https://doi.org/10.1070/RCR5024

Pickering emulsions: structure, properties and the use as colloidosomes and stimuli-responsive emulsions

Marina Yu. Koroleva,* Evgeny V. Yurtov

Mendeleev University of Chemical Technology, Miusskaya pl. 9, 125047 Moscow, Russian Federation

Pickering emulsions are emulsions that are stabilized by solid micro- and nanoparticles. These emulsions are in most demand for applications where the use of surfactants is restricted. The review addresses stabilization of Pickering emulsions. The attention is focused on the flocculation, coalescence, sedimentation and Ostwald ripening processes taking place in these emulsions. The structures formed by particles in the emulsion dispersion medium and in thin interlayers between the dispersed phase droplets are analyzed. Methods for preparing colloidosomes, that is, microcapsules of assembled particles, from Pickering emulsions are considered. Colloidosomes are promising for the encapsulation and prolonged release of active substances. Conversely, Pickering stimuli-responsive emulsions provide intense release of encapsulated substances upon the change in the environmental parameters. This can be used not only in medicine and pharmacology, but also in sensors, food industry, paint and varnish industry, petroleum production, *etc.*
The bibliography includes 340 references.

Contents

1. Introduction 1
2. Stabilization of Pickering emulsions 2
3. Stability of Pickering emulsions 4
3.1. Flocculation 4
3.1.1. Thin films 4
3.1.2. A droplet on the surface 5
3.1.3. Emulsions 5
3.2. Coalescence 6
3.3. Sedimentation and creaming 7
3.4. Ostwald ripening 8
4. Types of Pickering emulsions 9
4.1. Oil-in-water and water-in-oil emulsions 9
4.2. Multiple water-in-oil-in-water and oil-in-water-in-oil emulsions 9
4.3. Bicontinuous emulsions 10
4.4. Water-in-water and oil-in-oil emulsions 11
5. Types of stabilizing particles 12
5.1. Silica particles 13
5.2. Latexes 14
5.3. Carbon nanoparticles 15
5.4. Hydroxyapatite particles 17
5.5. Clay particles 17
5.6. Starch particles 17
5.7. Cellulose particles 18
5.8. Lipid particles 19
5.9. Microgel particles 19
5.10. Particles of bioactive polymers 20
5.11. Particles of biological origin 21
5.12. Janus particles 22
6. Colloidosomes 23
7. Stimuli-responsive Pickering emulsions 25
7.1. Emulsions responsive to pH change in the aqueous dispersion medium 25
7.2. Emulsions responsive to the action of chemicals 26
7.3. Emulsions responsive to temperature variation 26
7.4. Emulsions responsive to magnetic field 27
7.5. Emulsions responsive to light 27
8. Conclusion 27
9. List of abbreviations and symbols 28
10. References 28

1. Introduction

Pickering emulsions are emulsions stabilized by solid particles. The accumulation of solid protein fibres, iron acetate or copper acetate particles, *etc.* on gas bubble surface was observed for the first time by W.Ramsden [1] in 1903. On the basis of his experiments on foams, the author proposed that particles can also be located at the interface between two liquids, and this gives rise to stable emulsions. These emulsions were later called Pickering emulsions after S.U.Pickering, who discovered this type of stabilization in

M.Yu.Koroleva. Doctor of Chemical Sciences, Professor at the Department of Nanomaterials and Nanotechnology, MUCTR.
E-mail: m.yu.kor@gmail.com
Current research interests: nanomaterials and nanostructures, nanoemulsions, liquid nanostructured systems, liquid extraction.
E.V.Yurtov. Corresponding Member of the RAS, Doctor of Chemical Sciences, Professor at the same Department.

Translation: Z.P.Svitanko

Received 12 May 2021

© 2022 Uspekhi Khimii, ZIOC RAS, Russian Academy of Sciences and IOP Publishing Limited

1907.[2] Pickering studied paraffin oil-in-water emulsions stabilized by particles of lime and copper hydroxide sulfate $CuSO_4 \cdot 3\,Cu(OH)_2$ or iron hydroxide sulfate $Fe(OH)SO_4$ and concluded that the solid particles were attracted to oil droplets and formed a film on their surface, thus preventing the droplets from coalescence.

Pickering emulsions can be stable for a long period of time, and an undoubted advantage of these emulsions is the absence (or very low concentration) of surfactants, which are used to stabilize conventional emulsions.[3] This is especially important for pharmaceutical and food industry applications.

Like conventional emulsions, Pickering emulsions can be of oil-in-water (O/W), water-in-oil (W/O) and multiple [water-in-oil-in-water (W/O/W) and oil-in-water-in-oil (O/W/O)] types.

The most intensive studies of these emulsions have been carried out in the last several decades. Quite a few reviews and books are devoted to Pickering emulsions. However, the number of publications addressing physicochemical aspects of Pickering emulsions and processes taking place in them is moderate.[4–7] Most reviews discuss separate issues of stabilization of these emulsions by a particular sort of particles[8–15] and their applications, most often, in food industry.[16–20] A lot of attention is devoted to the formation and stabilization of Pickering emulsions, which have been studied rather comprehensively. Characteristic features of stabilization of Pickering emulsions by particles of various morphology are addressed in reviews.[21,22] Low *et al.*[23] give a detailed account of methods used for analysis of the structure and stability of these emulsions. The key differences between stabilization of emulsions by conventional surfactants and colloidal particles have been discussed.[4,7]

In this review, attention is concentrated on mechanisms of phase separation of Pickering emulsions and processes that result in the formation of various structures of stabilizing particles at the interface and in the dispersion medium of emulsions. Despite numerous studies, experimental evidence for the existence of these structures, especially in the case of nanoparticle stabilization, is rarely reported. Meanwhile, particle organization in the emulsions determines their potential applicability.

A promising trend is application of Pickering emulsions as colloidosomes. Colloidosomes are porous microcapsules formed by colloidal particles that are locked together. These structures do not degrade upon the removal of the internal or external phase. Colloidosomes are promising for encapsulation of biologically active agents. Their controlled porosity ensures prolonged release of encapsulated compounds. A number of reviews[24–26] address methods for the preparation of colloidosomes, including methods that use solid templates, and methods for particle linking to form a strong capsule.

One more interesting and promising is the application of Pickering emulsions as stimuli-responsive systems, which undergo phase separation under definite external conditions, resulting in avalanche release of encapsulated compounds. Tang *et al.*[27] surveyed the most recent research achievements and the application prospects of materials obtained using stimuli-responsive Pickering emulsions. Successful development of some materials requires understanding of not only stabilization mechanisms of Pickering emulsions, which is considered in detail in many publications, but also phase separation mechanism, which is considered in detail in this review.

2. Stabilization of Pickering emulsions

The type of Pickering emulsion depends on the contact angle (θ) between the particle and the interface. Hydrophilic particles characterized by $\theta < 90^\circ$ measured through the aqueous phase stabilize oil-in-water emulsions, while hydrophobic particles with $\theta > 90^\circ$ stabilize water-in-oil emulsions (Fig. 1).

Stability of a particle layer depends on the energy of particle desorption from the interface

$$E = \pi r^2 \gamma_{ow}(1 \pm \cos\theta)^2 \quad (1)$$

where r is the radius of the adsorbed particle, γ_{ow} is the surface tension at the oil/water interface. The minus sign in the parentheses is used for particles with $\theta < 90^\circ$ when the particles are desorbed from the surface to the aqueous phase, while this sign is plus for particles characterized by $\theta > 90^\circ$ and desorbed to the organic phase.

The desorption energy of non-spherical particles is determined from the following expressions:

for plate-like particles[28]

$$E = \pi r^2 \gamma_{ow}(1 \pm \cos\theta) \quad (2)$$

for rod-like particles[8]

$$E = lb\gamma_{ow}(1 \pm \cos\theta) \quad (3)$$

where l and b are rod length and thickness, respectively.

The dependences of desorption energy on the diameter of spherical particles for various contact angles are shown in Fig. 2.[29] The energies of particle detachment from the surface are very high in comparison with the energy of thermal motion kT (k is the Boltzmann constant, T is temperature); therefore, it can be conventionally considered that the particles with the diameter $d > 10$ nm are irreversibly adsorbed at the interface. This constitutes an important difference between emulsion stabilization by particles and by conventional surfactants, which can be both adsorbed and desorbed at the interface.[4] As the angle θ decreases, the desorption energy of particles from the interface decreases, but still remains relatively high, ranging from tens to thousands of kT.

According to Eqn (1), the desorption energy of particles is maximum for $\theta = 90^\circ$. However, for efficient stabilization of O/W emulsions, this angle should be $< 90^\circ$, while

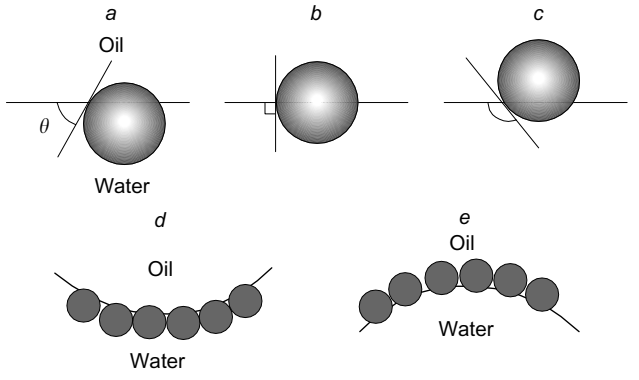


Figure 1. Position of particles at a planar water/oil interface ($a-c$) and on a curved surface (d, e) depending on the contact angle measured through the aqueous phase. θ, deg.: (a) <90, (b) 90, (c) >90, (d) <90, oil-in-water emulsion, (e) >90, water-in-oil emulsion.[4] Published with permission from Elsevier.

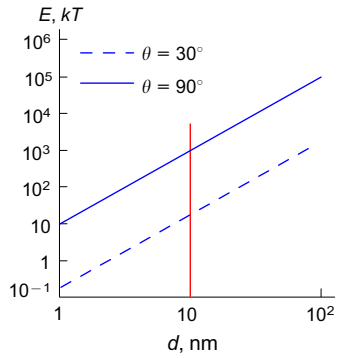


Figure 2. Dependences of the desorption energy of a particle from the interface (E) in kT units on the particle diameter for various contact angles.[29] Published with permission from Elsevier.

stabilization of W/O emulsions requires $\theta > 90°$.[30] The desorption energy sharply decreases with decreasing wetting contact angle of particles. When θ is in the range of $0-20°$ or $160-180°$, the desorption energy is less than 10 kT. In this case, particles are easily detached from the interface and do not act as effective stabilizers of emulsions.[4]

The efficiency of emulsion stabilization by so-called Janus particles, consisting of parts of different composition and, hence, possessing different surface properties (see Section 5), depends on the interfacial contact angles for the polar region of the particle θ_p and for the non-polar region of the particle θ_a (Fig. 3). The equation of the total surface energy of these particles located at the W/O interface was reported by Ondarçuhu *et al.*[31] If $\theta_a < \alpha < \theta_p$, the desorption energies from the interface and removal of a particle into the bulk aqueous (E_{water}) and organic (E_{oil}) phases are determined by the following equations:[32]

$$E_{water} = 2\pi r^2 \gamma_{ow}\left[\frac{1}{2}\sin^2\alpha + \cos\theta_a(\cos\alpha + 1)\right] \quad (4)$$

$$E_{oil} = 2\pi r^2 \gamma_{ow}\left[\frac{1}{2}\sin^2\alpha + \cos\theta_p(\cos\alpha - 1)\right] \quad (5)$$

Unlike homogeneous particles, Janus particles have a higher desorption energy. If the contact angle approaches 0 or 180°, the desorption energy of Janus particles is ~3 times higher than that of homogeneous particles, *i.e.*, they retain the surface activity.[33]

A similar trend was identified in a molecular dynamics simulation of the behaviour of silica nanoparticles of 3 nm in diameter at the water/decane interface. The desorption of Janus particles bearing surface groups with different properties requires higher energy than the desorption of homogeneous nanoparticles.[34]

The stability of Pickering emulsions depends not only on the desorption energy of particles from the interface, but also on the stability of the interfacial film between the droplets of the dispersed phase. Below (see Section 3) it is shown in more detail that the droplets of the dispersed phase approach one another to form floccules in which the droplets are separated by a mono- or bilayer of adsorbed particles (Fig. 4).

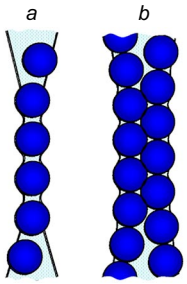


Figure 4. Schematic image of monolayer (*a*) and bilayer (*b*) between two flocculated droplets in a Pickering emulsion.[35] Published with permission from Elsevier.

The stability of the interfacial film formed by a monolayer or bilayer of adsorbed particles [35–39] was evaluated in terms of the maximum capillary pressure (P_c^{max}) at which the meniscus of the dispersion medium between two adsorbed particles is stable.[36]

The probability of formation of a stable emulsion with a dispersed phase fraction of 0.5 was calculated for a hexagonally packed single layer of particles separating two droplets (Fig. 5 *a*). In this case, the highest probability of

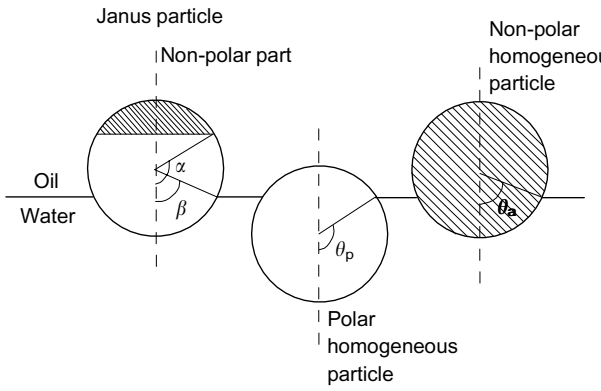


Figure 3. Schematic image of amphiphilic and homogeneous particles at the W/O interface. α is the angle characterizing the position of the boundary between the polar and non-polar parts of the Janus particle, *i.e.*, the degree of particle asymmetry; β is the angle between the solid phase and the interface; θ_a and θ_p are contact angles for the non-polar and polar parts (in the oil), respectively.[32] Published with permission from AIP Publishing.

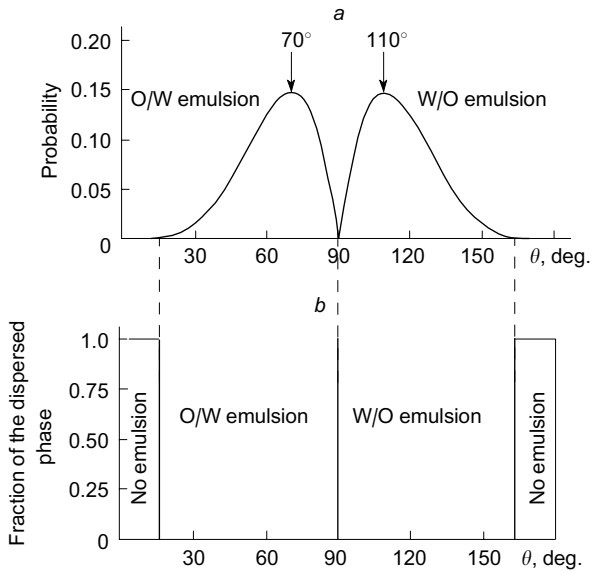


Figure 5. Probability of stability of emulsions with a dispersed phase fraction of 0.5 (*a*) and diagram of existence of emulsions in which the droplets are separated by a monolayer of adsorbed particles (*b*) as a function of contact angle.[39] Published with permission from Elsevier.

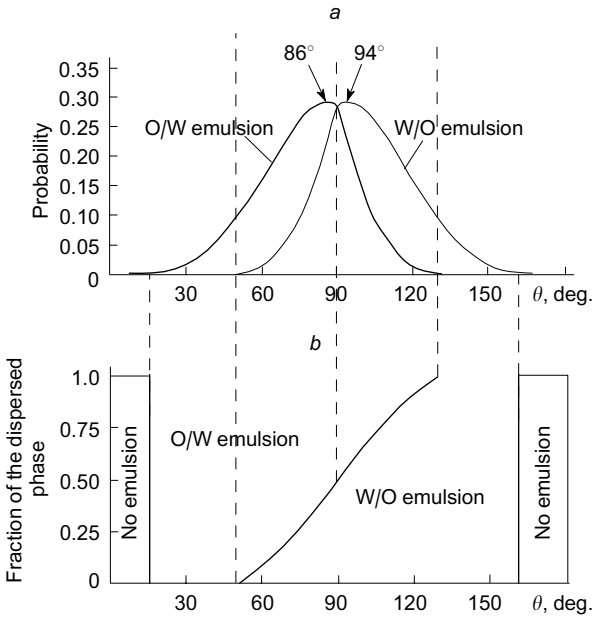


Figure 6. Probability of stability of emulsions with a dispersed phase fraction of 0.5 (*a*) and diagram of existence of emulsions in which the droplets are separated by a bilayer of adsorbed particles (*b*) as a function of contact angle.[39] Published with permission from Elsevier.

stabilization of O/W emulsions corresponds to the contact angle of 70°; in the case of W/O emulsions, this angle is 110°. Thus, O/W emulsions are formed in the θ range from 15 to 90°, while W/O emulsions are obtained for angles from 90 to 165° (Fig. 5 *b*).[39]

If the droplets of the dispersed phase are separated by a bilayer of adsorbed particles, the highest probability of stabilization of O/W emulsions is attained when the contact angle is 86°, while this angle for W/O emulsions is 94° (Fig. 6 *a*). Since the probability curves overlap, both O/W and W/O emulsions can exist in the range of contact angles from 50.7 to 129.3° (Fig. 6 *b*). According to calculations performed by Kaptay,[39] if $15 < \theta < 50.7°$, an O/W emulsion is formed, while in the $129.3 < \theta < 165.0°$ range, a W/O emulsion exists. Hence, the type of emulsion formed in the $50.7 < \theta < 129.3°$ range is that for which the probability of existence is higher.

The above calculated contact angles required for the formation of stable emulsions are in line with experimental data. Indeed, the smallest droplets, which are, hence, more stable to coalescence, were formed when the Bayol-35 paraffin oil was stabilized by clay particles with $\theta = 65°$;[40] the greatest amount of hexadecane was emulsified in the aqueous phase when stabilized by the *Acinetobacter venetianus* cells with $\theta = 55°$;[41] in the case of foam stabilization in aqueous ethanol, the highest stability was observed when the contact angle for polymer particles was 75–85°.[42]

3. Stability of Pickering emulsions

3.1. Flocculation

Pickering emulsions undergo the same processes as surfactant-stabilized emulsions, particularly, flocculation, coalescence, sedimentation and Ostwald ripening.

A decrease in the distance between the dispersed phase droplets leads to flocculation, that is, the formation of floccules in which the droplets are separated by interlayers, which represent mono- or bilayers of particles adsorbed on the droplet surfaces (see Fig. 4). If such interlayer is insufficiently tough of if droplets migrate from the contact zone, coalescence of droplets necessarily takes place.

The flocculation and the subsequent coalescence were studied for both Pickering emulsions and model systems — thin films separating two bulk phases and for an oil or water drop approaching a water/oil interface from the side of opposite polarity phase.

3.1.1. Thin films

Horozov *et al.*[43] investigated aqueous and octane films simulating an interlayer of the dispersion medium between droplets of the dispersed phase. Upon thinning of a water film in octane containing a low concentration of silica particles with a diameter of 3 μm and a contact angle of 99°, the particles migrated towards the periphery to give a dimple (Fig. 7 *a*). Subsequently, the film ruptured. At $\theta = 65°$, the dimple was surrounded by a ring of particles adsorbed at its periphery (Fig. 7 *b*). These films were relatively stable, since the dimple was arrested, and the particles that were in contact with the aqueous phases on the two sides did not migrate towards the film periphery (Fig. 7 *c*). The lateral mobility of the particles in the film played the crucial role in the stabilization. If the packing density of particles on the surface was low, the particles were dragged by the hydrodynamic flow of the liquid out of the film, and the thinnest part of the film between the droplets approaching one another turned bare.

The octane films in water containing silica particles with $\theta = 152°$ were stable. Thinning of the film gave rise to a hexagonal packing of particles (Fig. 8 *a*), with the distance between the particles gradually decreasing. On further film thinning, a spherical area of close-packed particles located at ~1.2 μm distances from one another and contacting with both aqueous phases on the two sides of the film appeared in the thinnest part of the film (Fig. 8 *b*). A sketch depicting the arrangement of particles in the octane film as the film is thinned is given in Fig. 8 *c*.

In the case of high particle concentration, thinning of water films in octane and thinning of octane films in water resulted in the formation of an area of close-packed particles. As the close-packed particle areas approached each other, a bilayer formed; subsequently, it transformed into a monolayer, with the bilayer structure being retained at the periphery.[43] Experimental data and results of calculations

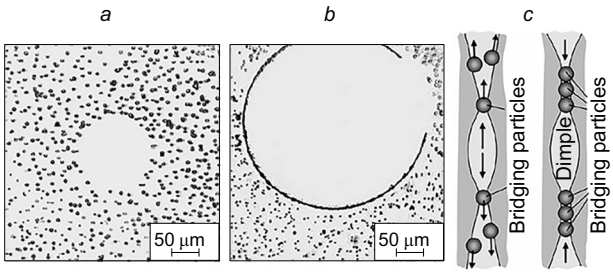


Figure 7. Optical microscopy images illustrating the dimple formation upon thinning of the water film with a low concentration of silica particles with contact angles of 99° (*a*) and 65° (*b*) and diagram of particle location in the films (*c*) depicted in Figs *a* and *b*.[43] Published with permission from the American Chemical Society.

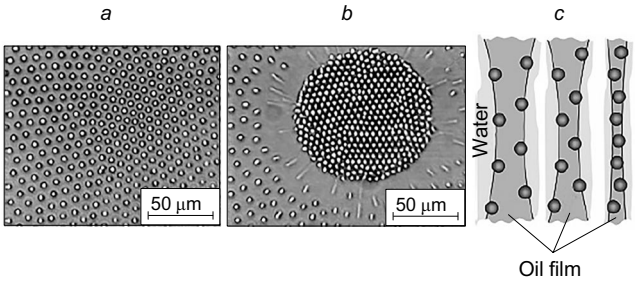


Figure 8. Micrographs of an octane film in water containing silica particles with $\theta = 152^\circ$ (*a*, *b*) and schematic image of the arrangement of particles following film thinning (*c*).[43] The structure with a hexagonal packing of particles (*a*) becomes denser in the central part as the film is thinned (*b*). Published with permission from the American Chemical Society.

showed that the critical capillary pressure at which the bilayer is transformed into a monolayer is markedly lower than the critical pressure needed for rupture of a film stabilized by a bilayer of particles; therefore, the film stability depended on the stability of the particle monolayer.

3.1.2. A droplet on the surface

Stancik *et al.*[44] reported the results of studying the behaviour of droplets approaching a water/decane interface from the side of opposite polarity (Fig. 9 *a*). Adsorbed spherical polystyrene particles with an average diameter of 3.1 μm were located on the droplet surface and on the flat interface.

In all cases, thinning of the film led to the formation of a dimple. At low particle concentration on the flat surface, most of the particles migrated from the contact zone during film drainage before coalescence. However, some of the particles were trapped in the dimple, being arranged as a thin ring consisting of a single row of particles (Fig. 9 *b*). As the concentration of particles adsorbed at the interface increased, the ring became thicker (Fig. 9 *c*). Further increase in the particle concentration on the surface gave rise to a round area with a regular hexagonal packing of particles inside the dimple (Fig. 9 *d*). Despite the film drainage, the particles inside the dimple were located at a certain distance from one another due to repulsion forces between them.

When a water droplet approached the water/decane interface from the side of decane, an area of close-packed particles formed in the contact zone, as the repulsion forces between the particles were much weaker in non-polar decane.

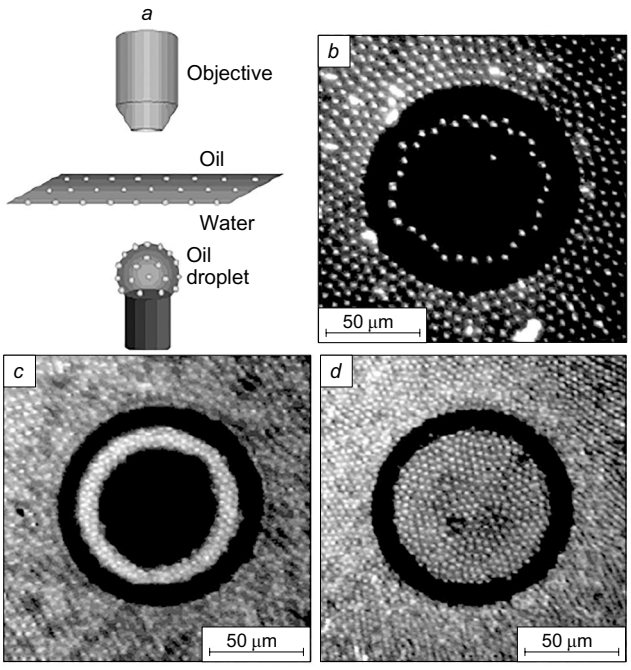


Figure 9. Schematic image of the system consisting of a drop of decane approaching the water/decane interface from the side of water (*a*) and micrographs illustrating the formation of a ring from one particle row (*b*), thick ring (*c*), and a round zone with an ordered packing of particles (*d*) inside the dimple. The polystyrene particle concentration on the decane droplet surface is 1%, that at the water/decane interface is 13 (*b*), 38 (*c*), 55% (*d*).[44] Published with permission from the American Chemical Society.

3.1.3. Emulsions

There are not a lot of reported visual data confirming the structure of the interfacial layer in the contact zone between the flocculated droplets of the dispersed phase in Pickering emulsions. French *et al.*[45] investigated dodecane emulsions in water stabilized by silica particles of 860 nm in diameter with the surface modified with isopropyl myristate. The freeze fracture scanning electron microscopy (SEM) image is shown in Fig. 10 *a*. In the contact zone between two droplets with a diameter of ~60 μm, a monolayer of adsorbed silica particles formed.

Horozov and Binks[46] reported optical microscopy images of the contact zone between the flocculated drops taken using an extra-long working distance objectives. An emulsion of water in octane with a drop size of 300 μm was

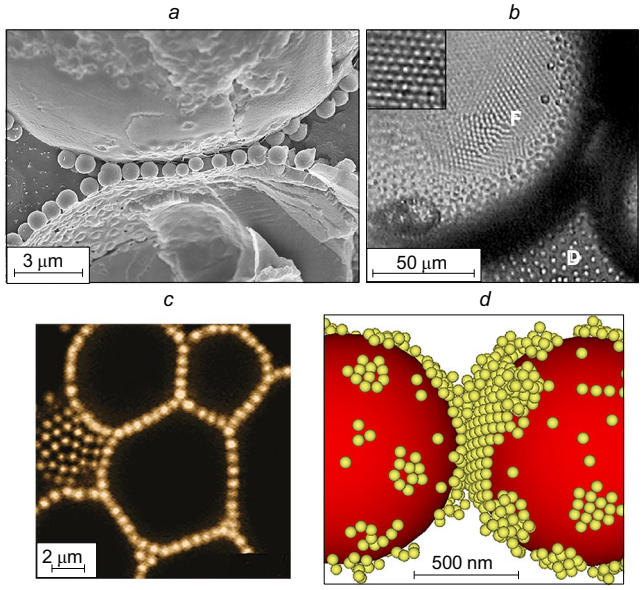


Figure 10. SEM images of dodecane-in-water (*a*)[45] and water-in-octane (*b*)[46] emulsions; confocal microscopy image of an emulsion consisting of a solution of dimethyl sulfoxide in water dispersed in a mixture of toluene and dodecane (*c*),[47] and image of oil droplets in water obtained by Langevin dynamics simulation (*d*).[48] The images illustrate the formation of a monolayer of adsorbed silica particles in the contact zone between the droplets. For zones *F* and *D*, see text. Figures *a* and *d* are published with permission from Elsevier, Fig. *b* is published with permission from Wiley, Fig. *c* is published with permission from the American Chemical Society.

stabilized by silica particles with a diameter of 3 μm with $\theta = 152^\circ$. It can be seen (see Fig. 10 *b*) that the contact zone designated by the letter *F* is a rounded area consisting of a monolayer of close-packed particles. At the periphery outside the contact zone designated by the letter *D*, the particles are located rather sparsely.

Lee *et al.*[47] studied W/O emulsions consisting of a solution of dimethyl sulfoxide in water dispersed in a mixture of toluene and dodecane. Droplet flocculation resulted in a monolayer of silica particles with a diameter of 975 nm (Fig. 10 *c*).

Langevin dynamics simulation of the adsorption of silica nanoparticles on the surface of oil droplets of 1 μm in diameter showed[48] that flocculation in the contact zone also gives a monolayer of adsorbed silica nanoparticles (Fig. 10 *d*). When the ionic strength of the aqueous dispersion medium changes from 0.01 to 3 mol L^{-1} and if flocculation of oil droplets took place, they were located at 50 nm distance from one another, which corresponded to the diameter of a silica nanoparticle. An area of close-packed nanoparticles appeared in and around the contact zone. In other regions, the surface of an oil droplet was only slightly covered by adsorbed nanoparticles.

The formation of mono- and bilayers in the contact zone was observed by confocal microscopy during flocculation of decane droplets stabilized by poly(*N*-isopropylacrylamide) microgel particles of ~950 nm in diameter in water (Fig. 11).[49] Possibly, in these emulsions, the bilayer in the contact zone was not transformed into a monolayer, since the hydrogel microparticles were easily deformed.[50]

In a monolayer, the capillary forces acting between the particles connecting two droplets of the dispersed phase attract the particles to one another, which leads to the formation of a closer packing of particles in the thinnest parts of the film of the dispersion medium. Even if the long-range repulsion forces between the particles on the drop surface are relatively high, the particles are attracted to one another in the contact zone of the droplets.

Depending on the capillary pressure, the structure of the layer separating the flocculated droplets of the dispersed phase may be different. In the case of small-droplet emulsions, the formation of a monolayer in the contact zone is more likely, as the capillary pressure is high. In large droplets, the capillary pressure is lower; therefore, the particle bilayer between the droplets may exist for longer periods of time.[43]

However, this conclusion is valid only theoretically. In practice, a monolayer of non-deformable particles is typically formed in the contact zone between flocculated droplets in emulsions. As a result, the emulsions are stable to coalescence, even if the droplet surface is only partly covered by adsorbed particles. It is noteworthy that when the monolayer is formed in the contact zone of droplets, the flocculation becomes irreversible.

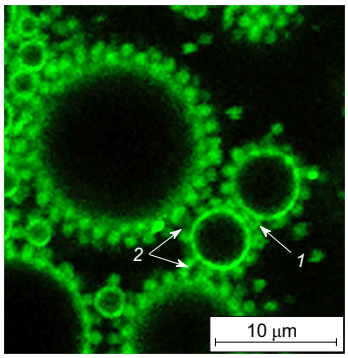


Figure 11. Confocal microscopy image of a decane-in-water emulsion stabilized by poly(*N*-isopropylacrylamide) hydrogel microparticles.[49] (*1*) Monolayer, (*2*) bilayer of adsorbed particles in the contact zone. Published with permission from Elsevier.

3.2. Coalescence

Many authors noted that immediately after preparation, so-called limited coalescence of dispersed phase droplets takes place in Pickering emulsions, like in surfactant-stabilized emulsions.[51] The cause for this process is the formation of a too large interfacial area upon dispersion, so that the available amount of the surfactant or particles is insufficient for stabilization. The limited coalescence phenomenon was first described by Hardy[52] in 1928 in relation to emulsions formed by lubricating oils. In emulsions stabilized by solid particles, the occurrence of limited coalescence is in line with the Pickering's statement that the droplet size depends on the number and size of stabilizing particles rather than on the stirring intensity.[1]

The rate of limited coalescence gradually decreases with time and then becomes virtually zero. As a rule, this process takes from approximately several seconds to several minutes after preparation of the emulsion.[46, 53] After limited coalescence is over, Pickering emulsions with a narrow droplet size distribution stable to coalescence for a long period of time (several months to several years) are formed rather often.

Arditty *et al.*[53] studied emulsions of polydimethylsiloxane in water with a fraction of the dispersed phase of 90 mass %, which were prepared by manual shaking. The emulsions were stabilized by silica nanoparticles of 25 nm in diameter with n-octyltriethoxysilane grafted to the surface. The photographs taken in various time intervals after formation of the emulsion are depicted in Fig. 12. In the initial period, the average droplet size rapidly increased, while later it remained nearly constant. When limited coalescence took place, a narrow droplet size distribution was retained, while the average droplet diameter increased from 0.59 to 3.39 mm in 151 s (Fig. 13).

The specific interfacial area of emulsions after completion of the limited coalescence depended on the dispersion

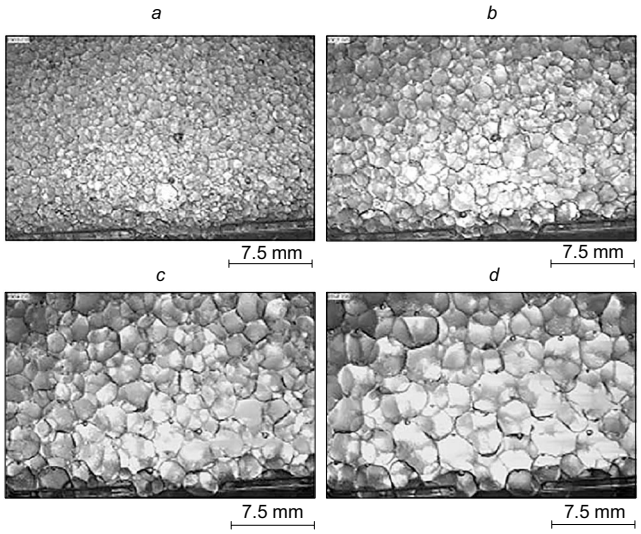


Figure 12. Micrographs of polydimethylsiloxane-in-water emulsions with a dispersed phase fraction of 90 mass % stabilized by silica nanoparticles taken 9 (*a*), 21 (*b*), 54 (*c*) and 141 s (*d*) after the preparation.[53] Published with permission from Springer Nature.

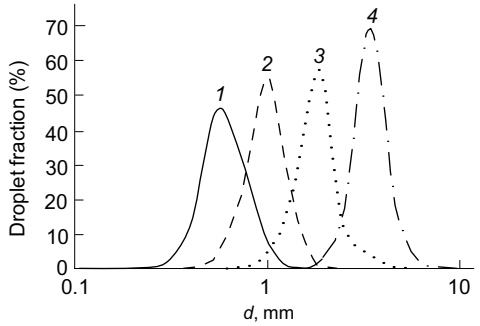


Figure 13. Droplet size distributions presented as a fraction of the total surface area occupied by droplets of a given size in polydimethylsiloxane-in-water emulsions with a dispersed phase fraction of 90 mass % stabilized by silica nanoparticles 0 (*1*), 3 (*2*), 15 (*3*) and 151 s (*4*) after the preparation.[53] Published with permission from Springer Nature.

intensity during the preparation of initial emulsions. Due to the turbulent stirring, the specific interfacial area was approximately equal to the surface area at which the monolayer of hexagonally close-packed particles was formed. During the preparation of coarse emulsions by gentle manual shaking (see Fig. 12), aggregates of silica nanoparticles were adsorbed on the droplet surface. The specific interfacial area in these emulsions after the limited coalescence was ~10 times smaller than in the case of turbulent stirring fabrication of the emulsions. The authors attributed this result to the fact that the initial nanoparticles were aggregated in water. The energy of manual shaking was insufficient to breakup the aggregates; therefore, the aggregates of nanoparticles were adsorbed on the droplet surface. The turbulent stirring resulted in not only more efficient dispersion, but also in the breakup of nanoparticle aggregates. Hence, the emulsions were stabilized by adsorption of single silica nanoparticles on the droplet surface.

Thus, with efficient adsorption of particles on the droplet surface, Pickering emulsions are, most often, highly stable to coalescence.[5] The layer of adsorbed particles acts as a mechanical barrier that prevents coalescence,[4, 6, 54] and these disperse systems remain stable to this process for a long period of time.

Pawar *et al.*[55] observed the formation of non-spherical droplets upon partial coalescence (Fig. 14). Droplets partially covered by adsorbed particles were squeezed out of two micropipettes and brought together. First, the formation of a dimple in the contact zone was observed and then coalescence took place. The surface area of the partially coalesced droplets decreased, and at some time point, a layer of close-packed particles formed on the surface of the two initial droplets and in the neck netween them (Fig. 14 *d*). This phenomenon was called arrested coalescence.

The non-spherical droplets were transformed with time into spherical droplets even in the presence of close-packed adsorbed particles on the surface, no matter how great the energy of particle desorption from the interface was. Structures of this type can exist for relatively long time in highly concentrated emulsions; for example, they were detected in a particle-stabilized emulsion obtained by bulk mixing (see Fig. 14 *e*).

Studying of the limited coalescence process demonstrated that preparation of a Pickering emulsion stable

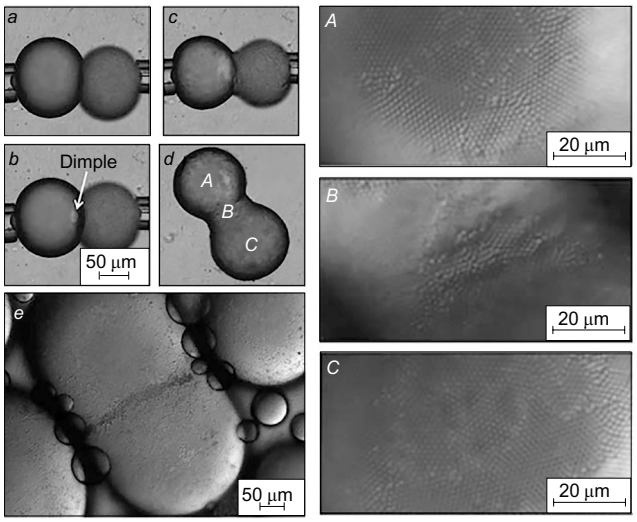


Figure 14. Micrographs illustrating partial coalescence. (*a*) two drops squeezed out of the capillary were brought in contact with each other; (*b*) dimple formation between the droplets; (*c*) initiation of droplet coalescence; (*d*) partially coalesced droplets and close packing of adsorbed particles on the surface of these droplets (*A* and *C*) and in the neck region between them (*B*); (*e*) similar structure of partly coalesced droplets stabilized by particles for an emulsion obtained by bulk mixing.[55] Published with permission from the Royal Society of Chemistry.

against coalescence for a long period of time requires the formation of a close-packed layer of adsorbed particles on the surface of dispersed phase droplets. Some authors (see, *e.g.*, Refs 46, 48, 54, 56, 57) emphasized that emulsions can be stable against coalescence even if the concentration of particles in the system is insufficient to form a close-packed layer on the droplet surface. This may be caused by several factors. On the one hand, an area of close-packed particles can be formed in the droplet contact zones (see Figs 9 *d* and 10 *b*), which serves as a mechanical barrier that prevents coalescence,[46, 54] while on the other hand, adsorbed particles migrate over the interface as a result of Brownian motion, which retards the coalescence of droplets barely covered with the particles.[56]

3.3. Sedimentation and creaming

The particles present in Pickering emulsions can not only be adsorbed on the interface, thus ensuring stability against coalescence, but also aggregate with one another to give a spatial network in the bulk of the dispersion medium.[58] The formation of the gel-like network increases the stability of the emulsion, as droplet coming in contact and sedimentation slow down.[59] Also, there is additional time for adsorption of particles at the interface, which results in emulsions more stable to coalescence.[60]

Emulsions that form a gel of aggregated particles in the dispersion medium may have different structures. In these systems, the surface of dispersed phase droplets may be covered by adsorbed particles (Fig. 15 *a*). Meanwhile, emulsions can be stable even if the layer of adsorbed particles is sparse or absent. In this case, stability is provided by the gel-like structure of aggregated particles in which dispersed phase droplets can exist in the isolated state for a long period of time. The Langevin dynamics calculations reported by Koroleva *et al.*[48] showed that in the case of formation of a rather dense network of aggregated SiO_2

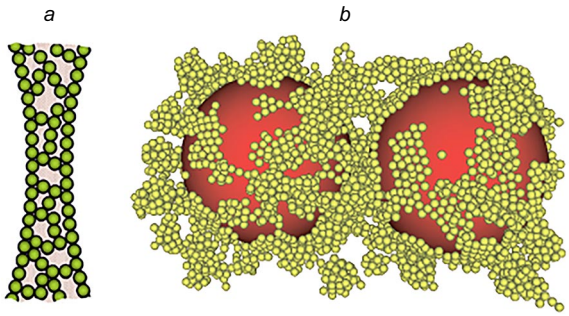


Figure 15. Schematic image of the dispersion medium of an emulsion with a network of aggregated particles in the interfacial film separating the dispersed phase droplets (*a*)[35] and snapshot of a model cell with oil droplets and aggregated SiO_2 nanoparticles obtained by Langevin dynamics simulation (*b*).[48] Published with permission from Elsevier.

nanoparticles in the bulk of the dispersion medium, only single clusters of close-packed nanoparticles were present on the surface of oil droplets (Fig. 15 *b*). The major part of the droplet surface was naked. Similar results were obtained in the simulation of stabilization of O/W emulsions by a mixture of SiO_2 and Fe_3O_4 nanoparticles.[29]

The Brownian dynamics method used to model particle aggregation showed the formation of aggregates with a fractal structure similar to the structure of polymer gels.[61] It was shown[62] that a gel-like network of aggregated nanoparticles, preventing the oil droplet coming in contact and flocculation, is formed at pH 8 in the dispersion medium of O/W emulsions stabilized by mixtures of Ludox CL silica and magnetite nanoparticles (Fig. 16).

The increase in the emulsion stability upon the formation of the gel-like network of aggregated particles in the dispersion medium was observed in numerous publications for O/W emulsions stabilized by spherical silica particles,[63] plate-like clay nanoparticles,[64, 65] palygorskite needle particles,[66] cellulose needle nano- and microcrystals,[67–69] chitin nanocrystals,[70] chitosan particles,[71] *etc.*

Rheological measurements for emulsions carried out by oscillation rheometry showed the formation of a gel-like network in the dispersion medium of emulsions stabilized by oppositely charged particles of the layered double hydroxide $[Mg_2Al(OH_6)]NO_3 \cdot 2\,H_2O$ and montmorillonite.[72] The gel structuring of the dispersion medium took place in water-in-water (W/W) emulsions stabilized by crystalline cellulose nanorods.[73] In all cases, the formation of gel-like network in the emulsion dispersion medium prevents droplets of the dispersed phase from approaching one another and thus hampers aggregation and subsequent coalescence.

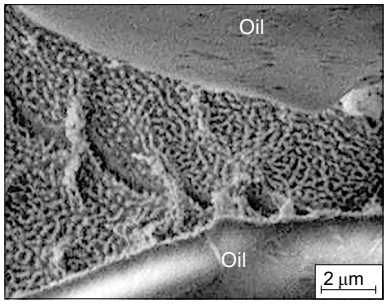


Figure 16. Cryo-SEM image of an emulsion stabilized by Ludox CL silica and Fe_3O_4 nanoparticles illustrating the formation of a gel-like network of aggregated nanoparticles between oil droplets.[62] Published with permission from the Royal Society of Chemistry.

3.4. Ostwald ripening

During the Ostwald ripening, caused by different Laplace pressures for small and large droplets, small droplets are dissolved, while large droplets becomer larger. The droplet size of the dispersed phase of Pickering emulsions is often several tens (and more) micrometres. In these disperse systems, Ostwald ripening is almost absent, since due to large radius of curvature of the interface, the Laplace pressure is relatively low. However, this process can take place in emulsions with smaller drops.

The Ostwald ripening (disproportionation) in foams proceeds in a similar way. It was shown experimentally that this process can be arrested almost completely by foam stabilization by solid particles.[74–77] In emulsions, the particles are adsorbed at the interface almost irreversibly; therefore, the Ostwald ripening can proceed in the initial time periods, and then its rate sharply decreases.[78] This occurs if the adsorbed particles form a barely packed layer on the droplet surface. The substance of the dispersed phase partially migrates from smaller droplets and the layer of adsorbed particles on the smaller droplets becomes close-packed. The particles are not desorbed from the interface, since the desorption energy is high, and Ostwald ripening almost stops.

It was shown[7] that in the Pickering emulsions with a barely packed particle layer at the interface, the radius of curvature of the droplet surface between adsorbed particles is equal to the droplet radius (Fig. 17). In emulsions with close-packed layer of particles, the sign of the surface curvature is reversed, as the adsorbed particles are mainly wetted by the dispersion medium; correspondingly, the Laplace pressure, which is the driving force of the Ostwald ripening, is different.[79]

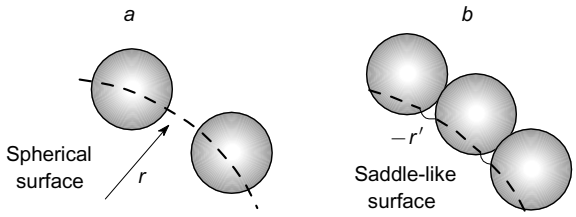


Figure 17. Schematic image of the droplet surface partially covered by adsorbed particles (*a*) and covered by a dense adsorption layer of particles (*b*);[7] r is the radius of the dispersed phase droplet in Pickering emulsions, r' is the radius of curvature of the saddle-like part of the surface with adsorbed particles. Published with permission from the Royal Society of Chemistry.

In some studies, it was shown experimentally that the Ostwald ripening in Pickering emulsions was either absent or substantially retarded. In emulsions stabilized by poly(glycerol monomethacrylate-b-2,2,2-trifluoroethyl methacrylate) copolymer nanoparticles of ~8.4 nm in size, the average size of dodecane and tetradecane droplets in water changed insignificantly for 6 weeks.[80] The 200–400 nm squalene droplets in water stabilized by Bindzil CC30 silica nanoparticles did not change in size for three years.[81] Ostwald ripening took place when hydrocarbons with a higher water solubility were used as the dispersed phase.[80, 81]

In W/O emulsions with dispersed phase droplet size of ~270 nm stabilized by ~28 nm nanoparticles of poly(stearyl methacrylate-co-2,2,2-trifluoroethyl methacry-

late) block copolymer, Ostwald ripening was absent if the NaCl concentration in the dispersed phase exceeded 0.11 mol L^{-1}.[82]

Thus, Ostwald ripening in O/W emulsions proceeds due to the diffusion of dispersed phase molecules dissolved in the dispersion medium. If the solubility is not negligibly low, Ostwald ripening most often does take place; when the solubility is very low, Ostwald ripening is absent. In W/O emulsions, the transport of water from smaller droplets to larger ones does take place if the Laplace pressure is not counterbalanced by the osmotic pressure created by the electrolyte.

It is noteworthy that the trends described above are valid for Pickering emulsions stabilized by non-modified particles. If the particles are modified with surfactant molecules for changing their hydrophobicity, a more intense Ostwald ripening is possible. In emulsions with modified particles, the surfactant micelles can transfer the dispersed phase substance between the droplets, which usually increases the rate of Ostwald ripening.[79]

4. Types of Pickering emulsions

Like conventional emulsions, Pickering emulsions may be of various types: O/W, W/O, multiple (W/O/W and O/W/O), bicontinuous, *etc*. Velankar[83] reported the non-equilibrium phase diagram illustrating the formation of various systems in various concentration ranges of components. The state diagram limited only to emulsion systems is shown in Fig. 18.

If the fraction of phase B (φ_B) is smaller than the fraction of phase A (φ_A), for an appropriate contact angle, a B/A emulsion is formed and *vice versa*. If the fractions of phases A and B are approximately equal, then at contact angles of particle wettability close to 90°, bicontinuous emulsions (bijels) are formed. Of course, this state diagram is not universal, as it is non-equilibrium. When the preparation procedure of emulsions is modified, for example, by varying the stirring intensity, order of component mixing and so on, the borders between the regions can considerably shift and the structure of emulsions can also change.[83]

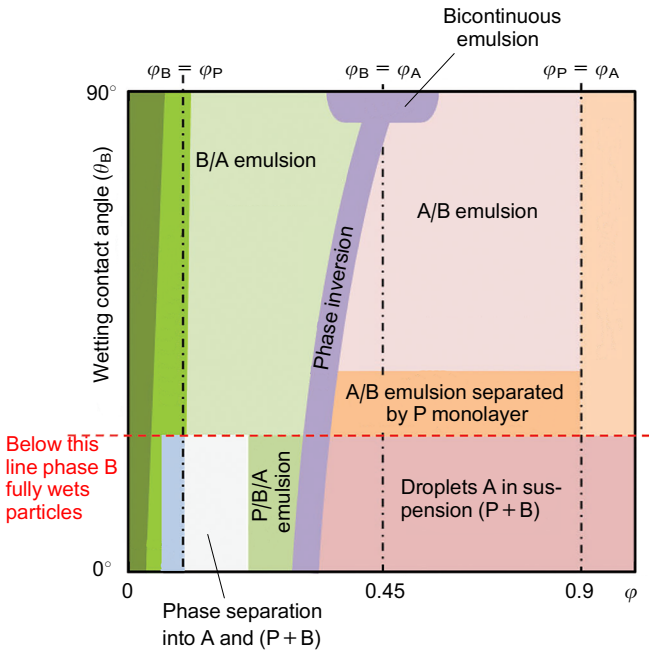


Figure 18. State diagram in the liquid A/liquid B/solid particles P. The fraction of solid particles in the system is 0.1.[83] Published with permission from the Royal Society of Chemistry.

4.1. Oil-in-water and water-in-oil emulsions

Oil-in-water and water-in-oil emulsions are typical among Pickering emulsions. The fraction of the dispersed phase in these emulsions can vary from very low values to ⩾74%, *i.e*., both dilute and highly concentrated emulsions are possible. As an example, Fig. 19 shows the SEM images of these emulsions. This review mainly addresses particularly these types of Pickering emulsions.

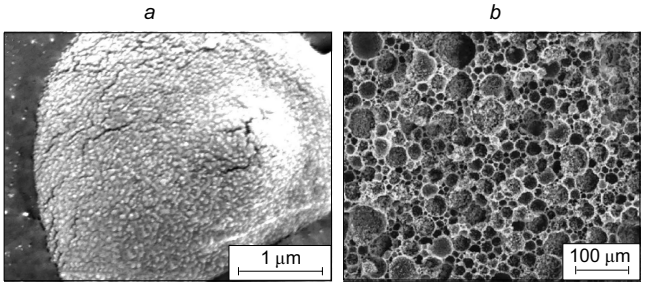


Figure 19. SEM images of a Miglyol 812 medium-chain triglyceride droplet with 1 mass % oleylamine in an emulsion containing 10 vol.% dispersed phase stabilized by 50 nm silica nanoparticles (*a*) [84] and highly concentrated W/O emulsion containing 85 vol.% dispersed phase stabilized by styrene particles after polymerization of the dispersion medium composed of styrene and divinylbenzene (9 : 1 volume ratio) (*b*).[85] Published with permission from the American Chemical Society.

4.2. Multiple water-in-oil-in-water and oil-in-water-in-oil emulsions

There are Pickering emulsions with different combinations of phases: W/O/W, O/W/O and O/O/O. The multiple Pickering emulsions are obtained when both the primary and secondary emulsions are stabilized by micro- or nanoparticles. Systems in which only one emulsion (primary or secondary) is stabilized by particles, while the other one is stabilized by conventional surfactants were also reported. For example, the primary W/O emulsion is stabilized by a surfactant, while the globules of the W/O emulsion dispersed in the external aqueous phase are stabilized by particles, or *vice versa*. It should be noted that multiple emulsions stabilized by particles with different contact angles are, as a rule, much more stable than the multiple emulsions stabilized by two surfactants.[3]

The structure and preparation of a W/O/W Pickering emulsion were considered by Nair *et al*.[86] The organic phase of this emulsion was a solution of terephthalic acid and bisphenol branched copolymers in ethyl acetate; the internal aqueous phase consisted of carboxymethyl cellulose hydrogel, with the droplet diameter of 100 – 500 nm. The droplets of the primary W/O emulsion were dispersed in the external aqueous phase and stabilized by Ludox TM silica nanoparticles with a size of 22 nm. Evaporation of ethyl acetate and water afforded hollow polymer particles the inner structure of which corresponded to the structure of the primary W/O emulsion (Fig. 20). Similar images were obtained upon polymerization of the organic phase of a water/styrene/water emulsion, in which the primary W/O

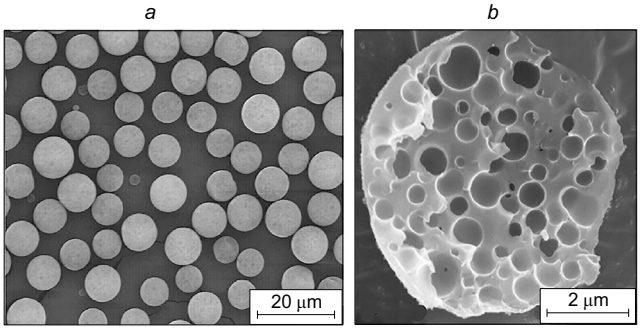


Figure 20. SEM images of capsules of a porous polymer formed from a W/O/W emulsion stabilized by Ludox TM silica nanoparticles (*a*) and a broken capsule with pores in place of water droplets in the primary W/O emulsion (*b*).[86] Published with permission from Elsevier.

emulsion was stabilized by hydrophobic silica nanoparticles, while the secondary emulsion was stabilized by Fe_3O_4 nanoparticles.[87]

The stabilization solely by particles resulted in the formation of W/O/W emulsions, stable for several months, with sunflower oil as the organic phase. The primary W/O emulsion was stabilized by ethyl cellulose particles, while the secondary emulsion was stabilized by rutoside particles.[88] Frasch-Melnik *et al.*[89] described a multiple W/O/W emulsion with sunflower oil, in which the primary emulsion was stabilized by crystalline mono- and triglycerides and the secondary emulsion was stabilized by sodium caseinate.

Water-in-dodecane-in-water emulsions were formed using a combination of worm-like particles of hydrophobic poly(lauryl methacrylate)–poly(benzyl methacrylate) and hydrophilic poly(glycerol monomethacrylate)–poly(2-hydroxypropyl methacrylate)–poly(benzyl methacrylate) copolymers for stabilization.[90]

Multiple O/W/O emulsions were studied by Szumała and Luty.[91] The external and internal oil phases consisted of liquid paraffin or jojoba oil. The emulsions were stabilized by carnauba wax particles. Cunha *et al.*[92] described hexadecane-in-water-in-hexadecane emulsions; the primary emulsion was stabilized by cellulose nanocrystals, while the secondary one was stabilized by lauryl chloride-modified cellulose nanocrystals.

Tyowua *et al.*[93] prepared emulsions of the O/O/O type, namely, olive oil-in-polydimethylsiloxane-in-olive oil and rapeseed oil-in-polydimethylsiloxane-in-rapeseed oil stabilized by silica nanoparticles the hydrophobicity of which was changed by surface modification with dimethyldichlorosilane (the fractions of the SiOH groups on the surface were 70 and 20%, respectively). The micrographs of multiple Pickering emulsions with rapeseed oil are shown in Fig. 21.[93] The emulsions were stable against coalescence, but tended to undergo sedimentation at low concentration of hydrophilic silica particles.

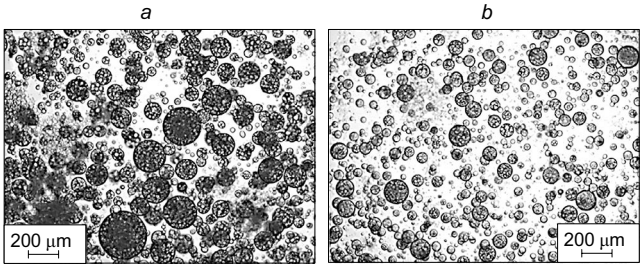


Figure 21. Micrographs of rapeseed oil-in-polydimethylsiloxane-in-rapeseed oil emulsions with concentrations of hydrophilic silica particles of 0.1 (*a*) and 0.5 mass % (*b*).[93] Published with permission from Elsevier.

Multiple Pickering emulsions are most in-demand in the food and pharmaceutical industry.

4.3. Bicontinuous emulsions

The possibility of existence of bicontinuous Pickering emulsions was shown for the first time by mathematical modelling. Stratford *et al.*[94] called thus structure bicontinuous intefacially jammed emulsion gel (or Bijel).[1] The images illustrating the stages of formation of a bicontinuous emulsion stabilized by particles of 10 nm in diameter are depicted in Fig. 22.

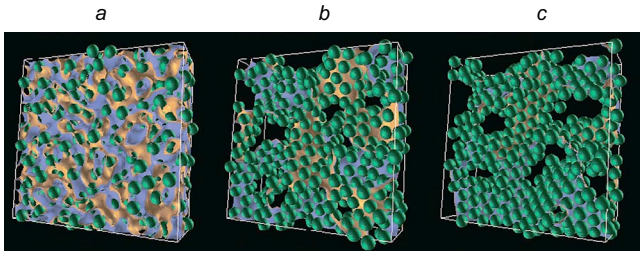


Figure 22. Snapshots of a part of 3D model cell illustrating the formation of a bicontinuous structure: 5000 (*a*), 50 000 (*b*), 500 000 simulation steps (*c*). The contact angle of particles is 90°; the volume concentration of particles in the system is 20%. The two liquids are coloured yellow and blue; monodispersed colloidal particles are green.[94] Published with permission from AAA Science.

The existence of these structures was confirmed experimentally.[95,96] Bicontinuous emulsions were formed upon spinodal decomposition on fast heating of the system. Confocal microscopy images of bicontinuous Pickering emulsions consisting of water and 2,6-lutidine and stabilized by silica particles with a diameter of 290 nm are shown in Fig. 23. These emulsions were stable for more than 7 months.

White *et al.*[97] showed that a decrease in the hydration of silica particles changes the type of emulsion from 2,6-lutidine-in-water to water-in-2,6-lutidine; in the case of intermediate hydrophilicity of stabilizing particles corresponding to phase inversion, the system was a bicontinuous Pickering emulsion.

Using phase separation *via* solvent diffusion from bicontinuous Pickering emulsions, unsymmetrical and hierarchical structures were formed.[98] Phase separation took place upon extraction of the solvent from a homogeneous three-component mixture. Emulsions were stabilized by silica nanoparticles with a size of 22 nm modified with cetyltrimethylammonium bromide for increasing their hydrophobicity. Hexane-1,6-diol diacrylate or butyl acrylate was used as the organic phase; they were polymerized for fixing the bicontinuous emulsion structure (Fig. 24).

Bicontinuous Pickering emulsions can be used as microreactors with liquid counter-current and as catalysts when stabilized by catalytically active particles.[96]

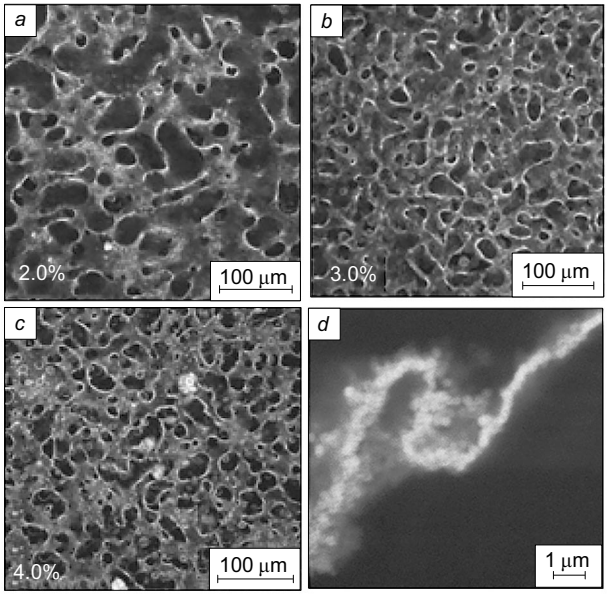


Figure 23. Confocal microscopy images of bicontinuous Pickering emulsions in the water/2,6-lutidine system (*a*–*c*) and enlarged image of the interfacial layer with adsorbed silica particles (*d*).[96] Figures *a*–*c* indicate concentrations of silica particles of 290 nm in diameter.[95] Emulsions were obtained by heating up to 40 °C at a 17 °C min^{-1} rate. Figures *a*–*c* are published with permission from Springer Nature, Fig. *d* is published with permission from the Royal Society of Chemistry.

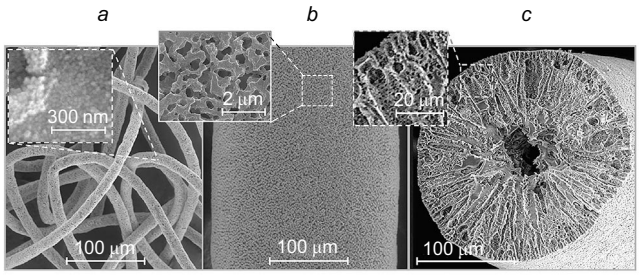


Figure 24. SEM images of fibres (*a*) and bulk material with a bicontinuous structure (*b*) and cross-section of a hollow fibre with a hierarchical wall structure (*c*) obtained after polymerization of the organic phase of a bicontinuous emulsion.[98] Published with permission from Wiley.

4.4. Water-in-water and oil-in-oil emulsions

Water-in-water emulsions are formed upon dispersion of two immiscible concentrated aqueous solutions of polymers. Each of the aqueous phases of these emulsions contains a solution enriched in one of the polymers, while the concentration of the other polymer is low. Subsequently, while describing the composition of phases of these emulsions, we will use the expression polymer solution, implying a solution enriched in one polymer and depleted in the other one.

Water-in-water emulsions, characterized by very low interfacial tension (1 μN m^{-1} to 1 mN m^{-1}) and thickness of the interfacial region up to several[73,99] or several tens[28] of nanometres, cannot be stabilized by conventional surfactants. Effective stabilization of these emulsions requires that the energy of particle removal from the interfacial region be noticeably larger than the energy of thermal motion kT, according to Eqn (1), which corresponds to particle size not smaller than 160 nm.[28]

Poortinga[100] showed that solid fat particles were adsorbed at the interface between two immiscible aqueous solutions of polysaccharides — dextran, maltodextrin and alginate — in various combinations. These emulsions were relatively stable.

Gonxalez-Jordan *et al.*[101] investigated emulsions containing a polyethylene oxide solution in an aqueous solution of dextran and a dextran solution in an aqueous solution of polyethylene oxide stabilized by polystyrene latex particles. It was shown that polystyrene latex particles modified with whey proteins stabilize emulsions consisting of a solution of polyethylene oxide dispersed in a solution of dextran. The particles without whey proteins stabilized emulsions containing a dextran solution dispersed in a solution of polyethylene oxide.

A micrograph of a drop of a dextran solution in a solution of polyethylene oxide with polystyrene latex particles with a diameter of 250 nm on the surface is shown in Fig. 25.[102] The contact angle of polystyrene particles through the dextran solution was 145°. The particles were preferably wetted by the phase containing polyethylene glycol; therefore, they stabilized dextran solution-in-polyethylene glycol solution emulsions.

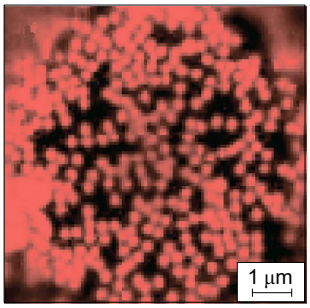


Figure 25. Confocal laser scanning microscopy image of a dextran droplet covered by polystyrene latex particles and dispersed in polyethylene oxide.[102] Published with permission from the American Chemical Society.

Vis *et al.*[28] produced W/W emulsions in which an aqueous solution of dextran was dispersed in an aqueous solution of fish gelatin. The emulsions were stabilized by plate-like gibbsite [$Al(OH)_3$] nanoparticles of ~170 nm in diameter and ~7 nm thickness; they were stable for several weeks. When larger and thicker particles were used for stabilization, emulsions were unstable and broke down.

Plate-like poly(lactide) particles were used to stabilize polyethylene glycol solution/dextran solution emulsions.[103] The particle size, that is, the length of up to 3.75 μm and the thickness of 12 nm, were determined by transmission electron microscopy (TEM) (Fig. 26 *a*). The interfacial tension at the boundary between two polymer solutions was 3.05 μN m^{-1}. According to investigations, 3.75 μm long polylactide particles more efficiently stabilized W/W emulsions (Fig. 26 *b*) than shorter particles of the same thickness. When the particle concentration was >0.3 mass %, the stability of the emulsions sharply increased (Fig. 26 *c*).

Emulsions containing a solution of polyethylene oxide dispersed in a solution of dextran were stabilized by rod-like nanoparticles of crystalline cellulose with 160 × 6 × 6 nm dimensions[73] and by protein particles with a diameter of ~300 nm.[104] Firoozmand *et al.*[105] obtained W/W bicontinuous emulsions from a gelatin solution and an oxidized starch solution using polystyrene latex particles for stabilization.

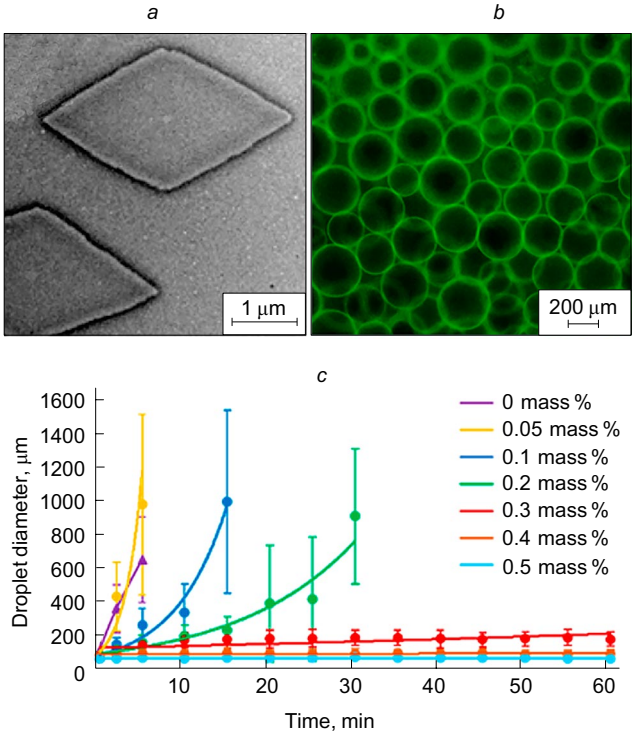


Figure 26. TEM image of plate-like poly(lactide) particles (*a*); confocal microscopy image of an emulsion of polyethylene glycol solution in a dextran solution stabilized by these particles (*b*); and time dependence of the droplet diameter in the emulsion at different particle concentrations, mass % (*c*).[103]

Emulsions consisting of two immiscible aqueous solutions of polymers stabilized by particles of various shapes and natures are promising for the use in food industry[99] and as stimuli-responsive systems and microreactors.

Oil-in-oil (O/O) Pickering emulsions are usually obtained from two immiscible liquids with different polarities. For example, Rozynek *et al.*[106] prepared emulsions of silicone oil in castor oil stabilized by 10 μm polystyrene particles. It can be seen in Fig. 27 that the particles form nearly regular hexagonal packing on the surface of a silicone oil droplet.

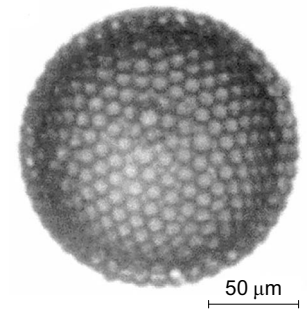


Figure 27. Micrograph of a silicone oil droplet in castor oil with polystyrene particles on the surface.[106] Published with permission from the Royal Society of Chemistry.

Rymaruk *et al.*[107] described the formation of emulsions of plant oils in silicone oil stabilized by block copolymer particles. The size of dispersed phase droplets in emulsions with castor oil or tall oil fatty acids almost did not change during four weeks at 20 °C (Fig. 28). In sunflower oil emulsions, the size of droplets increased with time. This difference was attributed to more intense Ostwald ripening

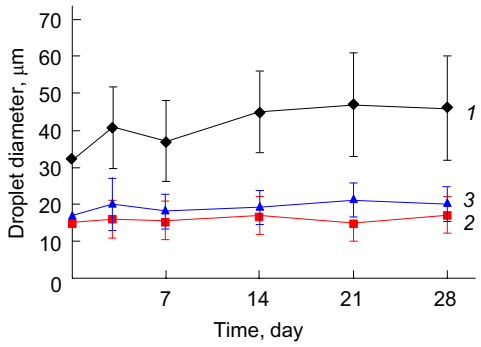


Figure 28. Time dependence of the diameter of dispersed phase droplets of sunflower oil (*1*), castor oil (*2*) and tall oil fatty acids (*3*) in silicone oil.[107] Published with permission from Elsevier.

caused by higher solubility of sunflower oil in silicone oil compared to other oils.

Using stabilization by graphene oxide nanoparticles modified with alkylamines with C_{12} or longer hydrocarbon chains, dimethylformamide-in-octane and acetonitrile-in-octane emulsions were obtained. If a C_6 hydrocarbon chain was present in alkylamine, octane emulsions in dimethylformamide or in acetonitrile were formed.[108]

Emulsions of diethylenetriamine in decalin were formed in the case of stabilization by ~6 μm montmorillonite particles modified with quaternary ammonium salt.[109] Hexane-in-methanol and dodecane-in-ethanol emulsions were formed when silica particles of 440 nm in diameter were used for stabilization.[110] Silica nanoparticles with a size of 20–30 nm were used to stabilize emulsions of olive oil in glycerol.[111]

Bicontinuous emulsions consisting of styrene trimer and low-molecular-mass polybutene were stabilized by silica nanoparticles.[112] Multiple O/O/O emulsions were obtained in the olive oil/silicone oil/olive oil and rapeseed oil/silicone oil/rapeseed oil systems and stabilized by silica nanoparticles with a size of 20–30 nm and different wettability.[93]

Oil-in-oil emulsions of various structures can be used for encapsulation of non-polar drug substances, in food industry, as lubricating materials, *etc.*

5. Types of stabilizing particles

Pickering emulsions are formed using stabilization by various particles with an appropriate contact angle and high energy of particle desorption from the interface. It is necessary to consider the density of stabilizing particles, as particle desorption and sedimentation are possible in the case of high density; this is accompanied by the loss of coalescence stability of emulsions. If the particles are not desorbed from the interface, droplets of the dispersed phase with a shell of adsorbed particles with high density can precipitate. These Pickering emulsions are unstable to sedimentation.

Below we consider the main types of particles stabilizing Pickering emulsions that have been studied most actively in recent years. The types of particles are rather arbitrary and are differentiated according to the proportion of publications and the application prospects of emulsions they stabilize rather than by chemical composition.

5.1. Silica particles

Silica micro- and (especially) nanoparticles have been considered most often as stabilizers for Pickering emulsions. Most studies use commercially available Ludox silica nanoparticles, which are obtained by sol–gel process *via* hydrolysis and polycondensation of silicate solutions, or Aerosil fumed silica, which is formed upon hydrolysis of silicon tetrachloride in water vapour. Nanoparticles of both types are hydrophilic. The surface of deposited particles (Ludox silica) bears numerous silanol groups Si–OH, while the fumed silica surface contains a lot of siloxane groups Si–O–Si; therefore, different sorts of nanoparticles respond differently to changes in the pH and electrolyte concentrations.[113] The authors of some publications used hand-made silica particles; as a rule, these particles were a few micrometres in size.

Many authors emphasize that preparation of stable oil-in-water Pickering emulsions requires the use of partly flocculated particles as small aggregates. This is reasonable, because particles with a high surface charge repel from one another and are slowly adsorbed on oil droplets, which usually have a relatively low surface charge. The particles on the droplet surface also repel from one another; hence, the adsorbed particle layer is not close-packed, which increases the probability of droplet coalescence. If the particles are highly flocculated, the adsorption of large flocs on the droplet surface would not result in uniform particle distribution and formation of a packed layer because of the attraction forces. Only the adsorption of small flocs may result in uniform distribution of the particles over the surface giving a layer in which the adsorbed particles are attracted to each other thus forming a close packing.

Maas *et al.*[114] suggested that clusters consisting of a small number of silica particles have a higher surface activity than single nanoparticles.

Binks and Lumsdon[113] studied toluene emulsions in water stabilized by Aerosil 200 fumed silica nanoparticles of 12 nm in diameter. In the dispersion medium pH range from 2 to 10, the emulsions were unstable to creaming and coalescence in the absence of electrolytes. After the addition of NaCl, the emulsions remained unstable; however, in the presence of $LaCl_3$ or tetraethylammonium bromide, the stability of the emulsions increased. The authors attributed the stability of emulsions to flocculation of silica nanoparticles. If the nanoparticles were weakly flocculated in the initial suspension, the emulsions were stable. Extensive flocculation of nanoparticles resulted in destabilization of emulsions. The use of precipitated silica nanoparticles in the presence of $CaCl_2$ markedly increased the stability of emulsions with an alkaline dispersion medium. The addition of dodecyldimethylammonium bromide afforded stable Pickering emulsions.[115]

An increase in the polarity of the oil molecule also increased the emulsion stability. This was attributed[115] to adsorption of oil molecules on the silica nanoparticle surface and change in their wettability. Similar results were mentioned in another publication.[116] Attempts to prepare emulsions with non-polar oils in the presence of fumed silica nanoparticles failed. Emulsions with the dispersed phase composed of ethyl acetate, butyl lactate, butanol, diethyl adipate, diisopropyl adipate or diisobutyl adipate were stable for >6 months.

The surface of hydrophilic silica particles can be modified with surfactant molecules which are adsorbed on the surface *via* hydrogen bonds or organic compounds that are linked to the surface *via* covalent bonds; most often, these are silane derivatives. This changes the wetting contact angle and the surface charge of particles.

If the dissociated surfactant molecules and particles are oppositely charged, the flocculation of particles takes place; by controlling this process, it is possible to obtain stable emulsions. Studies of dodecane-in-water emulsions stabilized by Ludox HS-30 nanoparticles with a negative surface charge at pH 9.5 and by a cationic surfactant, cetyltrimethylammonium bromide, showed[117] that the addition of the surfactant induced flocculation of nanoparticles in the initial suspension. This gave emulsions most stable to creaming and coalescence. A similar trend was observed when the emulsions were stabilized by positively charged Ludox CL nanoparticles and an anionic surfactant, sodium dodecyl sulfate, and the pH of the dispersion medium was 3.5; at this pH, the nanoparticles and surfactant molecules had opposite charges. A micrograph of the interface with a layer of adsorbed Ludox CL nanoparticles in this emulsion is shown in Fig. 29.[118]

Liu *et al.*[119] studied emulsions stabilized by negatively charged silica nanoparticles and dodecyl dimethyl carboxyl betaine, a zwitter-ionic surfactant. The emulsions were stable to coalescence at $pH \leqslant 5$ and completely broke down at $pH > 8.5$. In acidic solutions, carboxyl betaine molecules became positively charged and were adsorbed on silica nanoparticles. Correspondingly, at high pH values, the surfactant molecules did not modify the hydrophilic nanoparticles, and these nanoparticles did not stabilize the emulsion.

When stabilization was performed by hydrophilic fumed silica nanoparticles modified with non-ionic alkyl poly(oxyethylene), emulsions with flocculated nanoparticles were again most stable. Using experimentally determined contact angle and interfacial tension, the energy of desorption of modified nanoparticles from the interface was calculated. The dependence of the desorption energy on the surfactant concentration had a maximum, which corresponded to the most stable emulsion. The maximum energy of nanoparticle detachment from the interface was $\sim 550\,kT$ at an alkyl poly(oxyethylene) concentration of ~ 10 mmol L^{-1} (Ref. 120).

Binks *et al.*[63] used mixtures of negatively and positively charged SiO_2 nanoparticles to stabilize emulsions. The pH values of initial suspensions of Ludox HS-30 and Ludox CL were 9.9 and 3.6, respectively. The optimal mass ratio of negatively and positively charged particles was 2 : 1 (without

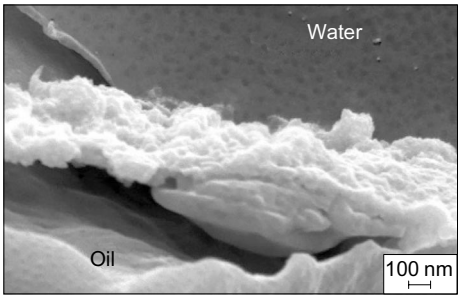


Figure 29. Cryo-SEM image of the interface in a dodecane emulsion in water stabilized by Ludox CL nanoparticles (2 mass %) modified with sodium dodecyl sulfate (3×10^{-2} mol L^{-1}).[118] Published with permission from the American Chemical Society.

correction of the mixture pH). The nanoparticles in the mixture flocculated, and dodecane-in-water emulsions containing 50 vol.% dispersed phase and stabilized by nanoparticle heteroaggregates were stable for >8 months. During this period, the size distribution of dispersed phase droplets almost did not change, which attested to the absence of coalescence. Heteroaggregates were adsorbed on the droplet surface and were located in the dispersion medium of emulsions. The fact that the dispersed phase droplets were covered by an adsorption layer of nanoparticles was confirmed by dilution of these emulsions with water: in dilute emulsions, the viscosity of the dispersion medium was lower, and creaming of oil droplets took place, but no coalescence occurred.

Emulsions of liquid paraffin in water stable to coalescence were formed when the mass ratio of Ludox HS-30 and Ludox CL nanoparticles was (0.3–1.0):1. When the nanoparticle ratio was (1.5–2.5):1, the emulsions were stable to flocculation and creaming. If the ratio of nanoparticles exceeded 3:1, the emulsions were unstable to coalescence and soon broke down (Fig. 30). This is due to the fact that at the 2:1 ratio (and total concentration of 3 mass %), the nanoparticles formed a gel-like network within the first 24 h after mixing. When the nanoparticle ratio was 1:1, the gel formation from heteroaggregates proceeded very slowly (within 20 days). Hence, the emulsions were stable to coalescence, but unstable to creaming. When the mass ratio of nanoparticles was 3:1, large heteroaggregates appeared, which were unable to stabilize emulsions.[62]

Oil-in-water Pickering emulsions were obtained using stabilization by silica nanoparticles modified with lecithin and oleylamine,[121] sodium alginate,[122] palmitic acid,[123] oleic acid,[124] didodecyldimethylammonium bromide,[125] alkyl poly(oxyethylene) monododecyl ethers,[126, 127] chitosan,[71] poly(*N*-isopropylacrylamide),[128] and by silica nanoparticles with surface-grafted benzaldehyde,[129] poly(styrene sulfonate),[130] methyl(polyethylene glycol)silane and organosilanes with propyl and methyl groups,[131] (3-glycidyloxypropyl)trimethoxysilane [132] and perfluorodecyldimethylchlorosilane.[133]

Water-in-paraffin oil emulsions were stabilized by fumed silica nanoparticles with a size of ~20 nm. If the pH value of the internal phase of the emulsion was low or high, intense flocculation of dispersed phase droplets took place. This was attributed to the destruction of the surface siloxane groups and increase in the number of surface silanol groups. Modification of silica nanoparticles with octadecyltrimethoxysilane gave water-in-oil Pickering emulsions containing 80 vol.% dispersed phase.[134]

Emulsions of hexadecane in water with 30 vol.% dispersed phase were stable for 4 months after preparation when stabilized by hydrophilic silica fibres with a length of 10 μm and a diameter of 200–250 nm. When the fibres used for stabilization had the same thickness and lengths of 1 and 5 μm, the emulsions completely broke down after 3 and 7 days respectively. The concentration of the fibres was 2 g L^{-1} with respect to the aqueous phase. When the fibre surface was modified with hexadecyltrimethoxysilane, the obtained water-in-hexadecane emulsions were stable for >4 months when stabilized by 1.5, 2.5 or 5 μm fibres.[135]

Water-in-lutidine emulsions were stabilized by hydrophobic silica rods with a length of ~4 μm. The dispersed phase droplets were covered by a multilayer shell consisting of chaotically arranged rods (Fig. 31).[136]

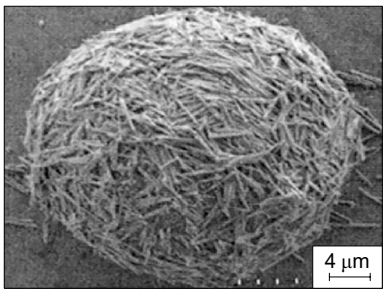


Figure 31. SEM image of the hollow sphere obtained after evaporation of water and lutidine from a W/O emulsion stabilized by silica rods.[136] Published with permission from the American Chemical Society.

5.2. Latexes

Pickering emulsions stabilized by polystyrene latex particles were investigated most often. It was shown [137] that the use of polystyrene latex particles with aldehyde and sulfate groups on the surface with an average size from 0.03 to 6.1 μm in the presence of 10^{-3} to 1 mol L^{-1} of NaCl in the aqueous phase resulted in the formation of W/O Pickering emulsions, which were stable to coalescence for >6 months. A micrograph of a water droplet in this emulsion, with particles forming a regular hexagonal packing on the surface, is shown in Fig. 32.

Not only spherical particles form ordered structures on the droplet surface. Gentle stirring of a mixture of water, hexadecane and rod-like epoxy resin particles yielded a W/O emulsion in which the rod-like particles were also self-assembled on the surface of water droplets [138] (Fig. 33).

Golemanov *et al.*[139] obtained W/O emulsions in which polystyrene latex particles with sulfate groups on the surface (190–220 nm in diameter) were initially dispersed in the aqueous phase. Water-in-oil emulsions were formed when non-polar oils such as hexadecane and tetradecane were used as the dispersion media. If the dispersion medium consisted of more polar molecules with a relatively high viscosity (50 mPa s), *e.g.*, soybean or silicone oil, the latex particles were not adsorbed on the droplet surface, but migrated into the bulk of the oil phase. When the silicone oil viscosity was lower (<5 mPa s), stable W/O emulsions were formed. The authors explained this by the fact that the adhesion of particles to the interface was higher in the case of emulsions with silicone oil of a low viscosity; therefore,

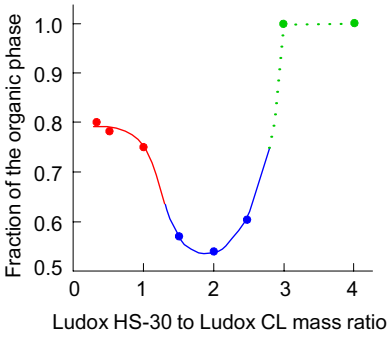


Figure 30. Fraction of the organic phase in the residual emulsion 20 days after preparation depending on the mass ratio of Ludox HS-30 and Ludox CL nanoparticles. The total concentration of nanoparticles is 3 mass %. The change in the curve colour corresponds to change in the emulsion stability from stable to coalescence (red dots) to stable to coalescence and creaming (blue dots), then to unstable emulsion (green dots).[62] Published with permission from the Royal Society of Chemistry.

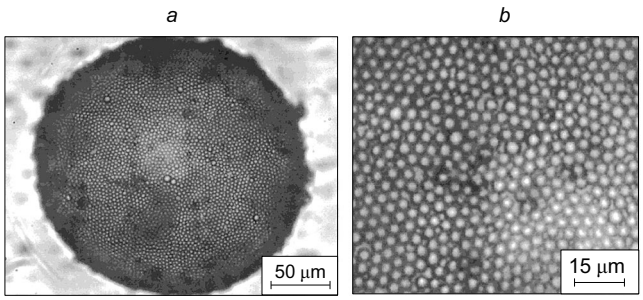


Figure 32. Micrograph of a water droplet in cyclohexane stabilized by polystyrene latex particles with aldehyde and sulfate groups on the surface (*a*) and fragment of the droplet surface with a close packing of particles (*b*).[137] Published with permission from the American Chemical Society.

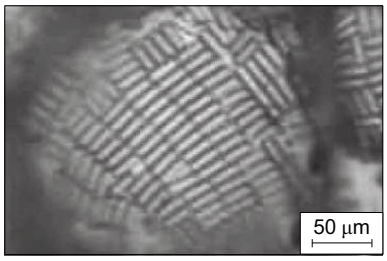


Figure 33. SEM image of rod-like epoxy resin particles on the surface of a water droplet in hexadecane.[138] Published with permission from the American Chemical Society.

during emulsification, the adsorbed particles did not detach from the droplet surface. The following should be mentioned: if the latex particles in the initial aqueous suspension were in the aggregated state, stable emulsions with both hexadecane and tetradecane as well as with the low-viscosity silicone oil were obtained.

Of course, a certain proportion of the particles are adsorbed on the droplet surface during preparation of the emulsion. However, particle adsorption does not stop after the preparation. Tarimala *et al.*[140] studied the rate of adsorption of polystyrene latex particles with sulfate groups (1.1 μm in diameter) on the surface of silicone oil droplets in water. The micrographs illustrating coverage of the droplet surface by particles over time are depicted in Fig. 34. The adsorption of latex particles on the droplet surface after the end of emulsion prepatation was relatively fast and ~1 min later it was substantially retarded; in this case, a relatively large part of droplet surface was not covered by particles.

Nallamilli *et al.*[141] prepared Pickering emulsions stabilized by polystyrene latex particles with opposite surface charges. The contact angles (measured through the aqueous phase) of polystyrene particles bearing amidine and sulfate groups amounted to $103.1 \pm 4.0^\circ$ and $116.1 \pm 12.3^\circ$, respectively. Usually, polystyrene latex particles with sulfate groups stabilize W/O emulsions, despite the fact that initially they were dispersed in the aqueous phase.[139] The charge values of the negatively and positively charged particles used by the authors[141] were high, and these particles did not stabilize emulsions if used not in a mixture. Oil-in-water emulsions with 50 vol.% fraction of dispersed phase were most stable to coalescence when the numerical ratio of oppositely charged particles was close to 1 : 1. The increase in the fraction of the dispersed phase to 80 vol.% at the same ratio of the particles resulted in phase inversion — oil-in-water emulsions were converted to water-in-oil ones.

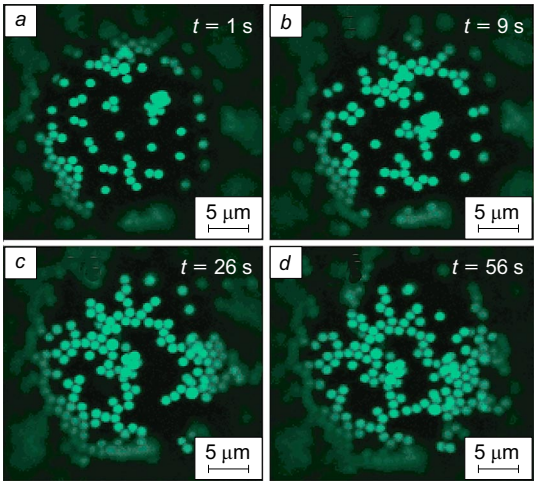


Figure 34. Confocal microscopy images illustrating the formation of the adsorption layer of polystyrene latex particles with sulfate groups on the surface of polydimethylsiloxane droplets (20 mPa s viscosity) in water.[140] The time (*t*) after the end of emulsion preparation is indicated. Published with permission from the American Chemical Society.

In various studies, Pickering emulsions were stabilized by various latex particles:

— polystyrene latex particles with surface-grafted polyethyleneimine molecules modified with 4-vinylbenzyl chloride,[142]

— polystyrene latex particles modified with chitosan,[143]

— particles consisting of a polystyrene core and a poly[(2-dimethylamino)ethyl methacrylate-*stat*-ethylene glycol dimethacrylate] shell,[144]

— *tert*-butylaminoethyl methacrylate – ethylene glycol methacrylate copolymer,[145]

— 2-diethylaminoethyl methacrylate – ethylene glycol methacrylate copolymer.[146]

Stabilization by the 10 – 40 nm nanoaggregates of poly(styrene-4-sulfonic acid-*co*-maleic acid) sodium salt afforded an emulsion of liquid paraffin in water with droplet size of ~200 nm.[147] Stable emulsions of dodecane in water with a droplet size from 50 to 250 mμ were obtained; stabilization was attained by using polymerosomes (block copolymer vesicles) of ~230 nm in diameter formed by cross-linked copolymer of glycerol monomethacrylate, 2-hydroxypropyl methacrylate and ethylene glycol dimethacrylate. If the copolymer was not cross-linked, the polymerosomes were destroyed during preparation of the emulsions, and copolymer molecules were adsorbed at the interface.[148]

5.3. Carbon nanoparticles

Graphene and graphene oxide particles, single- and multiwalled carbon nanotubes and soot were studied as stabilizers for Pickering emulsions.

Graphene oxide nanoparticles have a plate-like shape with a large number of carboxyl groups at the edges and numerous hydrophobic areas of non-oxidized benzene rings on the basal planes; therefore, these nanoparticles can be considered as amphiphilic.[149] SEM images of the monolayer formed by graphene oxide nanoparticles at the interface, and the surface pressure isotherm depending on the coverage of the interface by the particles, which illustrate the surface activity of graphene oxide particles, are presented in Fig. 35.[150]

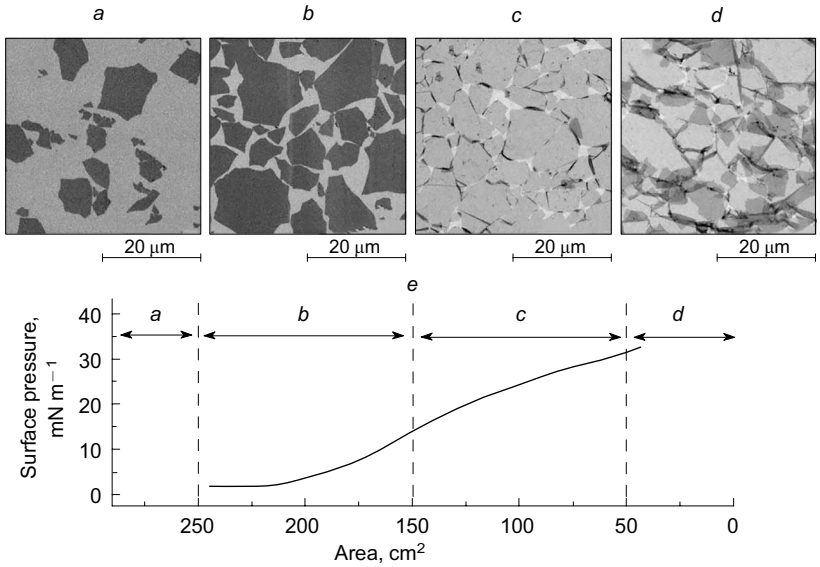


Figure 35. SEM images illustrating different degrees of packing of graphene oxide nanoparticles at the water/air interface: dilute monolayer with isolated nanoparticles (*a*), close-packed monolayer (*b*), partially overpacked layer (*c*), overpacked layer in which graphene oxide particles overlap (*d*) and surface pressure isotherm obtained by the Langmuir–Blodgett method (*e*), reflecting the states of the monolayer in Fig. *a*–*d*.[150] Published with permission from the American Chemical Society.

Graphene oxide nanoparticles with a size of several micrometres across the basal plane were used to stabilize emulsions of toluene in water.[149] When pH of the aqueous solution in the dispersion medium was 2, emulsions were stable for several months, despite the fact that the dispersed phase droplets were relatively large — several hundred micrometres.

Styrene-in-water emulsions with a droplet size of 200 nm were formed with graphene oxide nanoparticles for stabilization. A micrograph of such emulsion after styrene polymerization is shown in Fig. 36.[151]

Emulsions stabilized by graphene oxide nanoparticles were most stable if the dispersed phase was a substituted aromatic compound, *e.g.*, benzyl chloride.[152] A decrease in the emulsion stability was observed in the following series of dispersed phases: benzene > polar compounds (decanol or ethyl heptanoate) > non-polar or slightly polar compounds (hexane or cyclohexane). Upon the addition of electrolytes, the stability of emulsions increased, as graphene oxide nanoparticles were aggregated. A similar trend was identified by Thickett and Zetterlund,[153] who demonstrated that emulsions with styrene as the dispersed phase were more stable than the emulsions with methyl methacrylate. At low concentrations of graphene oxide nanoparticles, low pH, high oil to water ratio and high electrolyte concentrations, multiple W/O/W emulsions formed.[152]

Pickering emulsions were stabilized by graphene oxide nanoparticles modified with polyvinyl alcohol,[154] by silver nanoparticles [152, 155] and by iron oxide nanoparticles.[156]

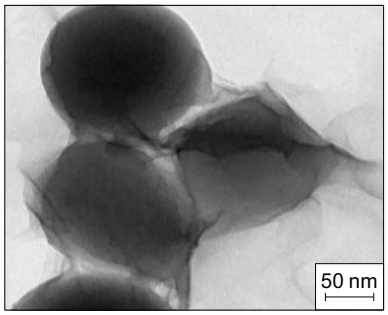


Figure 36. TEM image of the emulsion after polymerization of styrene droplets dispersed in water. The emulsion is stabilized by 2 mass % graphene oxide.[151] Published with permission from Elsevier.

Small graphene nanoparticles with a size of up to 10 nm across the basal plane that behaved as quantum dots were employed [157–159] to stabilize emulsions. For increasing the hydrophobicity of nanoparticles, they were subjected to heat treatment to remove a part of edge oxygen groups,[157] and their surface was modified with hexylamine [158] or dodecylamine.[159]

Carbon nanotubes can also serve as stabilizers for Pickering emulsions. The surface of a non-modified carbon nanotube is hydrophobic; therefore, they can stabilize W/O emulsions. Wang and Hobbie [160] were the first to use single-walled carbon nanotubes to stabilize emulsions of water in toluene.

When adsorbed at the interface in a water-in-1,2-dichlorobenzene emulsion, single-walled carbon nanotubes were bent along the interface and formed rings with an average diameter of 202 ± 76 nm (together with other structures such as slightly bent tubes, unclosed rings, irregular structures). The rings consisted of nanotubes combined into bundles comprising several tens to several hundreds of nanotubes.[161]

Briggs *et al.*[162] stabilized Pickering emulsions using up to 1 μm-long carbon nanotubes with a diameter of 6–9 nm and thickness of 3 to 6 carbon layers. Pristine nanotubes with a hydrophobic surface were used to stabilize water-in-dodecane emulsions. After nitric acid oxidation, the hydrophilicity of nanotubes increased, and O/W emulsions formed. Despite the presence of polar groups on the surface of oxidized carbon nanotubes, the attraction forces between them were relatively high, and a rigid network of adsorbed nanotubes formed on the interface and prevented droplets from coalescence.[163]

Baudouin *et al.*[164] described Pickering emulsions consisting of polyamide dispersed in the ethylene–acrylate copolymer; the emulsions were prepared at 180 °C, *i.e.*, at a temperature above the polymer melting point. Pristine multi-walled carbon nanotubes formed island structures on the droplet surface (Fig. 37).

It was shown [165] that carboxyl-terminated carbon black also has surfactant properties. Yu *et al.*[166] used carbonaceous microspheres to stabilize highly concentrated emulsions with styrene dispersion medium. The use of non-modified carbonaceous microspheres followed by polymer-

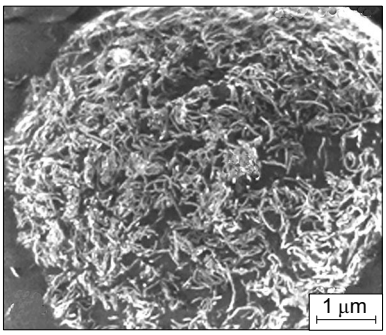


Figure 37. SEM image of the freeze-fractured emulsion consisting of polyamide dispersed in the ethylene–acrylate copolymer and stabilized by 2 mass % multiwalled carbon nanotubes.[164] Published with permission from Elsevier.

ization of the dispersion medium afforded closed-cell high-porosity polymer materials. When carbonaceous microspheres were modified with sorbitan monooleate, materials with interconnected pores were formed.

5.4. Hydroxyapatite particles

Hydroxyapatite particles are of interest for stabilization of Pickering emulsions, since they can be used to prepare microspheres and microfibres of biocompatible polymers, most often, polylactic acid polymers. These microspheres and microfibres are promising for the use in bone tissue reconstruction due to high adhesion of cells, including fibroblasts, to the hydroxyapatite shell.

Fujii *et al.*[167, 168] described emulsions with a dichloromethane solution of polylactic acid as the dispersed phase stabilized by hydroxyapatite nanoparticles of 40 nm in size. Polylactic acid microspheres coated by hydroxyapatite nanoparticles were formed upon evaporation of dichloromethane. Emulsions with polylactic acid solution in a mixture of dichloromethane and dimethylformamide as the dispersed phase were used for electrospinning of microfibres.[169]

The stability of Pickering emulsions with polylactic acid and hydroxyapatite nanoparticles depended on the pH of the dispersion medium. At pH 5, the emulsions were highly unstable; when pH increased from 7 to 10, the emulsion stability increased. If the concentration of polylactic acid in the dispersed phase was 5 mass %, the type of emulsion did not change within this pH range. In the case of polylactic acid concentration of 2 mass %, phase inversion took place with increasing pH in this range: an O/W emulsion was converted to a W/O emulsion.[170]

The use of rod-like hydroxyapatite nanoparticles of ~410 nm length and ~80 nm in diameter resulted in the formation of stable emulsions with methyl myristate dispersed phase. If the dispersed phase consisted of hexane, dodecane, chloroform, toluene, undecanol or dichloromethane, the emulsions stabilized by hydroxyapatite nanorods broke down within 24 h.[171]

Cooling of Pickering emulsions obtained under hydrothermal conditions gave biodegradable polymer microspheres. In these emulsions, dispersed phase droplets consisted of a polycaprolactone and poly(L-lactide-co-ε-caprolactone) melt and were stabilized by hydroxyapatite nanoparticles.[172]

Highly porous materials were obtained from highly concentrated W/O emulsions with hydroxyapatite nanoparticles. The dispersion medium of these emulsions was a solution of lactic acid–glycolic acid copolymer in dichloromethane. Evaporation of dichloromethane from the dispersion medium yielded a highly porous polymer nanocomposite.[173] Sun *et al.*[174] fabricated a highly porous material by polymerization of dopamine in the dispersion medium of emulsions stabilized by hydroxyapatite nanoparticles.

5.5. Clay particles

Particles of layered silicates, montmorillonite and laponite, are used most often to stabilize Pickering emulsions. Montmorillonite nanoparticles have a plate-like shape, ~200 nm length and 1 nm thickness. Laponite RD nanoparticles are 1 nm-thick discs of 30 nm in diameter. They are hydrophilic, have a negative surface charge, and are aggregated in aqueous solutions. It was shown that these particles stabilize O/W emulsions due to both the adsorption of clay nanoparticles on the droplet surface and the formation of a three-dimensional gel-like network in the emulsion dispersion medium.[64, 65] If laponite nanoparticles are in the flocculated state, the most stable emulsions are formed.[78]

Mica particles with a diameter of 8 μm and a thickness of 50 nm modified with polymethylmethoxysiloxane were used to prepare emulsions of water in silicone oil.[175] The addition of more water induced phase inversion to give an O/W emulsion; this was attributed to a change in the structure of aggregates formed by mica particles.

Dodecane emulsions in sea water were obtained using montmorillonite particles modified with bis(2-hydroxyethyl)oleylamine. The emulsions were stable even at a low particle concentration such as 0.1 mass %. Phase inversion to give a W/O emulsion took place as the amounts of bis(2-hydroxyethyl)oleylamine and montmorillonite increased.[176]

An increase in the stability of liquid paraffin-in-water emulsions was observed in the presence of laponite particles in the aqueous phase and paraffin wax in the organic phase.[177] Whitby *et al.*[178] studied dodecane-in-water emulsions containing laponite in the dispersion medium and oil-soluble compounds solid at room temperature and possessing amphiphilic properties as the dispersed phase. In the presence of octadecylamine, synergistic effect appeared, and the droplet size decreased. In the presence of stearic acid, antagonistic effect was manifested, and coalescence took place in the emulsions. Most likely, the difference in the emulsion stability was related not to the difference between the amphiphilic properties of oil-soluble additives but rather to the size of crystals formed by these compounds during the preparation and subsequent cooling of the emulsions.

Sunflower oil-in-water emulsions stabilized by illite particles with a size <2 μm were stable for more than three weeks.[179] Lu *et al.*[66] reported data on the stability of toluene emulsions in water containing several micrometre-long needle-shaped palygorskite particles with a diameter of 20–50 nm. The emulsions were stable in the pH range from 1.4 to 11.4, in particular due to the formation of a three-dimensional gel-like network of aggregated particles in the dispersion medium.

5.6. Starch particles

Since Pickering emulsions are being actively investigated for food industry applications, numerous publications are devoted to stabilization of the emulsions by biocompatible particles.[13, 20, 180] A typical example are spherical or elliptical natural starch particles. They are hydrophilic; the hydrophobicicity of the particles can be increased by esterification of octenylsuccinic anhydride.[9, 16, 181] Stable emulsions of corn oil in water were formed in the presence of

crystalline particles of esterified sago starch.[182] Comparison of the sunflower oil emulsions stabilized by various starch particles (rice, waxy maize, wheat and potato starch) demonstrated that rice starch-containing emulsions are most stable.[183] Emulsions containing native particles of rice starch, waxy maize starch and wheat starch were obtained, while attempts to prepare emulsions containing native potato starch particles failed.[184]

A comparison of emulsions of canola oil and tocoferol stabilized by amaranth starch particles (native and modified *via* esterification with lauroyl chloride) was reported.[185] The stabilization by modified starch particles resulted in the formation of emulsions with smaller droplets of the dispersed phase, which were hence more stable.

The use of sweet potato starch and corn starch particles of 100 to 220 nm in diameter afforded the most stable emulsions. When smaller or larger particles were used, the stability of emulsions decreased.[186]

If the emulsion was heat-treated, the particles adsorbed on the surface of oil droplets swelled. As a result, the particle shell became more compact and represented a continuous layer on the surface (Fig. 38). This was favourable for increasing the emulsion stability, but simultaneously the rate of material transport through this layer decreased. The degree of swelling of starch particles adsorbed on the droplet surface could be controlled by varying the temperature and duration of heating.[187, 188]

Saari *et al.*[189] observed a similar effect upon gelation of starch particles in emulsions with $CaCl_2$ in the dispersion medium at room temperature. After 30 min, a continuous layer formed on the droplet surface.

The use of rice starch particles gave rise to highly concentrated emulsions with a 0.75–0.85 fraction of the oil dispersed phase.[190]

Poly(butyl methacrylate) nanocomposite particles were obtained by polymerization of the dispersed phase of an emulsion consisting of the monomer and stabilized by starch particles.[191]

5.7. Cellulose particles

The first study[192] dealing with stabilization of Pickering emulsions by microcrystalline cellulose particles was published in 1986. However, cellulose nanocrystals with a length from 70 nm to several micrometres and a thickness from 5 to 20 nm, are more efficient emulsifiers.[8, 193] Due to high surface charge and, hence, electrostatic repulsion, cellulose nanocrystals are weakly adsorbed on the surface of dispersed phase droplets in emulsions with distilled water. The addition of electrolytes in low concentrations reduces the surface charge, and cellulose nanocrystals are adsorbed to form a denser surface layer.

The stabilizing ability of nano- and microparticles of cellulose depends on the type of plant material and the method used to extract cellulose from the plant.[12] When hexadecane droplets in water were stabilized by 200 nm-long needle-shaped nanocrystals of cotton cellulose with a diameter of 16 nm, more stable emulsions with smaller droplets were obtained than in the case of stabilization by 19 nm long granules with a diameter of 11 nm.[194]

Emulsions with the dispersed phase of coconut oil and canthaxanthin are more stable when stabilized by cotton cellulose nanocrystals with a length of 112 nm than in the case of ~1.2 μm-long bacterial cellulose particles.[195] The micrographs of polystyrene particles that were formed upon polymerization of styrene-in-water emulsions stabilized by cellulose nanocrystalss of various origin (5 g L^{-1} concentration) are presented in Fig. 39.[196] Using stabilization with bacterial cellulose nanocrystals, emulsions of hexadecane in water with a similar droplet size distribution were produced.[197]

Kalashnikova *et al.*[196] showed that the minimum coverage of the droplet surface by cellulose nanocrystals required for the formation of emulsions is ~44% for of Cladophora cellulose, ~60% for bacterial cellulose and ~84% for cotton cellulose. The nanocrystal length varied from 189 nm for cotton cellulose to 4 μm for cladophora cellulose; the diameter was 13–20 nm. The emulsions were more efficiently stabilized by small nanocrystals of cotton cellulose than by larger ones. The latter could not be completely adsorbed on the droplet surface and attached simutaneously to two droplets, which resulted in flocculation of droplets in the emulsion. This is a typical behaviour of bacterial cellulose particles and, to a higher extent, for cladophora cellulose ones (see Fig. 39 *c*,*f*).

Meanwhile, at lower concentrations of needle nano- and microcrystals of cellulose in a certain range of the solution ionic strength, the aggregation of crystals can take place in the dispersion medium, resulting in the formation of a gel-like network, which provides emulsions with additional sedimentation stability.[67–69]

The W/O Pickering emulsions were obtained using hydrophobized cellulose. For example, water-in-toluene

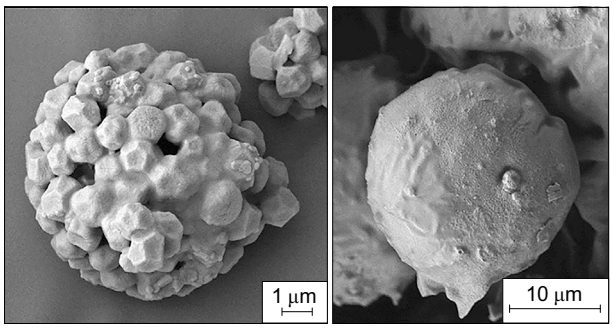


Figure 38. SEM images of the initial emulsion (*a*) and this emulsion after heat treatment at 70 °C for 1 min (*b*) illustrating swelling of the layer of starch particles on the oil droplet surface.[188] Published with permission from Elsevier.

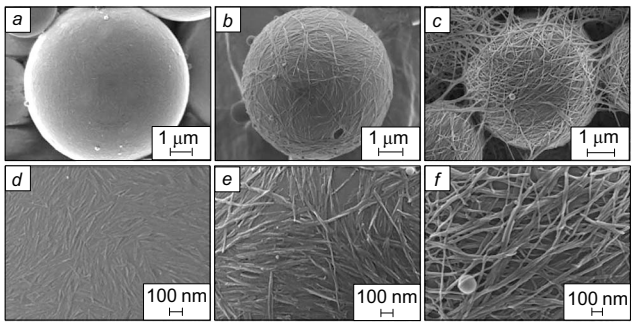


Figure 39. SEM images of polystyrene particles with a shell of cellulose nanocrystals derived from cotton (*a*, *d*), bacteria (*b*, *e*) and cladophora (*c*, *f*).[196] Published with permission from the Royal Society of Chemistry.

emulsions were formed in the presence of cellulose nanocrystals modified with cinnamic acid [198] or carboxylic acids.[199] Highly concentrated emulsions of water in toluene, cyclohexane or styrene with up to 89 vol.% fraction of the dispersed phase were prepared using microcrystalline cellulose modified with stearoyl chloride.[200]

Emulsions with Miglyol 812 medium-chain triglycerides as the dispersed phase were stabilized by a mixture of 170 nm-long cellulose nanoparticles of 17 nm in diameter and round-shaped quinoa starch particles with a size of 1.7 μm in 1 : 1 mass ratio. These emulsions were more stable to coalescence and sedimentation than those obtained with a single type of particles. The higher stability was attributed to the fact that the starch particles created a steric barrier that prevented coalescence. Possibly, cellulose nanoparticles on the droplet surface affected the Ostwald ripening.[201]

Oil-in-water emulsions stabilized by composite nanoparticles consisting of multiwalled carbon nanotubes and cellulose [202] or magnetite and cellulose [203] were reported.

5.8. Lipid particles

Stabilization of emulsions by lipid particles is mainly in demand in the food industry. For example, emulsions of water in soybean oil containing tristearin, palm stearin or palm oil crystals were obtained, but their stability was moderate.[204]

Emulsions containing canola oil as the dispersed phase and glycerylstearyl citrate particles of ~152 nm in diameter with a high ζ-potential (−49 mV) were stable for >6 months.[205, 206] A micrograph of this emulsion is shown in Fig. 40.[206]

Sunflower oil-in-water emulsions were stable to coalescence for long periods of time at a full coverage of the interface by ~170 nm tripalmitine particles modified with sodium caseinate.[207] The polarity of tripalmitine particles depended on the type of surfactant used for modification and decreased in the following order: whey protein isolate > soybean lecithin > soybean lecithin + Tween 20 > Tween 20 > polyglyceryl-polyricinoleate > no surfactant. Hence, lipid particles with a whey protein isolate were able to stabilizy sunflower oil-in-water emulsions. In the presence of lipid particles modified with soybean lecithin, O/W emulsions formed, but they were highly unstable. In the presence of lipid particles with soybean lecithin and Tween 20, W/O emulsions with a droplet size up to 30 μm were formed. Water-in-oil emulsions highly stable to coalescence with a dispersed phase droplet size of 5–15 μm were formed by using tripalmitine particles modified with Tween 20 or polyglyceryl-polyricinoleate or these lipid particles without surfactant modification.[208, 209]

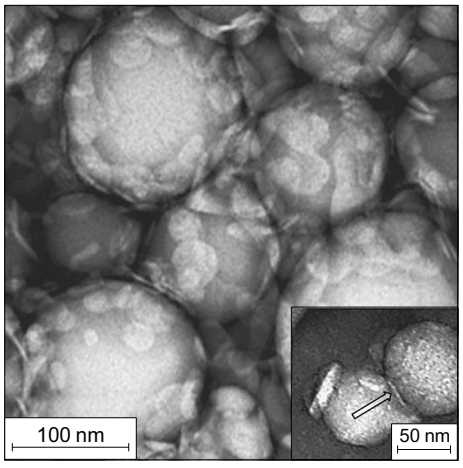


Figure 40. TEM image of an emulsion stabilized by glyceryl stearate citrate lipid particles.[206] The arrow in the inset marks the location of the lipid particle between the neighbouring droplets, which corresponds to a monolayer separating the particles (see Section 3.1). Published with permission from Elsevier.

Lipid particles consisting of Suppocires C (a mixture of $C_{10}-C_{18}$ fatty acid mono-, di- and triglycerides) modified with surfactant KolliphorsHS15 (a mixture of polyethylene glycol 660 and polyethylene glycol 660 12-hydrostearate, solid below 20 °C), were used to stabilize nanoemulsions with the LabrafacsWL 1349 dispersed phase (a mixture of medium-chain triglycerides).[210]

Corn oil droplets with added whey protein isolate, which have a positive surface charge, were stabilized by octadecane lipid particles modified with sodium dodecyl sulfate and, hence, having a negative surface charge.[211]

Zafeiri *et al.*[212] studied lyophilization and the subsequent resuspension of lipid particles of glyceryl tristearate or cetyl palmitate modified with sodium caseinate or Tween 80. Stabilization by sodium caseinate-modified lipid particles gives sunflower oil-in-water emulsion with droplet size of 8–15 μm. The droplet size did not change upon lyophilization and the subsequent resuspension.

Soybean oil-in-water emulsions stabilized by phytostyrene microparticles were obtained. An increase in the concentration of phytostyrene particles resulted in the formation of W/O emulsions.[213]

Gu *et al.*[214] described emulsions in which corn oil droplets were dispersed in water and stabilized by β-lactoglobulin. These droplets had a positive surface charge. After pectin modification, the surface charge of the droplets changed to negative. Then the emulsion of pectin-modified droplets with s size of 0.6 μm was mixed with an emulsion in which the droplets were not modified and had a 0.2 μm size. The smaller positively charged droplets were adsorbed on the surface of the larger, negatively charged ones. A relatively stable system formed if the concentration of the smaller droplets was sufficient to completely cover the surface of the larger droplets.

Pickering emulsions stabilized by particles of drugs are known. For example, Capmul® MCM C8 (caprylic acid monoglyceride) emulsions stabilized by ~340 nm silybin particles, consisting of a mixture of flavonolignans extracted from milk thistle, were obtained.[215] Sunflower oil-in-water emulsions were stabilized by amorphous curcumin particles [216] and flavonoid (rutin and naringin) particles.[217]

5.9. Microgel particles

Microgel particles are micrometre particles formed from a polymer gel.[218, 219] At temperatures below the critical solution temperature, microgel particles swell;[220] they become porous and are deformed.[14, 58, 221] Microgel particles of poly(*N*-isopropylacrylamide) and its copolymers are used, most often, to stabilize Pickering emulsions.[222] The first publication addressing this issue appeared in 2003.[223]

When the degree of cross-linking of polymer molecules was relatively low, the microgel particles had a spherical shape when located in the bulk of the dispersion medium and assumed a flattened or lens shape upon the adsorption at an interface in an emulsion (Fig. 41 *a*). As the degree of

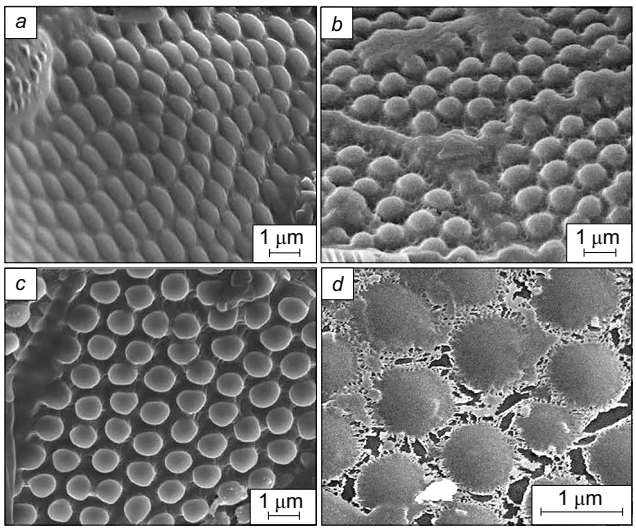


Figure 41. Cryo-SEM images of dodecane (*a*–*c*) and decane (*d*) droplets with adsorbed *N*-isopropylacrylamide–*N*,*N*′-methylenebis(acrylamide) copolymer microgel particles. Concentration of the *N*,*N*′-methylenebis(acrylamide) cross-linking agent, mol.%: 15 (*a*), 2.5 (*b*, *d*), 3.5 (*c*).[224] Published with permission from the Royal Society of Chemistry.

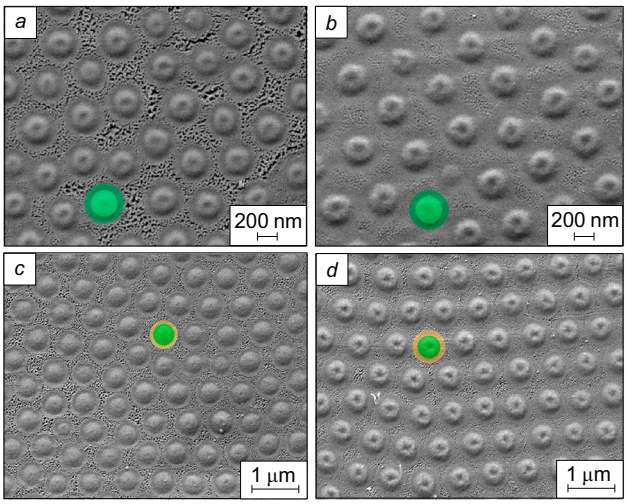


Figure 42. Cryo-SEM images of microgel particles at the water/heptane interface; view from the organic phase. Particles consisting only of the core (*a*, *b*) and core–corona structure (*c*, *d*); pH 3 (*a*, *c*), 9 (*b*, *d*). The core is shown in green and the corona is shown in yellow.[227] Published with permission from the American Chemical Society.

cross-linking increased, the shape of the microgel particles adsorbed at the interface became more and more spherical (see Fig. 41 *b*,*c*). It can be seen (see Fig. 41 *d*) that the filaments in the peripheral areas of the neighbouring deformed particles overlapped.[224]

The more deformable the microgel particles were upon adsorption, the higher was the tendency of the dispersed phase droplets in this emulsion for flocculation.[225] In relation to emulsions stabilized by poly(*N*-isopropylacrylamide) microgel particles with the same degree of cross-linking, but with different size, it was shown that particles with a size of 760 nm were more deformable than 250 nm particles. Thus, emulsions stabilized by larger particles were more flocculated.[226]

If the layer of the adsorbed microgel particles was dense and homogeneous, the probability of droplet flocculation to give a monolayer of bridging particles decreased. This situation occurred when stabilization was performed by small and derformable particles, which were more rapidly adsorbed at the interface; in this case, the adsorption layer was faster rearranged into a close-packed layer with a high degree of overlap of the peripheral areas of the microgel particles. The adsorption of larger particles with a greater degree of cross-linking was slower. Hence, the adsorption layer was less homogeneous due to the non-uniform core and shell size of the adsorbed particles, and this promoted the flocculation of droplets of the dispersed phase.[221]

Geisel *et al.*[227] obtained two types of microgel particles, those formed by the *N*-isopropylacrylamide–methacrylic acid copolymer and similar particles with a poly(*N*-isopropylacrylamide) shell. At pH 3, the particles without a shell were almost uncharged; at pH 9, they had a negative surface charge. As the pH changed from 3 to 9, the particle size increased from 276 to 362 nm. The size of particles with the poly(*N*-isopropylacrylamide) shell changed to a lesser extent upon the change in the pH from 3 to 9, namely, from 378 to 400 nm, that is, the degree of their swelling increased insignificantly. The surface charge did not change with increasing pH of the aqueous phase either. The particles with and without a shell both had a higher degree of cross-linking at the centre and a lower one at the periphery, *i.e.*, they had a core–corona morphology. When examined from the aqueous side, all particles were noted to be considerably deformed at the water/oil interface, in particular, the core was flattened and the corona with a low cross-linking degree was stretched (Fig. 42). Upon flattening, the particles were slightly immersed into the organic phase. On the side of the aqueous phase, the particles retained a bulk shape, which depended on the pH of the aqueous phase; thus, the adsorbed particles had a lens shape.

Massé *et al.*[228] emphasized that the charge distribution at the centre and on the surface of microgel particles did not affect significantly their ability to be adsorbed at the interface in the emulsion. Irrespective of the degree of swelling, microgel particles were adsorbed on the oil droplets to form a hexagonal packing. Thus, stabilization of emulsions *via* the adsorption of these particles depends on the viscoelastic properties of the interface with the microgel particles rather than on the electrostatic repulsion of the droplets.[229] The results of interfacial rheological measurements showed a correlation between the interfacial elasticity and stability of emulsions.[230]

5.10. Particles of bioactive polymers

Most of bioactive polymer particles are micro- and nanogel particles. Their main difference from the particles described in the previous Section is that they consist of natural polymers used in food industry. Protein and polysaccharide particles are used for stabilization of emulsions.[15,17] The starch and cellulose particles considered above also refer to bioactive polymer particles.

Milk can be regarded as a Pickering emulsion stabilized by casein micelles.[218] Despite this name, casein micelles are not conventional micelles formed by amphiphilic molecules. They are highly hydrated particles with an average diameter

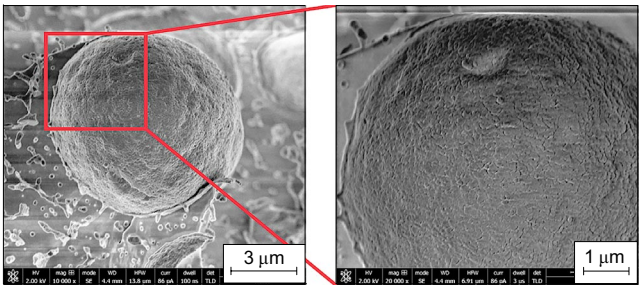


Figure 43. Cryo-SEM images of a medium-chain triglyceride droplet in an emulsion stabilized by gel-like casein particles of ~110 nm in size.[231] Published with permission from Elsevier.

of ~200 nm and consist of various phosphorylated milk proteins, caseins and calcium phosphate nanoclusters.

Wang *et al.*[231] studied emulsions of medium-chain triglycerides in water stabilized by genipin-cross-linked gel nanoparticles of casein with a size of ~18 nm and gel particles with a size of ~110 nm consisting of calcium-cross-linked casein nanoparticles subsequently cross-linked by genipin (Fig. 43). After 30 days of storage, the average size of dispersed phase droplets stabilized by smaller casein nanoparticles almost did not change: the initial diameter was 1.48 ± 0.06 μm, while 30 days later, the diameter was 1.51 ± 0.08 μm. In emulsions with larger gel casein particles, the average droplet size increased during 30 days from 3.66 ± 0.07 to 4.27 ± 0.51 μm.

In soybean oil-in-water emulsions stabilized by 100–400 nm-long β-lactoglobulin fibrils, dispersed phase droplets with a size of 11–19 μm did not coalesce for 56 days at room temperature.[232]

Canola oil-in-water emulsions were stabilized by zein particles with a size of ~136 nm.[233] When zein particles were modified with sodium caseinate, their adsorption on the droplet surface increased; hence, emulsion stability was enhanced. When soybean oil emulsions were stabilized by zein particles with a size of 360 nm modified with sodium stearate, the resulting emulsions were stable to flocculation and coalescence.[234]

Corn oil-in-water emulsions with ~400 nm particles of quinoa protein isolate were stable to flocculation at a particle concentration >1 mass %.[235] In the case of stabilization of corn oil droplets by 2 mass % whey protein isolate particles of 200–500 nm in size, stable emulsions were formed only at pH above or below the protein isoelectric point and at an ionic strength of the dispersion medium not exceeding 10 mmol L^{-1} (Ref. 236).

Zhu *et al.*[237] studied the stability of soy oil emulsions in freezing–thawing processes. Emulsions containing heat-treated soy protein isolate particles (~178 nm in size) and whey protein isolate particles (~266 nm in size) were more stable than the emulsions stabilized by the same particles (92 and ~130 nm in size, respectively) without heat treatment. In the presence of NaCl in the dispersion medium, the stability of the emulsions to freezing–thawing increased.[238]

Soybean oil emulsions stabilized by the particles of pea protein isolate of 40–500 nm in size were stable at pH 3.[239,240] The rate of release of encapsulated β-carotene decreased as the dispersed phase fraction increased to 0.6; the stability of emulsions under conditions mimicking the process of digestion increased.

Sarkar *et al.*[241] investigated emulsions containing lactoferrin particles of 100 nm in diameter and lactoferrin–inulin particles with a diameter of 116 nm. It was shown that in the acidic gastric medium *in vitro*, the adsorbed particles create a barrier that retarded the diffusion of pepsin and simultaneously prevented coalescence of droplets in the Pickering emulsions.

Highly concentrated emulsions with hexane or sunflower oil (80 vol.%) as the dispersed phase stabilized by gelatine microgel particles of ~200 nm in size have been prepared. The emulsions were stable at pH values differing from the isoelectric point.[242] Emulsions containing 50 vol.% dispersed phase were stabilized by gelatine microgel particles modified with glucomannan and tannic acid. The minimum concentration of the particles needed for the formation of emulsions of medium-chain triglycerides in water was 0.1 mass %.[243]

Whey protein isolate particles of 150 nm in size were used to stabilize W/W emulsions in which one aqueous phase contained waxy maize starch, while the other phase was an aqueous solution of the ceratonia siliqua gum.[244]

Pickering emulsions stabilized by chitosan particles are being actively studied.[10] Chitosan is insoluble in water at pH above its $pK_a = 6.5$ and forms nanometre-sized particles or micrometre-sized flocculated aggregates.[245] At pH 6.5, the size of gel-like chitosan particles is 82–84 nm.[245,246] Liquid paraffin, hexane, toluene, dichloromethane,[245] medium-chain triglycerides,[247] corn oil [246] and sunflower oil [248] emulsions in water stabilized by chitosan particles were prepared. The emulsions with a droplet size of 1.7 μm were stable for >5 months.[246] Chitosan nanoparticles modified with lecithin [249] and tripolyphosphate [250] were used to stabilize the Pickering emulsions.

Highly concentrated hexadecane-in-water emulsions with a dispersed phase fraction of 80 vol.% were stabilized by rod-shaped chitin nanocrystals with a length of 160 nm and a thickness of 16 nm.[251] In corn oil-in-water emulsions with a dispersed phase fraction of 10 mass %, chitin nanocrystals were adsorbed on oil droplets and formed a gel-like network in the bulk of the dispersion medium. Emulsions with a chitin concentration of 1 mass % were stable for 6 months.[70]

Owing to their biocompatibility and high stability, Pickering emulsions stabilized by bioactive polymer particles are used in food and pharmaceutical industry [11,18,252] and for targeted delivery of hydrophilic and lipophilic bioactive compounds.[19]

5.11. Particles of biological origin

Pickering emulsions can be obtained using non-traditional particles such as cells of microorganisms. The baker's yeast cells *Saccharomyces cerevisiae* and the lactic acid bacteria *Lactobacillus acidophilus* and *Streptococcus thermophilus* inactivated by heat treatment were studied as stabilizers for O/W emulsions.[253]

The *L. acidophilus* cells had a rod-like shape and were <5 μm long. Their adsorption resulted in the most complete (>90%) coverage of the olive droplet surface in the emulsion (Fig. 44). Upon the adsorption of the round-shaped *S. cerevisiae* cells with a diameter of <10 μm, the surface coverage was ~80%. The *Streptococcus thermophilus* cells were the smallest (<1 μm in diameter) and the surface coverage of the droplets did not exceed 65%. Correspondingly, emulsions stabilized by the *L. acidophilus* and *Saccharomyces cerevisiae* cells were more stable.

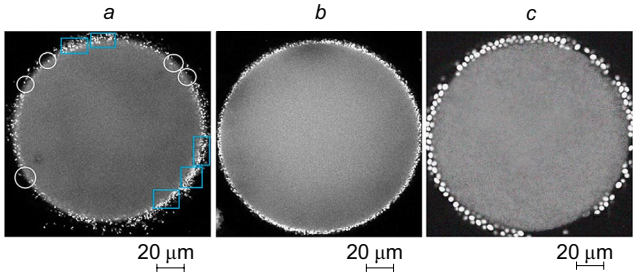


Figure 44. Confocal microscopy images of separate droplets of olive oil-in-water emulsions stabilized by *Streptococcus thermophilus* (*a*), *L. acidophilus* (*b*) and *Saccharomyces cerevisiae* (*c*).[253] Published with permission from Elsevier.

The yeast cells grown in the medium containing paraffin oil, water and inorganic salts stabilized the system with the formation of a Pickering emulsion.[254] Similar results on the cell adsorption at the interface between hexadecane, octane or *p*-xylene and water were obtained upon the growth of *Acinetobacter calcoaceticus*.[255]

Stable emulsions were formed using stabilization by *A. venetianus* cells, which surrounded droplets of hexadecane in water as a three-dimensional network.[41] The stability of hexadecane-in-water emulsions stabilized by the *Saccharomyces cerevisiae* yeast cells and the effect of various factors on phase separation of these emulsions were studied by Furtado *et al*.[256]

The yeast cells modified with oleic acid were used to stabilize toluene-in-water emulsions containing magnetite nanoparticles in the dispersed phase.[257] Emulsions of tetradecane in water were obtained when electrostatically bound associates of chitosan molecules with *Escherichia coli*, *Staphylococcus aureus*, *Bacillus subtilis*, *Bacillus cereus* and *Lactobacillus sakei* cells were adsorbed at the interface.[258]

5.12. Janus particles

Janus particles were named after the two-faced Roman god.[259] The surface of a Janus particle consists of two parts differing in the chemical composition or physical properties such as hydrophobicity, magnetic and optical properties and so on. Janus particles can consist of polymers, lipids or inorganic compounds.

If the particle consists of two parts differing in the hydrophobicity, this particle is considered to possess amphiphilic properties.[259] These particles are arranged at oil/water interfaces in the same way as surfactant molecules.[31–33]

On the one hand, Pickering emulsions can be used to obtain Janus particles and, on the other hand, they can be stabilized by such particles.[21]

Most often, Janus particles are obtained by changing the composition or by functionalizing a part of the surface of homogeneous particles. In Pickering emulsions, a part of a particle at the interface is immersed into the organic phase and, hence, it is protected from the chemical action of the aqueous phase. If the dispersed phase is an oil with a relatively high melting point, such as paraffin, cooling of a Pickering emulsion results in solidification of the parts of particles immersed into the organic phase, which prevents the particle migration over the interface or rotation. Meanwhile, the part of the particle located in the aqueous phase can be chemically modified (Fig. 45). This method is suitable for preparing large amounts of Janus particles.[260]

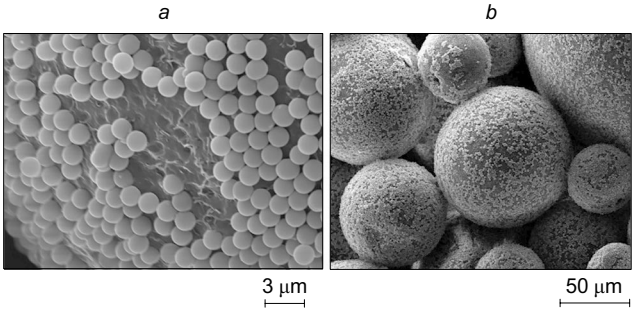


Figure 45. SEM images of SiO_2 particles partially immersed and fixed on a paraffin surface (*a*) and SiO_2 particles on the paraffin surface after 3-aminopropylsilane modification (*b*). The diameter of SiO_2 particles is 1.5 μm.[260] Published with permission from the American Chemical Society.

Janus particles made of silica were prepared in such a way that a half of their surface was covered by gold and modified with octadecanethiol to make it hydrophobic.[261] At a water/dodecane interface, these particles were immersed into both the aqueous and organic phases (Fig. 46 *a*). Almost all Janus particles were adsorbed on the droplet surface in a W/O emulsion (Fig. 46 *b*), which confirms that they were surface active.

Janus particles were formed when a part of the surface of a silica particle was modified with 3-aminopropyltrimethoxysilane and gold nanoparticles were then deposited on the modified part of the surface (Fig. 47 *a*).[262]

Water-in-oil and oil-in-water emulsions were stabilized by particles consisting of an aqueous gel of alginate and shellac (Fig. 47 *b*),[263] polystyrene and poly[3-(ethoxysilyl)-propyl methacrylate] (Fig. 47 *c*),[264] polystyrene and poly(2-vinylpyridine),[265] copolymer of methacrylic acid, methyl methacrylate and butyl acrylate and copolymer of methacrylic acid and methyl methacrylate.[266] Stabilization of W/O emulsions was attained by silica particles half of which were coated by gold nanoparticles.[267]

A micrograph of a W/O emulsion stabilized by three-component Janus particles, one part of which consisted of the styrene–divinylbenzene copolymer, and the other part consisted of silica-coated Fe_3O_4, is shown in Fig. 47 *d*.[268]

Stable O/W emulsions were obtained using Janus particles one part of which was composed of the styrene–polyvinyl alcohol copolymer and the other part of which

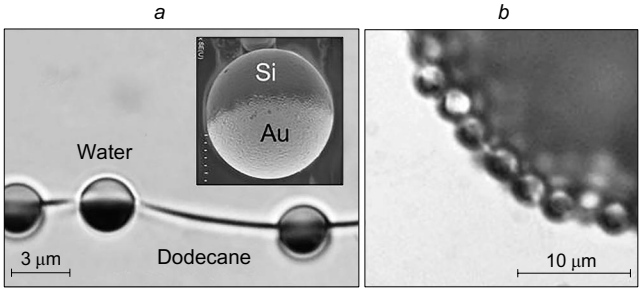


Figure 46. Micrographs of Janus particles at the water/dodecane interface (*a*) and W/O emulsion droplets stabilized by these particles (*b*).[261] The white band in the lower part of the particle in Fig. *a* is the hydrophobic Au; the dark part is hydrophilic SiO_2; the inset shows the SEM image of Janus particles. Published with permission from the American Chemical Society.

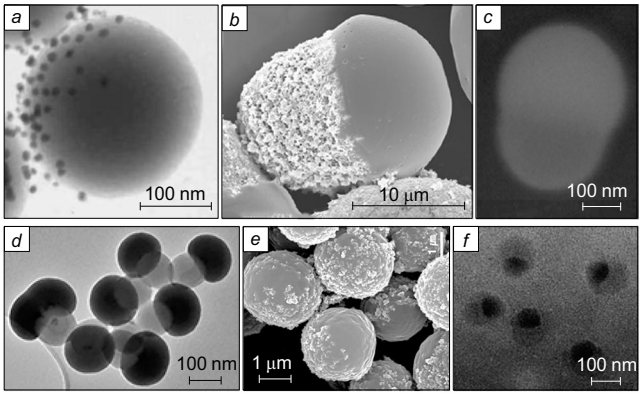


Figure 47. Micrographs of Janus particles consisting of silica and gold nanoparticles on a part of their surface (*a*),[262] alginate (porous part) and shellac (continuous part) (*b*),[263] polystyrene and poly[3-(ethoxysilyl)propyl methacrylate] (*c*),[264] styrene–divinylbenzene copolymer and Fe_3O_4 with a silica shell (*d*),[268] styrene–polyvinyl alcohol copolymer and Fe_2O_3 nanoparticles on a part of their surface (*e*),[269] and a particle with the core composed of methyl acrylate–butyl acrylate copolymer and a shell partly consisting of 2-(dimethylamino)ethyl methacrylate–butyl acrylate copolymer and partly consisting of pentafluorostyrene–butyl acrylate copolymer (*f*).[270] Figs *a*, *d*, *f* are TEM images; Figs *b*, *c*, *e* are SEM images. Figure *a* is published with permission from Elsevier, Figs *b*–*f* are published with permission from the American Chemical Society.

consisted of polytetradecyl acrylate. The styrene–polyvinyl alcohol copolymer surface was decorated with Fe_2O_3 nanoparticles stabilized by polyvinylpyrrolidone (Fig. 47 *e*).[269] In a magnetic field, these emulsions broke down, while in the absence of a magnetic field, they could be redispersed.

Oil-in-water emulsions with an alkaline dispersion medium were stabilized by particles the cores of which consisted of the methyl acrylate–butyl acrylate copolymer, a part of the surface was coated by a shell of 2-(dimethylamino)ethyl methacrylate–butyl acrylate copolymer, while the other part was coated by the pentafluorostyrene–butyl acrylate copolymer (Fig. 47 *f*).[270]

Many authors emphasize that Janus particles can be used to obtain emulsions responsive to various stimuli (see Section 7).

6. Colloidosomes

The preparation of colloidosomes was first described in 1996.[271] The term colloidosomes was proposed in 2002 by Dinsmore *et al.*[272] by analogy with liposomes. Colloidosomes are capsules formed upon self-assembly of colloidal particles at the interface. These are hollow shells the permeability and elasticity of which can be controlled by varying the size of particle being adsorbed and the matrix. These structures can be used for encapsulation of active ingredients.[273]

Currently, there are various methods for the fabrication of colloidosomes: self-assembly on the droplet surface in Pickering emulsions or on the surface of solid matrices; formation of capsules from liposomes with colloidal particles encapsulated in the space between the phospholipid chains. These methods are based on different self-assembly principles, but the resulting capsules have similar structures: they comprise a shell formed by one or several close-packed layers of colloidal particles.[274]

In this review, we consider the formation of colloidosomes by self-assembly of colloidal particles in Pickering emulsions. Liquid matrices have considerable advantages over solid ones, since the active substance can be encapsulated into the inner cavity of colloidosomes during the emulsion preparation.[24]

In the first study[271] where these structures were prepared, latex particles of 1 μm in diameter were deposited on octanol droplets with a diameter of 5–30 μm. Structures with a regular packing of particles on the droplet surface formed if the particle ζ-potential slightly exceeded 20 mV in magnitude. In this case, no flocculation of particles took place in the dispersion medium of the emulsions, and the adsorbed particles formed a close-packed layer on the droplet surface.

Dinsmore *et al.*[272] described capsules of polystyrene latex particles. They obtained colloidosomes from an emulsion with the droplets of the dispersed phase consisted of a vegetable oil and toluene in 1 : 1 ratio. The external aqueous phase was a mixture of glycerol and water also in 1 : 1 volume ratio. A micrograph of the dried capsule with a diameter of 10 μm, consisting of assembled 0.9 μm polystyrene particles is shown in Fig. 48. For binding the latex particles together, heat treatment at 105 °C for 5 min was carried out.

Connection of particles in colloidosomes is performed by processes such as thermal sintering, polyelectrolyte cross-linking on the external surface, gelling in the water core, polymerization on the external or internal surface and particle linking.[25]

Heat treatment at 50 °C was used to obtain colloidosomes from the particles of styrene–butyl acrylate copolymer[275] or methyl acrylate–butyl acrylate copolymer (Fig. 49 *a*).[276] Under solvothermal conditions, colloidosomes were formed from cubic particles of Fe metal-organic framework (Fig. 49 *b*).[277]

Colloidosomes were obtained from Pickering emulsions stabilized by styrene–methyl methacrylate copolymer particles. The dispersed phase of emulsions contained a copolymer of lactic and glycolic acids, which was deposited on the inner surface of the shell upon the removal of the dispersed phase and connected the particles.[278]

Colloidosomes were formed when polystyrene latex particles were adsorbed on acrylamide microgel droplets[279] and when magnetite nanoparticles were adsorbed on agarose gel droplets.[280] Hairy colloidosomes were obtained using agarose microgel particles with 10–70 μm-long

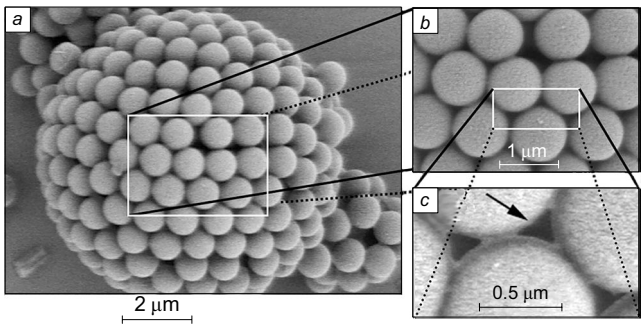


Figure 48. SEM image of a colloidosome formed by polystyrene latex particles (*a*); enlarged images of the delineated areas (*b*, *c*). The arrow in Fig. *c* points to a ~0.15 μm hole in the shell.[272] Published with permission from AAA Science.

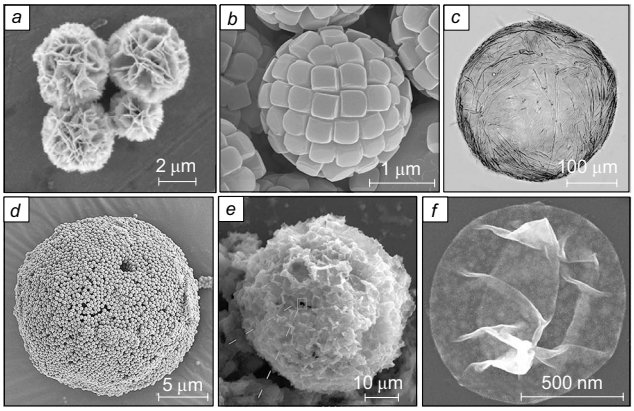


Figure 49. Micrographs of colloidosomes formed by silver-coated methyl acrylate–butyl acrylate copolymer particles (*a*),[276] Fe metal-organic framework cubic particles (*b*),[277] agarose microgel and cured epoxy resin nanorods (*c*),[281] spherical silica particles (*d*),[282] nanoparticles of double layered hydroxide modified with methyl orange (*e*) [283] and gold nanoparticles (*f*).[284] Figures *a*, *b*, *d*–*f* are SEM images, Fig. *c* is TEM image. Figures *a*, *b*, *c*, *f* are published with permission from the American Chemical Society, Figs *d* and *e* are published with permission from Elsevier.

cured epoxy resin microrods of 0.4–2.0 μm in diameter (Fig. 49 *c*).[281]

There are reported colloidosomes composed of laponite nanoparticles connected by polyethyleneimine cross-linking with polyethylene glycol diglycidyl ether;[285] cellulose nanocrystals cross-linked with silica;[198] silica particles connected by whey protein isolate (Fig. 49 *d*);[282] layered double hydroxide nanoparticles modified with methyl orange (Fig. 49 *e*);[283] gold nanoparticles connected by 11-[(ethoxycarbonylthiol)thio]undecyl methacrylate or 11-mercaptoundecyl methacrylate cross-linking (Fig. 49 *f*);[284] and polystyrene latex particles cross-linked with polyethyleneimine [142] or poly(glycerol monomethacrylate).[286]

In colloidosomes, binding took place upon oxidation of Cu_2O to give CuO particles consisting of ~9 nm-thick plates with a size of ~890 nm grown together (Fig. 50 *a*).[287] This gave colloidosomes with a size of ~250 μm (Fig. 50 *b*), which had a high catalytic activity owing to the large specific surface area of the stabilizing particles.

Formation of mono- and bilayer colloidosomes were reported.[288, 289] An emulsion of water (pH 1) in toluene was stabilized by silica nanoparticles with a diameter of 50 nm which were modified by octadecyltrimethoxysilane. Then a toluene solution of polyethoxysilane was added to the emulsion. Depending on the mass ratio of silica nanoparticles and water, monolayer (Fig. 51 *a*) or bilayer (Fig. 51 *b*) colloidosomes were obtained. The latter consisted of two layers of nanoparticles separated by a thin silica interlayer.

Williams *et al.*[290] described colloidosomes in colloidosomes formed from a multiple Pickering emulsion (Fig. 52). Water-in-oil-in-water emulsions were stabilized by silica nanoparticles modified with polyethyleneimine to different extents, which hence had different hydrophobicities. Nanoparticle layers were connected by cross-linking of polyethyleneimine chains with poly(ethylene glycol diglycidyl ether) or poly(propylene glycol diglycidyl ether).

Similar structures were prepared from oil-in-coacervate-in-oil multiple emulsions stabilized by silica nanoparticles

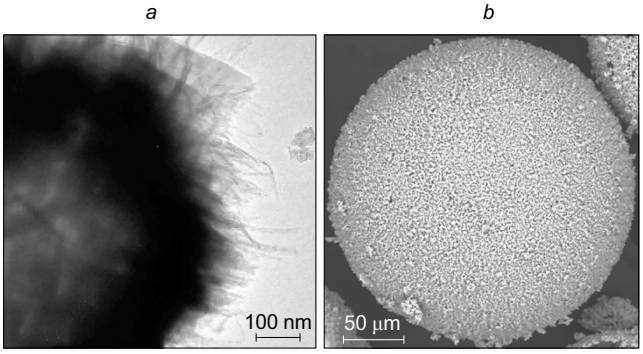


Figure 50. TEM image of CuO particles (*a*) and SEM image of colloidosome formed by these particles (*b*).[287] Published with permission from the American Chemical Society.

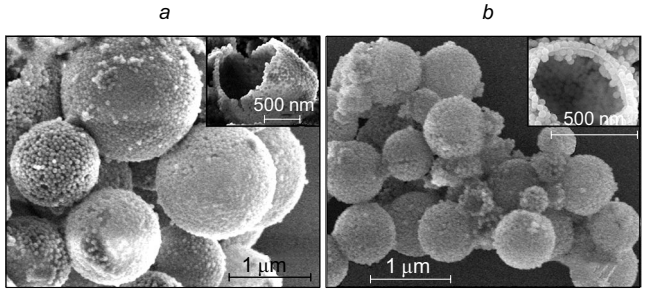


Figure 51. SEM images of mono- (*a*) and bilayer colloidosomes (*b*) obtained at mass ratios of silica nanoparticles to water of 0.2 (*a*) and 0.4 (*b*).[289] Published with permission from the American Chemical Society.

with different hydrophobicities connected by by tetramethoxysilane.[291]

Xu *et al.*[292] described doped colloidosomes (Fig. 53). Colloidosomes with a size of 2–15 μm were formed from phenol formaldehyde resin particles of ~450 nm in diameter. A ~900 nm particle with a core consisting of a gold (~70 nm in diameter) or silver (50 nm in diameter) nanoparticle and a phenol formaldehyde resin shell were incorporated in these colloidosomes.

The potential applications of colloidosomes include food, pharmaceutical and chemical industries. Initially, it was suggested that these systems could be used for encap-

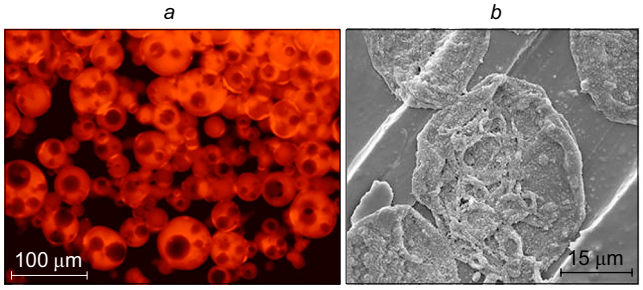


Figure 52. Confocal microscopy image of the W/O/W Pickering emulsion with 25 vol.% perfume oil and high content of aldehydes (*a*) and SEM image of the colloidosome-in-colloidosome system with silica particles after cross-linking (*b*).[290] Published with permission from the American Chemical Society.

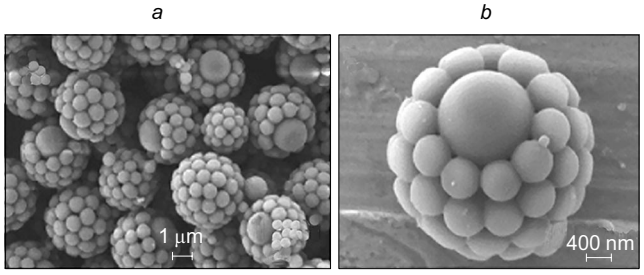


Figure 53. SEM images of colloidosomes consisting of phenol formaldehyde resin particles doped with a phenol formaldehyde resin particle with a silver nanoparticle in the core.[292] Published with permission from the American Chemical Society.

sulation and gradual release of active ingredients.[272] There are publications dealing with modelling of the diffusion rate of a substance encapsulated in the inner cavity of colloidosomes depending on the pore size and tortuosity of the diffusion path. For example, it was shown [293, 294] that in the case of diffusion across the monolayer shell of colloidosomes, the transport of small molecules almost does not depend on the size of particles that form the shell. However, in the close-packed thick layers, the rate of transfer considerably decreases with decreasing size of colloidal particles. The rate of release from colloidosomes was studied for aspirin,[295] caffeine,[295, 296] doxorubicin [276, 297] and fluorescein.[298] Colloidosomes were studied as containers for curcumin,[299] amylase,[300] cells and bacteria.[301–304]

The incorporation of magnetic nanoparticles into colloidosomes changes their transport properties, which makes it possible to accumulate nanoparticles in definite areas under the action of a magnetic field.[280] Colloidosomes can be used as parts of sensors that respond to the change of external characteristics such as temperature [305, 306] and pH of the medium.[307, 308] It was shown that colloidosomes can be used as catalysts,[309–311] sensors for ochratoxin A [312] and even artificial cells of living tissues.[313]

7. Stimuli-responsive Pickering emulsions

Depending on the potential application, it may be required that Pickering emulsions be stable for a long period of time, but lose stability under certain conditions. Such conditions are, for example, a change in the environmental temperature, pH or the ionic strength of the aqueous solution in which colloidosomes are dispersed, the action of light or magnetic field, *etc*.[27] Most often, external stimuli acting on Pickering emulsions change the following characteristics:

— contact angle of particles at the interface, resulting in particle migration into the dispersion medium; phase inversion of the emulsion is also possible;

— particle charge or droplet surface charge, resulting in electrostatic repulsion of the particle from the interface;

— degree of swelling of particles and, hence, the possibility of ion penetration into the inner areas of the particles.

7.1. Emulsions responsive to pH change in the aqueous dispersion medium

Among emulsions that respond to the change in the pH of the aqueous dispersion medium, most studied are those stabilized by microgel particles formed by polyacrylate derivatives that are hydrated in the acid medium and dehydrated in the alkaline medium. The effect of pH of the dispersion medium on the stability and breakdown of emulsions was studied by various researchers (see, for example, publications [144, 146, 229, 230, 270, 305, 307]).

The latex—microgel transition took place in the particles of 2-(diethylamino)ethyl methacrylate–ethylene glycol methacrylate copolymer cross-linked by divinylbenzene at pH < pK_a (pK_a = 6.9). Upon this transition, the particle size increased from ~220 to ~550 nm (Fig. 54). At pH 10, the particles existing in the latex state and having a negative surface charge stabilized emulsions of dodecane, sunflower oil, isononyl isononanoate or isopropyl myristate in water. Meanwhile, at pH 3, the particles existing as microgel had a positive surface charge; hence, they were desorbed from the interface and thus did not stabilize the emulsion. It was possible to carry out more than ten emulsification—demulsification cycles by changing the pH of the dispersion medium.[146]

Similar results were obtained when emulsions were stabilized by Janus particles with the core of the methyl acrylate–butyl acrylate copolymer, a part of the surface had a 2-(dimethylamino)ethyl methacrylate–butyl acrylate copolymer shell and the rest of the surface was covered by pentafluorostyrene–butyl acrylate copolymer. These emulsions were stable at pH 10. At pH 3, the particles were desorbed from the interface due to protonation of groups in poly[2-(dimethylamino)ethyl methacrylate].[270]

Water-in-water emulsions with a polyethylene oxide solution dispersed in a dextran solution or a dextran solution in a polyethylene oxide solution were obtained. The emulsions were stabilized by microgel particles of ethyl acrylate–methacrylic acid–butane-1,4-diol diacrylate terpolymer. When the pH was increased in a narrow range, the particle radius sharply increased from 60 to 220 nm at pH ~7. In the pH range from 5.0 to 7.5, the microgel particles were adsorbed at the interface, but only in the narrow pH range of 7.0–7.5, the emulsions were stable for more than a week.[314]

Most likely, the change in the microgel particle size and charge is not crucial for stabilization of emulsions. As shown by Brugger *et al.*,[230] in the emulsions stabilized by cross-linked microgel particles of the *N*-isopropylacrylamide–methacrylic acid copolymer of ~500 nm in size at

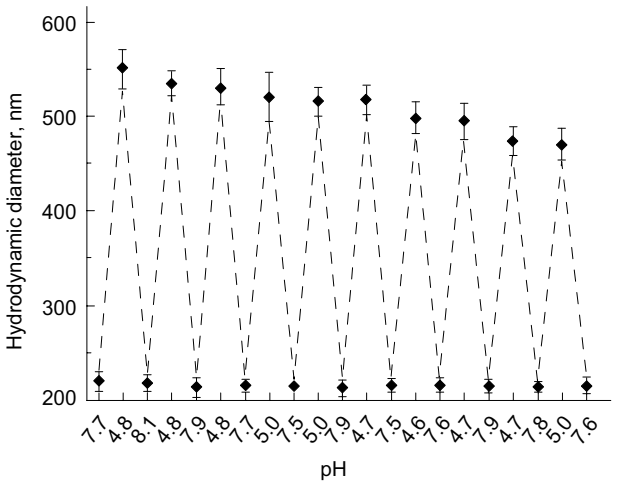


Figure 54. Cycles of variation of the hydrodynamic diameter of particles after the change in the pH of the aqueous phase upon the addition of 0.1 mol L^{-1} of HCl or KOH.[146] Published with permission from the American Chemical Society.

20 °C, the elastic modulus of the interfacial layer sharply decreased at pH < 5. An analogous decrease in the elasticity of the interfacial layer was observed upon temperature rise, which was attributed to decrease in the particle interactions with one another due to a decrease in their hydrophilicity. Meanwhile, in the case of the charged surface and counterions inside the microgel particles, the degree of particle swelling increases. The microgel particles become more deformable, which influences the viscoelastic properties of the interfacial layer.[229]

Emulsions responsive to a pH change were obtained when modified silica nanoparticles were used for stabilization. 3-Aminopropyltriethoxysilane was grafted on the surface of the silica nanoparticles and then benzaldehyde was bound to the amino groups. At pH 7.8, these nanoparticles were adsorbed at the interface and stabilized O/W emulsions. When pH decreased to 3.5, dissociation and elimination of benzaldehyde took place. The nanoparticle became hydrophilic and desorbed from the interface.[129]

Cellulose nanocrystals modified by poly[2-(dimethylamino)ethyl methacrylate] stabilized an emulsion with an alkaline dispersion medium. For poly[2-(dimethylamino)ethyl methacrylate], $pK_a \approx 7.4$. At pH > pK_a, the polymer molecules were hydrophobic and, in combination with hydrophilic cellulose nanocrystals, they were adsorbed at the interface in the emulsion. At pH < pK_a, the particles became hydrophilic due to hydration of poly[2-(dimethylamino)ethyl methacrylate] and migrated to the aqueous phase.[67]

At pH values above $pK_a = 6.5$, chitosan forms water-insoluble nanoparticles that stabilize O/W emulsions. At pH < pK_a, chitosan is dissolved in the dispersion medium and, hence, the emulsions break down. Five emulsification–demulsification cycles were carried out in these systems.[71,245]

Protein nanostructures shaped as dodecahedra with a size of ~25 nm were used to prepare emulsions responsive to pH changes. In neutral and alkaline media, stable O/W emulsions were formed. In acidic media, flocculation of oil droplets took place. This process was reversible; flocculation and redispersion of the emulsions occurred in five cycles.[315]

Emulsions stabilized by negatively charged silica nanoparticles and a zwitter-ionic surfactant, dodecyldimethyl carboxyl betaine, were stable to coalescence at pH ⩽ 5, while in acidic solutions, the surfactant molecules were charged oppositely to nanoparticles and were adsorbed on their surface. In alkaline solutions at pH > 8.5, the emulsions broke down.[119]

Stabilization by Ludox CL silica nanoparticles modified with the poly(sodium 4-styrenesulfonate) polyelectrolyte, which were positively charged in neutral medium, gave emulsions stable for >8 months. As pH decreased to 1 or increased to 13, phase separation in the emulsions took place.[316]

When Ludox CL nanoparticles modified with potassium hydrogen phthalate were used, O/W emulsions were formed in the pH range from 3.5 to 5.5. An increase or decrease in the pH resulted in phase inversion of emulsions.[317]

At pH > 9.5, an oil-in-water emulsion stabilized by $Mg(OH)_2$ particles was obtained; at lower pH, phase separation took place. This process was also reversible.[318]

Janus particles composed of polystyrene and poly(2-vinylpyridine) stabilized an emulsion of water in toluene at pH 7. A decrease in pH to 2 induced phase inversion and gave an O/W emulsion; as pH increased to 9, a W/O emulsion formed once again. Several cycles of pH variation from 2 to 9 were carried out. After phase inversion, the size of droplets of the dispersed phase in the emulsion changed within the error of measurements.[265] Janus particles consisting of polystyrene, 2-(diisopropylamino)ethyl methacrylate and 3-(triethoxysilyl)propyl methacrylate also stabilized the O/W emulsions at pH < 6.0 and W/O emulsions at pH > 7.0.[319]

7.2. Emulsions responsive to the action of chemicals

The action of certain ions changes the structure of polymer molecules, which can also be used for the design of stimuli-responsive Pickering emulsions. Tan *et al.*[320] obtained Pickering emulsions sensitive to perchlorate ions. Emulsions were stabilized by silica particles with surface-grafted poly[2-(methacryloyloxy)ethyltrimethylammonium] chloride molecules. The addition of $NaClO_4$ in a concentration of <10 or >40 mmol L^{-1} resulted in the formation of stable emulsions; in the concentration range of 10–40 mmol L^{-1}, the emulsions broke down.

In a system consisting of liquid paraffin and an aqueous phase containing >0.2 mol L^{-1} calcium cations, 10–40 nm nanoaggregates of the sodium salt of the 4-styrenesulfonic acid–maleic acid copolymer formed. In the presence of these nanoaggregates, stable O/W emulsions were formed. When the concentration of calcium ions was <0.2 mol L^{-1}, the polymer nanoaggregates split into separate molecules, and the emulsions broke down.[147]

Pickering emulsions sensitive to gases have been developed. For example, O/W emulsions stabilized by particles of the copolymer of 2-(diethylamino)ethyl methacrylate and sodium methacrylate cross-linked with *N*,*N*′-methylenebis(acrylamide) were sensitive to CO_2 and N_2 dissolved in water. On bubbling of CO_2, pH of the dispersion medium decreased from 8.8 to 5.6, and emulsions broke down. The subsequent bubbling of N_2 and homogenization resulted again in emulsification.[321] However, the response time was much longer than that of pH-responsive emulsions under the action of acids or alkalis: 15–20 min.

The emulsions stabilized by microgel particles of poly[2-(diethylamino)ethyl methacrylate-*co*-2,3,4,5,6-pentafluorostyrene] were sensitive to O_2 and CO_2.[322]

7.3. Emulsions responsive to temperature variation

Emulsions can respond to temperature changes because of the change in the hydration of molecules of the stabilizing particles. For example, the molecules of oxyethylated surfactants become hydrophobic upon dehydration at elevated temperature. The O/W emulsions stabilized by silica nanoparticles modified with alkyl polyoxyethylene monododecyl ethers were stable at room temperature, but broke down on heating. The process was reversible; the emulsions could be redispersed after a decrease in temperature.[127]

When temperature-responsive polymer particles are used to stabilize emulsions, phase separation takes place due to the sharp decrease in the particle volume upon temperature change. In systems with a lower critical solution temperature, if the temperature drops below this value, the molecules of a linear polymer are hydrated and dissolved. The cross-linked polymer molecules swell to form a hydrogel. Hence, upon the external stimulus, for example, on temperature rise, the particle size decreases (Fig. 55).[221] Thus latex particles with a size of ~1 μm obtained by copolymerization of *N*-isopropylacrylamide, acrylamide

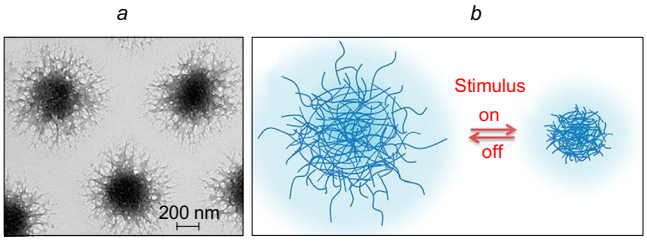


Figure 55. TEM image of poly(*N*-isopropylacrylamide) microgel particles (*a*) and schematic representation of decrease in the size of these particles upon external stimulus (*b*).[221] Published with permission from Elsevier.

and *N*,*N*′-methylenebis(acrylamide) decreased ~10-fold in the volume as the temperature increased above the critical solution temperature of poly(*N*-isopropylacrylamide).[220]

Diblock copolymer of sulfobetaine methacrylamide and *N*-isopropyl methacrylamide, which has both lower and upper solution temperatures, was grafted to silica nanoparticles. These nanoparticles stabilized O/W emulsions at 65 °C, while at 25 °C, the emulsions broke down.[323]

In O/W Pickering emulsions stabilized by star-shaped polyethylene oxide particles with a diameter of 24 nm, dispersed phase droplets were in the non-flocculated state at room temperature. On heating above the cloud point, flocculation of the oil droplets took place. Coalescence did not occur in the emulsion, but flocculation was irreversible.[324]

Tavacoli *et al.*[325] obtained microcapsules with the core made of a bicontinuous emulsion stabilized by silanized silica particles and the external surface formed by poly(12-hydroxystearic acid) particles, which responded to changes in the temperature and the phase ratio.

Heating of nanoemulsions stabilized by solid lipid nanoparticles above the lipid melting point resulted in coalescence of the dispersed phase droplets; hence, the rate of release of the ketoprofen encapsulated in the dispersed phase droplets increased.[210]

7.4. Emulsions responsive to magnetic field

A magnetic field induces demulsification, since magnetic particles are desorbed from the interface. In the absence of magnetic field, these emulsions can be mechanically redispersed. Most often, there emulsions are stabilized using iron oxide nanoparticles and nanocomposites with iron oxide nanoparticles.

In experiments carried out by Kaiser *et al.*,[326] cyclohexane droplets stabilized by FeO_x—polystyrene core–shell particles moved into the aqueous medium under the action of a permanent magnetic field. They could be separated from the aqueous phase, washed, and redispersed. Under the action of high-frequency magnetic field, demulsification took place. Melle *et al.*[327] determined the critical magnetic field strength for destabilization of a decane-in-water emulsion stabilized by iron carbonyl particles.

Magnetic field-responsive O/W emulsions were stabilized by non-modified Fe_3O_4 nanoparticles,[328,329] oleic acid-modified Fe_3O_4 nanoparticles,[330] ferrocenyl azine,[331] Fe_3O_4—cellulose nanocrystal nanocomposites,[332] Janus particles consisting of polymers and Fe_2O_3.[269] Water-in-oil emulsions were stabilized by graphene oxide nanoparticles modified with iron oxide nanoparticles.[156]

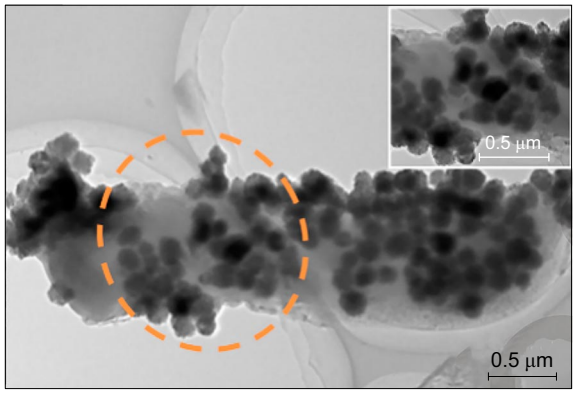


Figure 56. TEM image of the bacterium *Brevibacillus parabrev* with adsorbed Fe_3O_4 nanoparticles.[334] Published with permission from Elsevier.

Emulsions stabilized by Fe_3O_4 nanoparticles modified with poly[2-(dimethylamino)ethyl methacrylate] were responsive to the magnetic field and to the change in the pH of the aqueous medium.[333]

The crude oil-degrading *Brevibacillus parabrev* bacteria covered by a shell of Fe_3O_4 nanoparticles modified with poly(allylamine hydrochloride) (Fig. 56) proved to be efficient stabilizers for Pickering emulsions and emulsified kerosene, diesel fuel, tetradecane, dimethyl silicone oil and soya oil with an efficiency of >95%. Then the dispersed phase with adsorbed bacteria was separated by the action of a permanent magnet. This method was developed for cleaning the surface of water bodies after spillage of petroleum products.[334]

7.5. Emulsions responsive to light

Ultraviolet irradiation of TiO_2 nanoparticles with dodecylsilane molecules grafted to the surface induced cleavage of hydrocarbon chains, and chains with ~7 remained on the surface. The contact angle of the particles decreased from 140.5 to 105.5°; in the presence of such particles, water-in-oil emulsions broke down.[335]

On visible light irradiation, phase inversion took place in O/W emulsions with silica nanoparticles modified with 2,2-dimethyl-5-(furan-2-ylmethylene)-1,3-dioxane-4,6-dione.[336] The irradiation in the near-IR region resulted in phase inversion in W/O emulsions containing silica nanoparticles with grafted spiropyran molecules. On repeated exposure to visible light, Pickering emulsions were again converted to W/O emulsions.[337]

Some publications report the formation of Pickering emulsions responsive to combined stimuli such as pH change and temperature,[67,229,230] temperature and magnetic field,[338] pH and magnetic field,[330,333] light and magnetic field,[339] light and the presence of dissolved CO_2 or N_2 gases,[340] pH and the same dissolved gases.[268]

8. Conclusion

The most important difference of the Pickering emulsions from conventional emulsions is almost irreversible adsorption of >10 nm particles at the interface. In surfactant-stabilized emulsions, surfactant molecules in the bulk of the dispersion medium and at the interface occur in the dynamic equilibrium and can be adsorbed on and desorbed from the

droplet surface. Due to high energy of detachment of particles from the interface, which exceeds tens and thousands of kT, Pickering emulsions are stable to coalescence and, in some cases, remain stable for several years. The stability of Pickering emulsions increases when unadsorbed particles are aggregated in the dispersion medium and form a gel-like network. This structuring of the dispersion medium retards processes of droplet approaching one another and flocculation, and the rate of sedimentation decreases.

Pickering emulsions can be stabilized by particles with appropriate wettability by emulsion phases without additional modification of their surface with organic compounds. These emulsions are in most demand for applications in which the use of surfactants may be inappropriate, for example, in pharmaceutical industry. Currently, Pickering emulsions are actively used in food industry. These dispersion systems are promising as catalysts, microreactors, for the fabrication of nanocomposites based on latexes and porous materials.

Of special interest are Pickering emulsions for encapsulation of active substances. For example, colloidosomes, microcapsules of particles adsorbed on the droplet surface and connected with one another, can be obtained from Pickering emulsions. Colloidosomes are hollow shell; their permeability and elasticity can be controlled by varying the size of adsorbed particles and dispersed phase droplets. These structures can be used for encapsulation of active substances and subsequent prolonged or controlled release.

One more promising trend is development of stimuli-responsive Pickering emulsions, the stability of which varies under various impacts and changes in the environment properties. Stimuli-responsive emulsions provide intense release of encapsulated compounds, which can be used not only in medicine and in pharmacology, but also for the design of sensors and in food and paint industry.

This review was prepared with the financial support of the Russian Foundation for Basic Research (Project No. 20-13-50285).

9. List of abbreviations and symbols

O/W — oil-in-water emulsion,
W/O — water-in-oil emulsion,
W/W — water-in-water emulsion,
d — diameter,
E — energy,
k — Boltzmann constant,
P — pressure,
T — temperature,
r — radius,
γ — surface tension at the water/oil interface,
θ — contact angle of particles,
φ — fraction of the dispersed phase in the emulsion.

10. References

1. W.Ramsden. *Proc. R. Soc. London*, **72**, 156 (1903)
2. S.U.Pickering. *J. Chem. Soc., Transact.*, **91**, 2001 (1907)
3. R.Aveyard, B.P.Binks, J.H.Clint. *Adv. Colloid Interface Sci.*, **100–102**, 503 (2003)
4. B.P.Binks. *Curr. Opin. Colloid Interface Sci.*, **7**, 21 (2002)
5. Y.Chevalier, M.-A.Bolzinger. *Colloids Surf., A*, **439**, 23 (2013)
6. D.E.Tambe, M.M.Sharma. *Adv. Colloid Interface Sci.*, **52**, 1 (1994)
7. S.Tcholakova, N.D.Denkov, A.Lips. *Phys. Chem. Chem. Phys.*, **10**, 1608 (2008)
8. I.Capron, O.J.Rojas, R.Bordes. *Curr. Opin. Colloid Interface Sci.*, **29**, 83 (2017)
9. C.Guida, A.C.Aguiar, R.L.Cunha. *Curr. Opin. Food Sci.*, **38**, 52 (2021)
10. A.Sharkawy, M.F.Barreiro, A.E.Rodrigues. *Carbohydr. Polym.*, **250**, 116885 (2020)
11. A.Shi, X.Feng, Q.Wang, B.Adhikari. *Food Hydrocolloids*, **109**, 106117 (2020)
12. H.Dai, J.Wu, H.Zhang, Y.Chen, L.Ma, H.Huang, Y.Huang, Y.Zhang. *Trends Food Sci. Technol.*, **102**, 16 (2020)
13. F.Cui, S.Zhao, X.Guan, D.J.McClements, X.Liu, F.Liu, T.Ngai. *Food Hydrocolloids*, **119**, 106812 (2021)
14. I.N.Arrebola, L.Billon, G.Aguirre. *Adv. Colloid Interface Sci.*, **287**, 102333 (2021)
15. E.F.Ribeiro, P.Morell, V.R.Nicoletti, A.Quiles, I.Hernando. *Food Hydrocolloids*, **119**, 106839 (2021)
16. L.Chen, F.Ao, X.Ge, W.Shen. *Molecules*, **25**, 3202 (2020)
17. A.Niroula, T.D.Gamot, C.W.Ooi, S.Dhital. *Food Hydrocolloids*, **112**, 106303 (2021)
18. Abdullah, J.Weiss, T.Ahmad, C.Zhang, H.Zhang. *Trends Food Sci. Technol.*, **106**, 91 (2020)
19. W.W.Mwangi, H.P.Lim, L.E.Low, B.T.Tey, E.S.Chan. *Trends Food Sci. Technol.*, **100**, 320 (2020)
20. Q.Li, Y.Wu, R.Fang, C.Lei, Y.Li, B.Li, Y.Pei, X.Luo, S.Liu. *Trends Food Sci. Technol.*, **110**, 573 (2021)
21. Y.Iwashita. *Curr. Opin. Colloid Interface Sci.*, **49**, 94 (2020)
22. D.G.Ortiz, C.Pochat-Bohatier, J.Cambedouzou, M.Bechelany, P.Miele. *Engineering*, **6**, 468 (2020)
23. L.E.Low, S.P.Siva, Y.K.Ho, E.S.Chan, B.T.Tey. *Adv. Colloid Interface Sci.*, **277**, 102117 (2020)
24. F.J.Rossier-Miranda, C.G.P.H.Schroën, R.M.Boom. *Colloids Surf., A*, **343**, 43 (2009)
25. K.L.Thompson, M.Williams, S.P.Armes. *J. Colloid Interface Sci.*, **447**, 217 (2015)
26. A.M.B.Rodriguez, B.P.Binks. *Curr. Opin. Colloid Interface Sci.*, **44**, 107 (2019)
27. J.Tang, P.J.Quinlan, K.C.Tam. *Soft Matter*, **11**, 3512 (2015)
28. M.Vis, J.Opdam, I.S.J.van't Oor, G.Soligno, R.Roij, R.H.Tromp, B.H.Erné. *ACS Macro Lett.*, **4**, 965 (2015)
29. M.Koroleva, E.Yurtov. *Colloids Surf., A*, **601**, 125001 (2020)
30. J.H.Schulman, J.Leja. *Trans. Faraday Soc.*, **50**, 598 (1954)
31. T.Ondarçuhu, P.Fabre, E.Raphaël, M.Veyssié. *J. Phys. France*, **51**, 1527 (1990)
32. S.Jiang, S.Granick. *J. Chem. Phys.*, **127**, 161102 (2007)
33. B.P.Binks, P.D.I.Fletcher. *Langmuir*, **17**, 4708 (2001)
34. H.Fan, D.E.Resasco, A.Striolo. *Langmuir*, **27**, 5264 (2011)
35. T.S.Horozov. *Curr. Opin. Colloid Interface Sci.*, **13**, 134 (2008)
36. N.D.Denkov, I.B.Ivanov, P.A.Kralchevsky, D.T.Wasan. *J. Colloid Interface Sci.*, **150**, 589 (1992)
37. A.V.Nushtaeva, P.M.Kruglyakov. *Colloid J.*, **65**, 341 (2003)
38. P.M.Kruglyakov, A.V.Nushtayeva. *Adv. Colloid Interface Sci.*, **108–109**, 151 (2004)
39. G.Kaptay. *Colloids Surf., A*, **282–283**, 387 (2006)
40. N.Yan, J.C.Masliyah. *Colloids Surf., A*, **96**, 229 (1995)
41. L.S.Dorobantu, A.K.C.Yeung, J.M.Foght, M.R.Gray. *Appl. Environ. Microbiol.*, **70**, 6333 (2004)
42. Y.Q.Sun, T.Gao. *Metall. Mater. Trans. A*, **33**, 3285 (2002)
43. T.S.Horozov, R.Aveyard, J.H.Clint, B.Neumann. *Langmuir*, **21**, 2330 (2005)
44. E.J.Stancik, M.Kouhkan, G.G.Fuller. *Langmuir*, **20**, 90 (2004)
45. D.J.French, P.Taylor, J.Fowler, P.S.Clegg. *J. Colloid Interface Sci.*, **441**, 30 (2015)
46. T.S.Horozov, B.P.Binks. *Angew. Chem., Int. Ed.*, **45**, 773 (2006)
47. M.N.Lee, H.K.Chan, A.Mohraz. *Langmuir*, **28**, 3085 (2012)
48. M.Yu.Koroleva, A.M.Tokarev, E.V.Yurtov. *Mendeleev Commun.*, **27**, 518 (2017)

49. M.-H.Kwok, T.Ngai. *J. Colloid Interface Sci.*, **461**, 409 (2016)
50. E.Dickinson. *Food Hydrocolloids*, **23**, 1473 (2009)
51. R.M.Wiley. *J. Colloid Interface Sci.*, **9**, 427 (1954)
52. W.B.Hardy. *Colloid Symp. Monogr.*, **16**, 8 (1928)
53. S.Arditty, C.P.Whitby, B.P.Binks, V.Schmitt, F.Leal-Caldero. *Eur. Phys. J., E*, **11**, 273 (2003)
54. B.R.Midmore. *Colloids Surf., A*, **132**, 257 (1998)
55. A.B.Pawar, M.Caggioni, R.Ergun, R.W.Hartel, P.T.Spicer. *Soft Matter*, **7**, 7710 (2011)
56. E.Vignati, R.Piazza, T.P. Lockhart. *Langmuir*, **19**, 6650 (2003)
57. B.P.Binks, M.Kirkland. *Phys. Chem. Chem. Phys.*, **4**, 3727 (2002)
58. E.Dickinson. *Food Hydrocolloids*, **68**, 219 (2017)
59. G.Lagaly, M.Reese, S.Abend. *Appl. Clay Sci.*, **14**, 83 (1999)
60. E.Dickinson, R.Ettelaie, T.Kostakis, B.S.Murray. *Langmuir*, **20**, 8517 (2004)
61. B.H.Bijsterbosch, M.T.A.Bos, E.Dickinson, J.H.J.Opheusden, P.Walstra. *Faraday Discuss.*, **101**, 51 (1995)
62. M.Koroleva, D.Bidanov, E.Yurtov. *Phys. Chem. Chem. Phys.*, **21**, 1536 (2019)
63. B.P.Binks, W.Liu, J.A.Rodrigues. *Langmuir*, **24**, 4443 (2008)
64. S.Guillot, F.Bergaya, C.Azevedo, F.Warmont, J.-F.Tranchant. *J. Colloid Interface Sci.*, **333**, 563 (2009)
65. C.P.Whitby, P.C.Garcia. *Appl. Clay Sci.*, **96**, 56 (2014)
66. J.Lu, X.Tian, Y.Jin, J.Chen, K.B.Walters, S.Ding. *Appl. Clay Sci.*, **102**, 113 (2014)
67. J.Tang, M.F.X.Lee, W.Zhang, B.Zhao, R.M.Berry, K.C.Tam. *Biomacromolecules*, **15**, 3052 (2014)
68. T.Winuprasith, M.Suphantharika. *Food Hydrocolloids*, **43**, 690 (2015)
69. X.Jia, R.Xu, W.Shen, M.Xie, M.Abid, S.Jabbar, P.Wang, X.Zeng, T.Wu. *Food Hydrocolloids*, **43**, 275 (2015)
70. M.V.Tzoumaki, T.Moschakis, V.Kiosseoglou, C.G.Biliaderis. *Food Hydrocolloids*, **25**, 1521 (2011)
71. L.Alison, A.F.Demirörs, E.Tervoort, A.Teleki, J.Vermant, A.R.Studart. *Langmuir*, **34**, 6147 (2018)
72. S.Abend, N.Bonnke, U.Gutschner, G.Lagaly. *Colloid Polym. Sci.*, **276**, 730 (1998)
73. K.R.Peddireddy, T.Nicolai, L.Benyahia, I.Capron. *ACS Macro Lett.*, **5**, 283 (2016)
74. Z.Du, M.P.Bilbao-Montoya, B.P.Binks, E.Dickinson, R.Ettelaie, B.S.Murray. *Langmuir*, **19**, 3106 (2003)
75. R.G.Alargova, D.S.Warhadpande, V.N.Paunov, O.D.Velev. *Langmuir*, **20**, 10371 (2004)
76. M.Abkarian, A.B.Subramaniam, S.-H.Kim, R.J.Larsen, S.-M.Yang, H.A.Stone. *Phys. Rev. Lett.*, **99**, 188301 (2007)
77. N.Denkov, S.Tcholakova, N.Politova-Brinkova. *Curr. Opin. Colloid Interface Sci.*, **50**, 101376 (2020)
78. N.P.Ashby, B.P.Bink. *Phys. Chem. Chem. Phys.*, **2**, 5640 (2000)
79. M.Yu.Koroleva, E.V.Yurtov. *Russ. Chem. Rev.*, **90**, 293 (2021)
80. K.L.Thompson, M.J.Derry, F.L.Hatton, S.P.Armes. *Langmuir*, **34**, 9289 (2018)
81. K.H.Persson, I.A.Blute, I.C.Mira, J.Gustafsson. *Colloids Surf. A*, **459**, 48 (2014)
82. S.J.Hunter, E.J.Cornel, O.O.Mykhaylyk, S.P.Armes. *Langmuir*, **36**, 15523 (2020)
83. S.S.Velankar. *Soft Matter*, **11**, 8393 (2015)
84. S.Simovic, C.A.Prestidge. *Langmuir*, **24**, 7132 (2008)
85. Y.Zhu, S. Zhang, Y.Hua, H.Zhang, J.Chen. *Ind. Eng. Chem. Res.*, **53**, 4642 (2014)
86. M.Nair, C.P.Lusignan, D.C.Boris. *Colloids Surf., A*, **443**, 583 (2014)
87. S.Zou, H.Liu, Y.Yang, Z.Wei, C.Wang. *React. Funct. Polym.*, **73**, 1231 (2013)
88. F.Spyropoulos, L.J.Duffus, P.Smith, I.T.Norton. *Langmuir*, **35**, 15137 (2019)
89. S.Frasch-Melnik, F.Spyropoulos, I.T.Norton. *J. Colloid Interface Sci.*, **350**, 178 (2010)
90. K.L.Thompson, C.J.Mable, J.A.Lane, M.J.Derry, L.A.Fielding, S.P.Armes. *Langmuir*, **31**, 4137 (2015)
91. P.Szumała, N.Luty. *Colloids Surf., A*, **499**, 131 (2016)
92. A.G.Cunha, J.-B.Mougel, B.Cathala, L.A.Berglund, I.Capron. *Langmuir*, **30**, 9327 (2014)
93. A.T.Tyowua, S.G.Yiase, B.P.Binks. *J. Colloid Interface Sci.*, **488**, 127 (2017)
94. K.Stratford, R.Adhikari, I.Pagonabarraga, J.-C.Desplat, M.E.Cates. *Science*, **309**, 2198 (2005)
95. E.M.Herzig, K.A.White, A.B.Schofield, W.C.K.Poon, P.S.Clegg. *Nat. Mater.*, **6**, 966 (2007)
96. M.E.Cates, P.S.Clegg. *Soft Matter*, **4**, 2132 (2008)
97. K.A.White, A.B.Schofield, P.Wormald, J.W.Tavacoli, B.P.Binks, P.S.Clegg. *J. Colloid Interface Sci.*, **359**, 126 (2011)
98. M.F.Haase, K.J.Stebe, D.Lee. *Adv. Mater.*, **27**, 7065 (2015)
99. T.Nicolai, B.Murray. *Food Hydrocolloids*, **68**, 157 (2017)
100. A.T Poortinga. *Langmuir*, **24**, 1644 (2008)
101. A.Gonzalez-Jordan, T.Nicolai, L.Benyahia. *J. Colloid Interface Sci.*, **530**, 505 (2018)
102. G.Balakrishnan, T.Nicolai, L.Benyahia, D.Durand. *Langmuir*, **28**, 5921 (2012)
103. M.Inam, J.R.Jones, M.M.Pérez-Madrigal, M.C.Arno, A.P.Dove, R.K.O'Reilly. *ACS Cent. Sci.*, **4**, 63 (2018)
104. A.Gonzalez-Jordan, L.Benyahia, T.Nicolai. *Colloids Surf., A*, **532**, 332 (2017)
105. H.Firoozmand, B.S.Murray, E.Dickinson. *Langmuir*, **25**, 1300 (2009)
106. Z.Rozynek, R.Bielas, A.Józefczak. *Soft Matter*, **14**, 5140 (2018)
107. M.J.Rymaruk, V.J.Cunningham, S.L.Brown, C.N.Williams, S.P.Armes. *J. Colloid Interface Sci.*, **580**, 354 (2020)
108. B.Rodier, A.Leon, C.Hemmingsen, E.Pentzer. *ACS Macro Lett.*, **6**, 1201 (2017)
109. X.Lu, J.S.Katz, A.K.Schmitt, J.S.Moore. *J. Am. Chem. Soc.*, **140**, 3619 (2018)
110. P.S.Clegg, E.M.Herzig, A.B.Schofield, S.U.Egelhaaf, T.S.Horozov, B.P.Binks, M.E.Cates, W.C.K.Poon. *Langmuir*, **23**, 5984 (2007)
111. A.K.F.Dyab, L.A.Mohamed, F.Taha. *J. Dispers. Sci. Technol.*, **39**, 890 (2018)
112. L.Bai, J.W.Fruehwirth, X.Cheng, C.W.Macosko. *Soft Matter*, **11**, 5282 (2015)
113. B.P.Binks, S.O.Lumsdon. *Phys. Chem. Chem. Phys.*, **1**, 3007 (1999)
114. M.Maas, C.C.Silvério, J.Laube, K.Rezwan. *J. Colloid Interface Sci.*, **501**, 256 (2017)
115. B.P.Binks, C.P.Whitby. *Colloids Surf., A*, **253**, 105 (2005)
116. J.Frelichowska, M.-A.Bolzinger, Y.Chevalier. *Colloids Surf., A*, **343**, 70 (2009)
117. B.P.Binks, J.A.Rodrigues, W.J.Frith. *Langmuir*, **23**, 3626 (2007)
118. B.P.Binks, J.A.Rodrigues. *Langmuir*, **23**, 7436 (2007)
119. K.Liu, J.Jiang, Z.Cui, B.P.Binks. *Langmuir*, **33**, 2296 (2017)
120. B.P.Binks, A.Desforges, D.G.Duff. *Langmuir*, **23**, 1098 (2007)
121. N.G.Eskandar, S.Simovic, C.A.Prestidge. *J. Colloid Interface Sci.*, **358**, 217 (2011)
122. X.Zhao, G.Yu, J.Li, Y.Feng, L.Zhang, Y.Peng, Y.Tang, L.Wang. *ACS Sustain. Chem. Eng.*, **6**, 4105 (2018)
123. E.Santini, E.Guzmán, M.Ferrari, L.Liggieri. *Colloids Surf., A*, **460**, 333 (2014)
124. A.Sadeghpour, F.Pirolt, O.Glatter. *Langmuir*, **29**, 6004 (2013)
125. K.Lebdioua, A.Aimable, M.Cerbelaud, A.Videcoq, C.Peyratout. *J. Colloid Interface Sci.*, **520**, 127 (2018)
126. B.R.Midmore. *Colloids Surf., A*, **145**, 133 (1998)
127. Y.Zhu, T.Fu, K.Liu, Q.Lin, X.Pei, J.Jiang, Z.Cui, B.P.Binks. *Langmuir*, **33**, 5724 (2017)
128. C.Morishita, M.Kawaguchi. *Colloids Surf., A*, **335**, 138 (2009)
129. G.Ren, M.Wang, L.Wang, Z.Wang, Q.Chen, Z.Xu, D.Sun. *Langmuir*, **34**, 5798 (2018)
130. N.Saleh, T.Sarbu, K.Sirk, G.V.Lowry, K.Matyjaszewski, R.D.Tilton. *Langmuir*, **21**, 9873 (2005)

131. S Björkegren, L.Nordstierna, A.Törncrona, A.Palmqvist. *J. Colloid Interface Sci.*, **487**, 250 (2017)
132. C.Griffith, H.Daigle. *J. Colloid Interface Sci.*, **509**, 132 (2018)
133. I.E.Salama, A.Paul. *Colloids Surf., A*, **494**, 125 (2016)
134. X.Zheng, Y.Zhang, H.Wang, Q.Du. *Macromolecules*, **47**, 6847 (2014)
135. H.Yan, B.Zhao, Y.Long, L.Zheng, C.-H.Tung, K.Song. *Colloids Surf., A*, **482**, 639 (2015)
136. S.V.Daware, M.G.Basavaraj. *Langmuir*, **31**, 6649 (2015)
137. B.P.Binks, S.O.Lumsdon. *Langmuir*, **17**, 4540 (2001)
138. E.P.Lewandowski, M.Cavallaro Jr., L.Botto, J.C.Bernate, V.Garbin, K.J.Stebe. *Langmuir*, **26**, 15142 (2010)
139. K.Golemanov, S.Tcholakova, P.A.Kralchevsky, K.P.Ananthapadmanabhan, A.Lips. *Langmuir*, **22**, 4968 (2006)
140. S.Tarimala, S.R.Ranabothu, J.P.Vernetti, L.L.Dai. *Langmuir*, **20**, 5171 (2004)
141. T.Nallamilli, B.P.Binks, E.Mani, M.G.Basavaraj. *Langmuir*, **31**, 11200 (2015)
142. A.Walsh, K.L.Thompson, S.P.Armes, D.W.York. *Langmuir*, **26**, 18039 (2010)
143. S.Zhang, Y.Zhou, C.Yang. *Colloids Surf., A*, **482**, 338 (2015)
144. S.Fujii, D.P.Randall, S.P.Armes. *Langmuir*, **20**, 11329 (2004)
145. A.J.Morse, D.Dupin, K.L.Thompson, S.P.Armes, K.Ouzineb, P.Mills, R.Swart. *Langmuir*, **28**, 11733 (2012)
146. A.J.Morse, S.P.Armes, K.L.Thompson, D.Dupin, L.A.Fielding, P.Mills, R.Swart. *Langmuir*, **29**, 5466 (2013)
147. C.Zhao, J.Tan, W.Li, K.Tong, J.Xu, D.Sun. *Langmuir*, **29**, 14421 (2013)
148. K.L.Thompson, P.Chambon, R.Verber, S.P.Armes. *J. Am. Chem. Soc.*, **134**, 12450 (2012)
149. J.Kim, L.J Cote, F.Kim, W.Yuan, K.R.Shull, J.Huang. *J. Am. Chem. Soc.*, **132**, 8180 (2010)
150. L.J.Cote, F.Kim, J.Huang. *J. Am. Chem. Soc.*, **131**, 1043 (2009)
151. Y.Liu, Y.Zhang, L.Duan, W.Zhang, M.Su, Z.Sun, P.He. *Prog. Org. Coat.*, **99**, 23 (2016)
152. Y.He, F.Wu, X.Sun, R.Li, Y.Guo, C.Li, L.Zhang, F.Xing, W.Wang, J.Gao. *ACS Appl. Mater. Interfaces*, **5**, 4843 (2013)
153. S.C.Thickett, P.B.Zetterlund. *J. Colloid Interface Sci.*, **442**, 67 (2015)
154. T.D.Dao, H.M.Jeong. *Carbon*, **99**, 49 (2016)
155. M.Tang, T.Wu, X.Xu, L.Zhang, F.Wu. *Mater. Res. Bull.*, **60**, 118 (2014)
156. K.-Y.A.Lin, H.Yang, C.Petit, W.-D.Lee. *J. Colloid Interface Sci.*, **438**, 296 (2015)
157. H.Yang, D.J.Kang, K.H.Ku, H.-H.Cho, C.H.Park, J.Lee, D.C.Lee, P.M.Ajayan, B.J.Kim. *ACS Macro Lett.*, **3**, 985 (2014)
158. H.-H.Cho, H.Yang, D.J.Kang, B.J.Kim. *ACS Appl. Mater. Interfaces*, **7**, 8615 (2015)
159. W.Xuan, L.Ruiyi, L.Zaijun, L.Junkang. *J. Colloid Interface Sci.*, **505**, 847 (2017)
160. H.Wang, E.K.Hobbie. *Langmuir*, **19**, 3091 (2003)
161. W.Wang, E.D.Laird, Y.Gogotsi, C.Y.Li. *Carbon*, **50**, 1769 (2012)
162. N.M.Briggs, J.S.Weston, B.Li, D.Venkataramani, C.P.Aichele, J.H.Harwell, S.P.Crossley. *Langmuir*, **31**, 13077 (2015)
163. N.Briggs, A.K.Y.Raman, L.Barrett, C.Brown, B.Li, D.Leavitt, C.P.Aichele, S.Crossley. *Colloids Surf., A*, **537**, 227 (2018)
164. A.-C.Baudouin, D.Auhl, F.F.Tao, J.Devaux, C.Bailly. *Polymer*, **52**, 149 (2011)
165. K.C.Powell, A.Chauhan. *Langmuir*, **30**, 12287 (2014)
166. S.Yu, H.Tan, J.Wang, X.Liu, K.Zhou. *ACS Appl. Mater. Interfaces*, **7**, 6745 (2015)
167. S.Fujii, M.Okada, H.Sawa, T.Furuzono, Y.Nakamura. *Langmuir*, **25**, 9759 (2009)
168. S.Fujii, M.Okada, T.Nishimura, H.Maeda, T.Sugimoto, H.Hamasaki, T.Furuzono, Y.Nakamura. *J. Colloid Interface Sci.*, **374**, 1 (2012)
169. A.Samanta, S.Takkar, R.Kulshreshtha, B.Nandan, R.K.Srivastava. *Colloids Surf., A*, **533**, 224 (2017)
170. M.Zhang, A.-J.Wang, J.-M.Li, N.Song, Y.Song, R.He. *Mater. Sci. Eng., C*, **70**, 396 (2017)
171. S.Fujii, M.Okada, T.Furuzono. *J. Colloid Interface Sci.*, **315**, 287 (2007)
172. M Okada, S.Fujii, T.Nishimura, Y.Nakamura, S.Takeda, T.Furuzono. *Appl. Surf. Sci.*, **262**, 39 (2012)
173. Y.Hu, X.Gu, Y.Yang, J.Huang, M.Hu, W.Chen, Z.Tong, C.Wang. *ACS Appl. Mater. Interfaces*, **6**, 17166 (2014)
174. Y.Sun, Y.Li, J.Xu, L.Huang, T.Qiu, S.Zhong. *Colloids Surf., B*, **155**, 142 (2017)
175. Y.Nonomura, N.Kobayashi. *J. Colloid Interface Sci.*, **330**, 463 (2009)
176. J.Dong, A.J.Worthen, L.M.Foster, Y.Chen, K.A.Cornell, S.L.Bryant, T.M.Truskett, C.W.Bielawski, K.P.Johnston. *ACS Appl. Mater. Interfaces*, **6**, 11502 (2014)
177. C.Li, Q.Liu, Z.Mei, J.Wang, J.Xu, D.Sun. *J. Colloid Interface Sci.*, **336**, 314 (2009)
178. C.P.Whitby, D.Fornasiero, J.Ralston. *J. Colloid Interface Sci.*, **323**, 410 (2008)
179. I.Jurgelane, V.Sevjakova, L.Dzene. *Colloids Surf., A*, **529**, 178 (2017)
180. A.K.Pawlik, I.T.Norton. *Food Struct.*, **1**, 24 (2014)
181. Y.Ai, B.Nelson, D.F.Birt, J.-L.Jane. *Carbohydr. Polym.*, **98**, 1266 (2013)
182. A.Azfaralariff, F.F.Fazial, R.S.Sontanosamy, M.F.Nazar, A.M.Lazim. *J. Food Eng.*, **280**, 109974 (2020)
183. X.Song, F.Ma, F.Zheng, H.Ren, H. Gong. *Int. J. Food Sci. Technol.*, **55**, 2408 (2020)
184. C.Li, Y.Li, P.Sun, C.Yang. *Colloids Surf., A*, **431**, 142 (2013)
185. E.J.Leal-Castañeda, Y.García-Tejeda, H.Hernández-Sánchez, L.Alamilla-Beltrán, D.I.Téllez-Medina, G.Calderón-Domínguez, H.S.García, G.F.Gutiérrez-López. *Food Hydrocolloids*, **80**, 177 (2018)
186. S.Ge, L.Xiong, M.Li, J.Liu, J.Yang, R.Chang, C.Liang, Q.Sun. *Food Chemistry*, **234**, 339 (2017)
187. M.Sjöö, S.C.Emek, T.Hall, M.Rayner, M.Wahlgren. *J. Colloid Interface Sci.*, **450**, 182 (2015)
188. A.Marefati, M.Bertrand, M.Sjöö, P.Dejmek, M.Rayner. *Food Hydrocolloids*, **63**, 309 (2017)
189. H.Saari, D.B.Johansson, N.Knopp, M.Sjöö, M.Rayner, M.Wahlgren. *Food Hydrocolloids*, **82**, 288 (2018)
190. T.Yang, J.Zheng, B.-S.Zheng, F.Liu, S.Wang, C.-H.Tang. *Food Hydrocolloids*, **82**, 230 (2018)
191. S.B.Haaj, W.Thielemans, A.Magnin, S.Boufi. *ACS Appl. Mater. Interfaces*, **6**, 8263 (2014)
192. K.P.Oza, S.G.Frank. *J. Dispers. Sci. Technol.*, **7**, 543 (1986)
193. Y.Habibi, L.A.Lucia, O.J.Rojas. *Chem. Rev.*, **110**, 3479 (2010)
194. X.Li, J.Li, J.Gong, Y.Kuang, L.Mo, T.Song. *Carbohydr. Polym.*, **183**, 303 (2018)
195. S.Hedjazi, S.H.Razavi. *Int. J. Biol. Macromol.*, **106**, 489 (2018)
196. I.Kalashnikova, H.Bizot, P.Bertoncini, B.Cathala, I.Capron. *Soft Matter*, **9**, 952 (2013)
197. I.Kalashnikova, H.Bizot, B.Cathala, I.Capron. *Biomacromolecules*, **13**, 267 (2012)
198. Z.Zhang, K.C.Tam, X.Wang, G.Sèbe. *ACS Sustain. Chem. Eng.*, **6**, 2583 (2018)
199. K.-Y.Lee, J.J.Blaker, R.Murakami, J.Y.Y.Heng, A.Bismarck. *Langmuir*, **30**, 452 (2014)
200. B.Pang, H.Liu, P.Liu, X.Peng, K.Zhang. *J. Colloid Interface Sci.*, **513**, 629 (2018)
201. M.Matos, A.Marefati, R.Bordes, G.Gutiérrez, M.Rayner. *Carbohydr. Polym.*, **169**, 127 (2017)
202. C.Avendano, N.Brun, O.Fontaine, M.In, A.Mehdi, A.Stocco, A.Vioux. *Langmuir*, **32**, 3907 (2016)

203. L.E.Lowa, B.T.Tey, B.H.Ong, E.S.Chan, S.Y.Tang. *Carbohydr. Polym.*, **155**, 391 (2017)
204. N.Garti, H.Binyamin, A.Aserin. *JAOCS*, **75**, 1825 (1998)
205. R.Gupta, D.Rousseau. *Food Funct.*, **3**, 302 (2012)
206. D.Rousseau. *Curr. Opin. Colloid Interface Sci.*, **18**, 283 (2013)
207. A.Schröder, J.Sprakel, K.Schroën, J.N.Spaen, C.C.Berton-Carabin. *J. Food Eng.*, **234**, 63 (2018)
208. A.Pawlik, D.Kurukji, I.Norton, F.Spyropoulos. *Food Funct.*, **7**, 2712 (2016)
209. G.I.Sakellari, I.Zafeiri, A.Pawlik, D.Kurukji, P.Taylor, I.T.Norton, F.Spyropoulos. *J. Colloid Interface Sci.*, **587**, 644 (2021)
210. S.M.Dieng, N.Anton, P.Bouriat, O.Thioune, P.M.Sy, N.Massaddeq, S.Enharrar, M.Diarrab, T.Vandamme. *Soft Matter*, **15**, 8164 (2019)
211. H.Salminen, T.Helgason, B.Kristinsson, K.Kristbergsson, J.Weiss. *Food Res. Int.*, **79**, 11 (2016)
212. I.Zafeiri, P.Smith, I.T.Norton, F.Spyropoulos. *Colloids Surf., A*, **599**, 124916 (2020)
213. F.Liu, C.-H.Tang. *J. Agric. Food Chem.*, **62**, 5133 (2014)
214. Y.-S.Gu, E.A.Decker, D.J.McClements. *Food Hydrocolloids*, **21**, 516 (2007)
215. T.Yi, C.Liu, J.Zhang, F.Wang, J.Wang, J.Zhang. *Eur. J. Pharm. Sci.*, **96**, 420 (2017)
216. N.P.Aditya, I.E.Hamilton, I.T.Norton. *Food Chem.*, **224**, 191 (2017)
217. L.J.Duffus, J.E.Norton, P.Smith, I.T.Norton, F.Spyropoulos. *J. Colloid Interface Sci.*, **473**, 9 (2016)
218. E.Dickinson. *Trends Food Sci. Technol.*, **43**, 178 (2015)
219. O.S.Deshmukh, D.Ende, M.C.Stuart, F.Mugele, M.H.G.Duits. *Adv. Colloid Interface Sci.*, **222**, 215 (2015)
220. R.H.Pelton, P.Chibante. *Colloids Surf.*, **20**, 241 (1986)
221. V.Schmitt, V.Ravaine. *Curr. Opin. Colloid Interface Sci.*, **18**, 532 (2013)
222. M.A.Fernandez-Rodriguez, A.Martín-Molina, J.Maldonado-Valderrama. *Adv. Colloid Interface Sci.*, **288**, 102350 (2021)
223. T.Ngai, S.H.Behrens, H.Auwetera. *Chem. Commun.*, 331 (2005)
224. M.Destribats, V.Lapeyre, M.Wolfs, E.Sellier, F.Leal-Calderon, V.Ravaine, V.Schmitt. *Soft Matter*, **7**, 7689 (2011)
225. M.Destribats, M.Wolfs, F.Pinaud, V.Lapeyre, E.Sellier, V.Schmitt, V.Ravaine. *Langmuir*, **29**, 12367 (2013)
226. M.Destribats, M.Eyharts, V.Lapeyre, E.Sellier, I.Varga, V.Ravaine, V.Schmitt. *Langmuir*, **30**, 1768 (2014)
227. K.Geisel, L.Isa, W.Richtering. *Langmuir*, **28**, 15770 (2012)
228. P.Massé, E.Sellier, V.Schmitt, V.Ravaine. *Langmuir*, **30**, 14745 (2014)
229. W.Richtering. *Langmuir*, **28**, 17218 (2012)
230. B.Brugger, B.A.Rosen, W.Richtering. *Langmuir*, **24**, 12202 (2008)
231. P.Wang, C.Chen, H.Guo, H.Zhang, Z.Yang, F.Ren. *Food Hydrocolloids*, **77**, 689 (2018)
232. Z.Gao, J.Zhao, Y.Huang, X.Yao, K.Zhang, Y.Fang, K.Nishinari, G.O.Phillips, F.Jiang, H.Yang. *LWT — Food Sci. Technol.*, **76**, 1 (2017)
233. Y.Feng, Y.Lee. *Food Hydrocolloids*, **56**, 292 (2016)
234. Z.-M.Gao, X.-Q.Yang, N.-N.Wu, L.-J.Wang, J.-M.Wang, J.Guo, S.-W.Yin. *J. Agric. Food Chem.*, **62**, 2672 (2014)
235. X.-S.Qin, Z.Luo, X.Peng. *J. Agric. Food Chem.*, **66**, 4449 (2018)
236. J.Wu, M.Shi, W.Li, L.Zhao, Z.Wang, X.Yan, W.Norde, Y.Li. *Colloids Surf., B*, **127**, 96 (2015)
237. X.-F.Zhu, N.Zhang, W.-F.Lin, C.-H.Tang. *Food Hydrocolloids*, **69**, 173 (2017)
238. X.-F.Zhu, J.Zheng, F.Liu, C.-Y.Qiu, W.-F.Lin, C.-H.Tang. *Food Hydrocolloids*, **74**, 37 (2018)
239. Y.Shao, C.-H.Tang. *Food Res. Int.*, **79**, 64 (2016)
240. H.-N.Liang, C.-H.Tang. *LWT — Food Sci. Technol.*, **58**, 463 (2014)
241. A.Sarkar, V.Ademuyiwa, S.Stubley, N.H.Esa, F.M.Goycoolea, X.Qin, F.Gonzalez, C.Olvera. *Food Hydrocolloids*, **84**, 282 (2018)
242. H.Tan, G.Sun, W.Lin, C.Mu, T.Ngai. *ACS Appl. Mater. Interfaces*, **6**, 13977 (2014)
243. W.Jin, J.Zhu, Y.Jiang, P.Shao, B.Li, Q.Huang. *J. Agric. Food Chem.*, **65**, 1401 (2017)
244. B.S.Murray, N.Phisarnchananan. *Food Hydrocolloids*, **56**, 161 (2016)
245. H.Liu, C.Wang, S.Zou, Z.Wei, Z.Tong. *Langmuir*, **28**, 11017 (2012)
246. X.-Y.Wang, M.-C.Heuzey. *Langmuir*, **32**, 929 (2016)
247. W.W.Mwangi, K.-W.Ho, B.-T.Tey, E.-S.Chan. *Food Hydrocolloids*, **60**, 543 (2016)
248. A.L.R.Costa, A.Gomes, R.L.Cunha. *Food Res. Int.*, **107**, 717 (2018)
249. I.Dammak, P.J.A.Sobral. *J. Food Eng.*, **229**, 2 (2018)
250. B.R.Shah, Y.Li, W.Jin, Y.An, L.He, Z.Li, W.Xu, B.Li. *Food Hydrocolloids*, **52**, 369 (2016)
251. E.Perrin, H.Bizot, B.Cathala, I.Capron. *Biomacromolecules*, **15**, 3766 (2014)
252. Q.Zhao, F.Zaaboul, Y.Liu, J.Li. *Compr. Rev. Food Sci. Food Safety.*, **19**, 1934 (2020)
253. H.Firoozmand, D.Rousseau. *Food Res. Int.*, **81**, 66 (2016)
254. S.P.Srivastava. H.D.Singh, J.N.Baruah, P.V.Krishna, M.S.Iyengar. *J. Appl. Chem.*, **20**, 105 (1970)
255. M.Rosenberg, E.Rosenberg. *Oil Petrochem. Pollut.*, **2**, 155 (1985)
256. G.F.Furtado, C.S.F.Picone, M.C.Cuellar, R.L.Cunha. *Colloids Surf., B*, **128**, 568 (2015)
257. W.Zhu, W.Ma, C.Li, J. Pan, X.Dai, M.Gan, Q.Qu, Y.Zhang. *Colloids Surf., A*, **453**, 27 (2014)
258. P.Wongkongkatep, K.Manopwisedjaroen, P.Tiposoth, S.Archakunakorn, T.Pongtharangkul, M.Suphantharika, K.Honda, I.Hamachi, J.Wongkongkatep. *Langmuir*, **28**, 5729 (2012)
259. C.Casagrande, P.Fabre, E.Raphaël, M.Veyssié. *Europhys. Lett.*, **9**, 251 (1989)
260. L.Hong, S.Jiang, S.Granick. *Langmuir*, **22**, 9495 (2006)
261. T.G.Noguchi, Y.Iwashita, Y.Kimura. *Langmuir*, **33**, 1030 (2017)
262. A.Perro, F.Meunier, V.Schmitt, S.Ravaine. *Colloids Surf., A*, **332**, 57 (2009)
263. D.Chen, E.Amstad, C.-X.Zhao, L.Cai, J.Fan, Q.Chen, M.Hai, S.Koehler, H.Zhang, F.Liang, Z.Yang, D.A.Weitz. *ACS Nano*, **11**, 11978 (2017)
264. D.Wu, B.P.Binks, A.Honciuc. *Langmuir*, **34**, 1225 (2018)
265. K.H.Ku, Y.J.Lee, G.-R.Yi, S.G.Jang, B.V.K.J.Schmidt, K.Liao, D.Klinger, C.J.Hawker, B.J.Kim. *Macromolecules*, **50**, 9276 (2017)
266. W.Zhai, B.Wang, Y.Wang, Y.-F.He, P.Song, R.-M.Wang. *Colloids Surf., A*, **503**, 94 (2016)
267. W.Cao, R. Huang, W.Qi, R.Su, Z.He. *ACS Appl. Mater. Interfaces*, **7**, 465 (2015)
268. E.Passas-Lagos, F.Schüth. *Langmuir*, **31**, 7749 (2015)
269. H.Kim, J.Cho, J.Cho, B.J.Park, J.W.Kim. *ACS Appl. Mater. Interfaces*, **10**, 1408 (2018)
270. C.Lu, M.W.Urban. *ACS Macro Lett.*, **3**, 346 (2014)
271. O.D.Velev, K.Furusawa, K.Nagayama. *Langmuir*, **12**, 2374 (1996)
272. A.D.Dinsmore, M.F.Hsu, M.G.Nikolaides, M.Marquez, A.R.Bausch1, D.A.Weitz. *Science*, **298**, 1006 (2002)
273. D.J.McClements. *Curr. Opin. Colloid Interface Sci.*, **17**, 235 (2012)
274. T.Bollhorst, K.Rezwan, M.Maas. *Chem. Soc. Rev.*, **46**, 2091 (2017)
275. S.Laïb, A.F.Routh. *J. Colloid Interface Sci.*, **317**, 121 (2008)

276. Q.Sun, H.Gao, G.B.Sukhorukov, A.F.Routh. *ACS Appl. Mater. Interfaces*, **9**, 32599 (2017)
277. M.Pang, A.J.Cairns, Y.Liu, Y.Belmabkhout, H.C.Zeng, M.Eddaoudi. *J. Am. Chem. Soc.*, **135**, 10234 (2013)
278. Z.Ao, Z.Li, G.Zhang, T.Ngai. *Colloids Surf., A*, **384**, 592 (2011)
279. J.-W.Kim, A.Fernández-Nieves, N.Dan, A.S.Utada, M.Marquez, D.A.Weitz. *Nano Lett.*, **7**, 2876 (2007)
280. H.Duan, D.Wang, N.S.Sobal, M.Giersig, D.G.Kurth, H.Möhwald. *Nano Lett*, **5**, 949 (2005)
281. P.F.Noble, O.J.Cayre, R.G.Alargova, O.D.Velev, V.N.Paunov. *J. Am. Chem. Soc.*, **126**, 8092 (2004)
282. F.J.Rossier-Miranda, K.Schroën, R.Boom. *Food Hydrocolloids*, **27**, 119 (2012)
283. W.Li, C.Zhao, J.Tan, J.Jiang, J.Xu, D.Sun. *Colloids Surf., A*, **421**, 173 (2013)
284. G.Sobczak, T.Wojciechowski, V.Sashuk. *Langmuir*, **33**, 1725 (2017)
285. M.Williams, S.P.Armes, D.W.York. *Langmuir*, **28**, 1142 (2012)
286. K.L.Thompson, S.P.Armes, J.R.Howse, S.Ebbens, I.Ahmad, J.H.Zaidi, D.W.York, J.A.Burdis. *Macromolecules*, **43**, 10466 (2010)
287. J.Xu, X.Li, X.Wu, W.Wang, R.Fan, X.Liu, H.Xu. *J. Phys. Chem., C*, **120**, 12666 (2016)
288. H.Wang, X.Zhu, L.Tsarkova, A.Pich, M.Möller. *ACS Nano*, **5**, 3937 (2011)
289. C.Zhang, C.Hu, Y.Zhao, M.Möller, K.Yan, X.Zhu. *Langmuir*, **29**, 15457 (2013)
290. M.Williams, S.P.Armes, P.Verstraete, J.Smets. *Langmuir*, **30**, 2703 (2014)
291. J.Fothergill, M.Li, S.A.Davis, J.A.Cunningham, S.Mann. *Langmuir*, **30**, 14591 (2014)
292. X.-W.Xu, X.-M.Zhang, C.Liu, Y.-L.Yang, J.-W.Liu, H.-P.Cong, C.-H.Dong, X.-F.Ren, S.-H.Yu. *J. Am. Chem. Soc.*, **135**, 12928 (2013)
293. R.T.Rosenberg, N.R.Dan. *J. Colloid Interface Sci.*, **354**, 478 (2011)
294. N.Dan. *Curr. Opin. Colloid Interface Sci.*, **17**, 141 (2012)
295. R.T.Rosenberg, N.R.Dan. *J. Colloid Interface Sci.*, **349**, 498 (2010)
296. M.R.Amiryousefi, M.Mohebbi, S.Golmohammadzadeh, A.Koocheki, F.Baghbani. *J. Food Eng.*, **212**, 181 (2017)
297. Y.Yang, Y.Cai, N.Sun, R.Li, W.Li, S.C.Kundu, X.Kong, J.Yao. *Colloids Surf., B*, **151**, 102 (2017)
298. H.N.Yow, A.F.Routh. *Langmuir*, **25**, 159 (2009)
299. Y.Zhao, Y.Pan, N.Nitin, R.V.Tikekar. *LWT — Food Sci. Technol.*, **58**, 667 (2014)
300. P.H.R.Keen, N.K.H.Slater, A.F.Routh. *Langmuir*, **30**, 1939 (2014)
301. P.H.R.Keen, N.K.H.Slater, A.F.Routh. *Langmuir*, **28**, 16007 (2012)
302. A.Jana, L.Bai, X.Li, H.Ågren, Y.Zhao. *ACS Appl. Mater. Interfaces*, **8**, 2336 (2016)
303. P.H.R.Keen, N.K.H.Slater, A.F.Routh. *Langmuir*, **28**, 1169 (2012)
304. Y.Gong, A.M.Zhu, Q.G.Zhang, M.L.Ye, H.T.Wang, Q.L.Liu. *ACS Appl. Mater. Interfaces*, **5**, 10682 (2013)
305. D.B.Lawrence, T.Cai, Z.Hu, M.Marquez, A.D.Dinsmore. *Langmuir*, **23**, 395 (2007)
306. R.K.Shah, J.-W.Kim, D.A.Weitz. *Langmuir*, **26**, 1561 (2010)
307. A.J.Morse, J.Madsen, D.J.Growney, S.P.Armes, P.Mills, R.Swart. *Langmuir*, **30**, 12509 (2014)
308. J.S.Sander, A.R.Studart. *Langmuir*, **29**, 15168 (2013)
309. R.Kluger. *Bioorg. Chem.*, **49**, 59 (2013)
310. G.Lv, F.Wang, X.Zhang. *Appl. Catal., A*, **547**, 191 (2017)
311. S.Lin, S.Sun, K.Shen, D.Tan, H.Zhang, F.Dong, X.Fu. *Appl. Clay Sci.*, **159**, 42 (2018)
312. T.Zhang, B.Xing, Q.Han, Y.Lei, D.Wu, X.Ren, Q.Wei. *Anal. Chim. Acta*, **1032**, 114 (2018)
313. W.K.Spoelstra, S.Deshpande, C.Dekker. *Curr. Opin. Biotechnol.*, **51**, 47 (2018)
314. B.T.Nguyen, W.Wang, B.R.Saunders, L.Benyahia, T.Nicolai. *Langmuir*, **31**, 3605 (2015)
315. M.Sarker, N.Tomczak, S.Lim. *ACS Appl. Mater. Interfaces*, **9**, 11193 (2017)
316. S.Shahid, S.R.Gurram, M.G.Basavaraj. *Langmuir*, **34**, 5060 (2018)
317. J.Li, H.D H.Stöver. *Langmuir*, **24**, 13237 (2008)
318. J.Tan, J.Wang, L.Wang, J.Xu, D.Sun. *J. Colloid Interface Sci.*, **359**, 155 (2011)
319. D.Wu, A.Honciuc. *ACS Appl. Nano Mater.*, **1**, 471 (2018)
320. K.Y.Tan, J.E.Gautrot, W.T.S.Huck. *Langmuir*, **27**, 1251 (2011)
321. P.Liu, W.Lu, W.-J.Wang, B.-G.Li, S.Zhu. *Langmuir*, **30**, 10248 (2014)
322. L.Lei, Q.Zhang, S.Shi, S.Zhu. *Langmuir*, **33**, 6108 (2017)
323. M.Ranka, H.Katepalli, D.Blankschtein, T.A.Hatton. *Langmuir*, **33**, 13326 (2017)
324. T.Saigal, A.Yoshikawa, D.Kloss, M.Kato, P.L.Golas, K.Matyjaszewski, R.D.Tilton. *J. Colloid Interface Sci.*, **394**, 284 (2013)
325. J.W.Tavacoli, J.H.J.Thijssen, A.B.Schofield, P.S.Clegg. *Adv. Funct. Mater.*, **21**, 2020 (2011)
326. A.Kaiser, T.Liu, W.Richtering, A.M.Schmidt. *Langmuir*, **25**, 7335 (2009)
327. S.Melle, M.Lask, G.G.Fuller. *Langmuir*, **21**, 2158 (2005)
328. J.Zhou, L.Wang, X.Qiao, B.P.Binks, K.Sun. *J. Colloid Interface Sci.*, **367**, 213 (2012)
329. H.Yang, H.Zhang, J.Peng, Y.Zhang, G.Du, Y.Fang. *J. Colloid Interface Sci.*, **485**, 213 (2017)
330. Q.Lan, C.Liu, F.Yang, S.Liu, J.Xu, D.Sun. *J. Colloid Interface Sci.*, **310**, 260 (2007)
331. N.Sun, Q.Li, D.Luo, P.Sui, Q.Jiang, J.Liu, A.Li, W.Si, Y.Ma. *Colloids Surf., A*, **608**, 125588 (2021)
332. L.E.Low, L.T.-H.Tan, B.-H.Goh, B.T.Tey, B.H.Ong, S.Y.Tang. *Int. J. Biol. Macromol.*, **127**, 76 (2019)
333. L.E.Low, C.W.Ooi, E.S.Chan, B.H.Ong, B.T.Tey. *J. Environ. Chem. Eng.*, **8**, 103715 (2020)
334. H.Cheng, Z.Li, Y.Li, Z.Shi, M.Bao, C.Han, Z.Wang. *J. Colloid Interface Sci.*, **560**, 349 (2020)
335. R.-X.Bai, L.-H.Xue, R.-K.Dou, S.-X.Meng, C.-Y.Xie, Q.Zhang, T.Guo, T.Meng. *Langmuir*, **32**, 9254 (2016)
336. Y.Chen, Z.Li, H.Wang, Y.Pei, Y.Shi, J.Wang. *Langmuir*, **34**, 2784 (2018)
337. Z.Chen, L.Zhou, W.Bing, Z.Zhang, Z.Li, J.Ren, X.Qu. *J. Am. Chem. Soc.*, **136**, 7498 (2014)
338. Y.Chen, Y.K.Bai, S.B.Chen, J.P.Jup, Y.Q.Li, T.M.Wang, Q.H.Wang. *ACS Appl. Mater. Interfaces*, **6**, 13334 (2014)
339. C.-Y.Xie, S.-X.Meng, L.-H.Xue, R.-X.Bai, X.Yang, Y.Wang, Z.-P.Qiu, B.P.Binks, T.Guo, T.Meng. *Langmuir*, **33**, 14139 (2017)
340. J.Z.Jiang, Y.Ma, Z.Cui, B.P.Binks. *Langmuir*, **32**, 8668 (2016)